Physics – Uspekhi **65** (10) 1039 – 1070 (2022)

REVIEWS OF TOPICAL PROBLEMS

PACS numbers: **05.45.–a**, **47.10.–g**, 47.20.Ft, 47.20.Ky, 47.27.Cn, **47.32.–y**, 47.32.Ef, 47.32.cd, 47.85.Dh, 92.10.Lq, **92.60.–e**, 92.60.hk

Baroclinic instability in geophysical fluid dynamics

M V Kalashnik, M V Kurgansky, O G Chkhetiani

DOI: https://doi.org/10.3367/UFNe.2021.08.039046

Contents

Abstract. **Baroclinic instability is that of flows in a rotating stratified fluid with a vertical velocity shear. The generation of large-scale vortical flows in the atmospheres of Earth and other planets is associated with this instability. The review presents modern theoretical approaches dealing with this instability. They include a description of baroclinic instability through the interaction of edge Rossby waves, the study of the problem of optimal perturbations, i.e., those characterized by the largest growth of energy or other functionals, and an analysis of the nonlinear dynamics of perturbations that relies on a low-mode approximation of the Galerkin method. Classical energy criteria for the stability of zonal flows obtained by the direct Lyapunov–Arnold method are also considered. The results presented may be of interest to specialists in the field of continuum mechanics and astrophysics.**

Keywords: geophysical fluid dynamics, baroclinic instability, energy criteria of stability, nonlinear perturbation dynamics, Galerkin method

M V Kalashnik***, M V Kurgansky, O G Chkhetiani**
Obukhov Institute of Atmospheric Physics,
Russian Academy of Sciences,
Pyzhevskii per. 3, 119017 Moscow, Russian Federation
E-mail: (*) kalashnik_obn@mail.ru

Received 2 June 2021, revised 20 August 2021
Uspekhi Fizicheskikh Nauk **192** (10) 1110 – 1144 (2022)
Translated by S D Danilov

1. Introduction

Geophysical fluid dynamics is a branch of science dealing with motions in rotating and stratified fluids, first and foremost, the motions in planetary atmospheres and oceans. The background rotation and stratification endow such motions with two main specific features. The first one is that, in rotating atmospheres at large scales, air moves along isobars (lines of constant pressure) and not from high to low pressure. The respective motions were discovered only two centuries after the beginning of regular meteorological pressure measurements in the 17th century, with the establishment of Buys Ballot's law, and were dubbed geostrophic motions (from the Greek *geo* for Earth and *strophe* for a turn, twist). Buys Ballot wrote in 1857: "If in the Northern hemisphere you stand with your back to the wind, pressure is lower on your left hand than on your right. In the Southern hemisphere the reverse is true" (see [1]). The second feature stems from stratification — the density structure of the atmosphere in the gravity field. As a measure of stratification, the buoyancy frequency squared $N^2 = -(g/\rho_0)(\mathrm{d}\rho_0/\mathrm{d}z + g\rho_0/c_s^2)$ is traditionally used, where $\rho_0(z)$ is the background (reference) vertical density profile (in the direction of the gravity force), g is the acceleration due to gravity, and c_s is the speed of sound (see, e.g. [2]). In a practically incompressible ocean, the last term in the second parentheses can be disregarded. For a convectively stable stratification ($N^2 > 0$), motions in the atmosphere acquire a wave character, in particular, in the form of internal gravity waves.

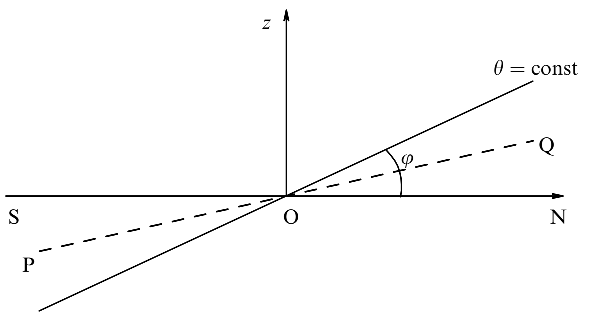

Figure 1. Schematic of isentropic surfaces in conditions of baroclinic instability; φ is the angle the surfaces $\theta = \text{const}$ are inclined toward the horizontal plane.

The fundamentals of geophysical fluid dynamics are presented in a number of monographs and textbooks [2–4]. They devote a central place to the description of various types of hydrodynamical instabilities in rotating flows and related mechanisms of vorticity generation in the atmosphere. These mechanisms are well known to specialists; however, for certain reasons, their description was not included in classical courses in physics, in particular, the volume *Fluid Dynamics* for the course by Landau and Lifshitz [5]. For physicists, the existing gap is partly filled by articles in the *Journal of Experimental and Theoretical Physics* (*JETP*) and *JETP Letters*, as well as by reviews [6–11] published in *Physics–Uspekhi* in various years.

These reviews focus attention on studies of hydrodynamical instability in rotating flows in fluids of uniform density. In geophysical fluid dynamics, such an instability is called barotropic. The present review is devoted to a description of so-called baroclinic instability, which occurs in flows of stratified rotating fluid with vertical velocity shear. Since the vertical velocity shear in a rotating fluid is maintained by the horizontal temperature gradient, baroclinic instability is interpreted as the one caused by the release of available potential energy (Fig. 1).

The first step in exploring baroclinic instability was made in Ref. [12]. In 1949, a classical paper by Eady [13] was published, in which the parameters of unstable perturbations (baroclinic waves) were found for an ideal flow with a uniform vertical shear, which agreed well with the parameters of midlatitude cyclones and anticyclones in the atmosphere. The Eady work stimulated an avalanche of publications contributing to the theory of baroclinic instability, which to date has not ceased. Only in 1990 were two monographs [14, 15] and a review [7] touching on different aspects of this problem published in this country. The accumulation of theoretical results, as well as results obtained in the laboratory [16], led to the present understanding that the generation of vortical structures (cyclones and anticyclones) in the midlatitude atmosphere is a realization of baroclinic instability. According to the author of monograph [15], the elaboration of this fact is one of the most significant achievements in meteorology in the second half of the 20th century. This statement is equally valid for oceanography and astrophysics.

We present a physical interpretation of baroclinic instability, which is considered a slantwise form of convection in the field of gravity. In classical convection driven by gravity (without background rotation), the isolines of background equilibrium distribution of potential temperature (and pressure) are strictly horizontal. The buoyancy force acting on each particle is directed vertically. Taking into account background rotation, i.e., in the model of baroclinic instability, the isolines of background temperature are sloping. For a fluid particle moving at an angle to the horizontal plane that is smaller than the slope of constant potential temperature surfaces (isoentropic surfaces), the buoyancy force acquires a nonzero component which tries to displace the particle from its initial position along its initial inclined trajectory. It is the horizontal slope of the lines of background potential temperature distribution that leads to the baroclinic instability.

As an illustration, consider a simple schematic (see Fig. 1) which presents isoentropic (having a constant potential temperature $\theta = \text{const}$, which is uniquely related to entropy) and equipotential (horizontal), $z = \text{const}$, surfaces in a baroclinic atmosphere. These surfaces form a so-called instability wedge. For this wedge, the potential temperature monotonically increases with height [5] and does so toward the equator (Fig. 1 displays the northern hemisphere). The slope of isoentropic surfaces to the horizontal plane, characterized by small angle $\varphi \approx 1/300$, is maintained by Earth's rotation and vertical wind shear, which is needed to ensure balance between the meridional pressure gradient and the Coriolis force at each horizontal level.

Let an air particle be displaced along the ray from point O to point P (to the south) or Q (to the north), i.e., along the trajectory within the instability wedge. In this case, it is found among particles with higher (at P) or lower (at Q) values of potential temperature. The buoyancy force accompanying such a displacement has a nonzero projection on the sloping trajectory PQ and tends to move the particle further away from point O. This is why the unfolding baroclinic instability is referred to as a form of sloping convection [3, 4, 16]. In the Eady baroclinic instability model [13] (see above), the maximum release rate for the available potential energy stored in the background zonal flow is reached for particles moving along the bisectrix of small angle φ.

For further exposition, it is useful to give some parameters helping to describe the dynamics of rotating atmospheres and baroclinic instability. The first of them is the so-called baroclinic Rossby deformation radius, which is a geometric scale given by the expression $L_{\mathrm{R}} = NH/f_0$. Here, H is the effective thickness of the atmosphere (ocean) and N is the mean value of the buoyancy frequency. The Coriolis parameter f_0 is twice the projection of planet angular velocity on the local vertical ($f_0 = 2\Omega_0 \sin\varphi_0$, Ω_0 is the module of angular velocity, and φ_0 is the local latitude). Moving forward, we note that L_{R} defines, up to a numerical factor, the scale of eddies that develop as a result of baroclinic instability. For the characteristic parameters of Earth's troposphere at midlatitudes $H = 10$ km, $N = 10^{-2}$ s^{-1}, $f_0 = 10^{-4}$ s^{-1}, the radius of deformation $L_{\mathrm{R}} = NH/f_0 = 1000$ km. For values $H = 5$ km, $N = 10^{-3}$ s^{-1}, and $f_0 = 10^{-4}$ s^{-1} that correspond to oceanic motions, $L_{\mathrm{R}} = NH/f_0 = 50$ km, which is smaller by more than an order of magnitude. Note that the expression for L_{R} can be written as $L_{\mathrm{R}} = c/f_0$, where $c = NH$ is the speed of long internal gravity waves. An analogous expression is valid for the so-called barotropic deformation radius that characterizes motions in a rotating shallow water layer with the phase speed of long waves $c = \sqrt{gH}$ [4, 17].

In the description of motions with characteristic horizontal velocity U and horizontal scale L, an important role is played by the Rossby number $\mathrm{Ro} = U/f_0 L$, which is a dimensionless parameter giving the ratio of the time scale due to rotation f_0^{-1} to the advective time scale $T = L/U$. If

$\mathrm{Ro} \ll 1$, the motion time scale is much larger that the Coriolis period. For $L = L_\mathrm{R}$ and a characteristic speed of atmospheric motions $U_* = 10\ \mathrm{ms}^{-1}$, the Rossby number $\mathrm{Ro} = 0.1$. This number is an order of magnitude smaller for motions in the ocean where the characteristic velocity is $U_* = 0.1\ \mathrm{m\ s}^{-1}$. Note that, for motions with a characteristic size $L = L_\mathrm{R} = c/f_0$, the Rossby number $\mathrm{Ro} = U/f_0 L$ is an analog of the Mach number $\mathrm{Ro} = U/c$. Motions characterized by $\mathrm{Ro} \ll 1$ are therefore analogs of motions at low Mach numbers.

A theoretical description of baroclinic instability is traditionally carried out in the framework of the quasigeostrophic model of the atmosphere, which is valid for motions with a horizontal scale $L \sim L_\mathrm{R}$ and Rossby number $\mathrm{Ro} \ll 1$. The model deals with deviations in pressure p' and density ρ' from the background hydrostatic distributions and introduces the streamfunction $\psi = p'/(f_0 \rho_*)$, where ρ_* is the constant reference value of background density. The horizontal components of fluid velocity u, v and the buoyancy distribution $\theta = -g\rho'/\rho_*$ are related to the streamfunction through

$$u = -\psi_y, \quad v = \psi_x, \quad \theta = f_0 \psi_z \,. \tag{1.1}$$

Here and below, along with the common notation, partial derivatives are denoted with subscript letters. The evolution of the streamfunction (in the Boussinesq approximation) is described by the potential vorticity (PV) evolution equation

$$\frac{\mathrm{D}q}{\mathrm{D}t} \equiv q_t + [\psi, q] = 0, \quad q = \Delta\psi + \frac{\partial}{\partial z}\left(\frac{f_0^2}{N^2}\frac{\partial\psi}{\partial z}\right), \tag{1.2}$$

where $[\psi, q] = \psi_x q_y - \psi_y q_x$ is the two-dimensional Jacobian, and $\Delta\psi = \psi_{xx} + \psi_{yy}$ is the two-dimensional Laplace operator. The asymptotic derivation of Eqn (1.2) based on the expansion of a full equation system in a series in small parameter $\varepsilon = \mathrm{Ro}$ can be found in monographs [3, 4]. For motions in a horizontal layer $0 < z < H$, Eqn (1.2) is complemented by nonstationary boundary conditions

$$z = 0, H: \quad \frac{\mathrm{D}\theta}{\mathrm{D}t} \equiv \frac{\partial\theta}{\partial t} + [\psi, \theta] = 0, \quad \theta = f_0 \psi_z \,. \tag{1.3}$$

Conditions (1.3) imply that the vertical velocity component w is zero on rigid horizontal layer boundaries and follow from the general buoyancy transport equation $\mathrm{d}\theta/\mathrm{d}t + N^2 w = 0$ linearized with respect to the background stratification [3, 4]. The upper boundary $z = H$ in atmospheric models (in the framework of the Boussinesq approximation) is commonly associated with the level of tropopause that corresponds to a sharp jump in the gradient of the vertical background temperature profile. We stress that, according to (1.1), (1.3) features a normal streamfunction derivative.

It should be noted that taking into account additional physical factors modifies Eqn (1.2). The latitudinal dependence of the Coriolis parameter (beta effect) adds the term $f = f_0 + \beta y$ in the expression for PV (1.2), where $\beta y \ll f_0$. Different functions of pressure [18, 19] are often taken as the vertical coordinate in meteorological models to account for compressibility. It is also important to stress that Eqn (1.2) is valid for motions satisfying the condition $\mathrm{Ro} \ll 1$, which, as shown above, holds for large-scale motions in Earth's atmosphere at midlatitudes. The validity of this condition for other planetary atmospheres depends on the planet's angular rotation speed and radius (maximum horizontal size). In the atmosphere of slowly rotating Venus, whose angular speed is 200 times smaller than Earth's, condition $\mathrm{Ro} \ll 1$ is not valid. However, for the rapidly rotating Jovian atmosphere (one Jovian day is 10 Earth hours), condition $\mathrm{Ro} \ll 1$ obviously holds, and Eqn (1.2) can be used to describe large-scale motions [4].

Practically all solutions pertaining to baroclinic instability were obtained in the framework of the quasigeostrophic (QG) model of atmospheric dynamics based on Eqns (1.2) and (1.3) [3, 4, 19, 20]. An informal derivation of these equations, together with an explanation of the general law of potential vorticity conservation, is presented in Section 2. This section also contains general integral criteria of baroclinic instability following from these equations. These criteria are obtained with the help of the direct Lyapunov–Arnold method. Section 3 presents a simplified version of the QG model that came to be known as the surface quasigeostrophic model (SQG). Flows with zero potential vorticity are considered, which are analogous to potential flows in classical fluid mechanics. Nonstationary boundary conditions (1.3) are a primary factor defining their dynamics. Section 3 points to a class of exact model solutions for stationary zonal flows, which includes the flow with constant vertical shear treated by Eady [13]. Its baroclinic instability is considered in Section 4, which devotes a central place (Section 4.1) to a description of linear baroclinic instability in terms of interacting edge Rossby waves, as obtained in Ref. [21], which are related to periodic buoyancy perturbations localized near boundaries with given amplitudes and phases. The process of wave interaction is described by a dynamical system of equations governing amplitudes and the phase difference between the boundary buoyancy distributions. Its solutions illustrate the fundamental role of the phase difference in the onset of instability. Section 4.2 deals with the problem of optimal perturbations, which are the ones with the largest growth rate for energy or the ratio of final to initial energies. The representation of the solution to the initial-value problem as a superposition of two edge Rossby waves allows the energetic characteristics to be expressed in terms of initial parameters. By searching for function extrema, the parameters of optimal perturbations are found in an analytical form.

The nonlinear dynamics of perturbations on a flow with uniform vertical velocity shear and a spatially periodic flow are considered in Section 4.3 and 5, respectively. To describe these dynamics, maximally truncated systems of the Galerkin method are used, which preserve the full energy and potential energies at the boundaries. The solutions indicate that the exponential growth of perturbations on the linear stage of instability evolution is replaced by the stage of regular nonlinear oscillations. This result explains the onset of oscillatory regimes in laboratory experiments [22, 23].

Section 6 considers a discrete variant of the SQG model that contains two vertical levels and is analogous to the classical Phillips model. In this framework, the long-wave instability of an isolated jet and two oppositely directed jets at each level is explored. Analytical expressions are obtained for increments and spatial scales of unstable modes.

Section 7 describes the instability of a zonal flow in the presence of the beta effect.

Section 8 deals with the so-called problem of symmetric instability of zonal flows, which is an instability with respect to perturbations that do not depend on the coordinate along the flow. An instability of this type, playing an important role in the atmosphere, is of a wave character and cannot be described by geostrophic equations. The full system of equations for the dynamics of symmetric perturbations leads to additional Lagrangian conservation laws for angular (geostrophic) momentum, which are used to build Lyapunov functionals to obtain sufficient conditions of nonlinear symmetric stability by the variational (energy) method.

Section 9 briefly presents manifestations of baroclinic instability in astrophysics: the development of turbulence in disk systems, the transport of angular momentum and maintenance of differential rotation, the evolution of seeds of planetary formation through the development of vortices, and matter accumulation in them.

2. Potential vorticity and energetic criteria of baroclinic stability in a quasigeostrophic model of atmospheric dynamics

2.1 On the notion of potential vorticity

Fluid dynamics as a science took shape in the middle of the 18th century after L Euler derived his celebrated equations. Since then, and during the entire 19th century, fluid dynamics has evolved either in the framework of models or for incompressible homogeneous fluids, or, at most, for a compressible barotropic fluid when the fields of pressure p and density ρ are in a one-to-one correspondence, which closes the system of fluid dynamical equations. At the beginning of the 20th century, triggered by the application of fluid dynamics to natural media (called geophysical at present), such as the atmosphere or ocean, it has become necessary to consider more complex realistic models in which ρ depends not only on p but also on some second independent thermodynamical variable (in the simplest case, on two independent thermodynamic functions of state). The most fundamental is the choice of the second variable as the kinetic temperature T (in degrees Kelvin) or specific (per unit mass) thermodynamic entropy s. A model of this type is called a baroclinic fluid. The name stems from the fact that surfaces of constant pressure (isobars) and constant density (isopycnals) do not coincide, in contrast to the case of a barotropic fluid, but cross at an angle (forming a wedge). This entails far-reaching consequences. In a baroclinic fluid, Helmholtz's well-known theorems on conservation of vortices in an ideal fluid cease to hold, while Kelvin's circulation theorem is no longer valid. Vortices can be created (generated) in an ideal fluid because of baroclinicity. The effect of vorticity generation is expressed, on the one hand, in the form of the Bjorkness theorem, which is a generalization of Kelvin's theorem. On the other hand, a baroclinic term appears in the vorticity equation (the Helmholtz equation), which is proportional to the vector product of the gradients of ρ and p, as has been shown by A A Friedman (the Friedman equation) (see Ref. [24]). It is a remarkable fact that a baroclinic fluid also possesses a dynamical conservation law following from the general theorem on vorticity, which is the essence of the dynamics of baroclinic fluid and which is written in the form (cf. [2])

$$\frac{\mathrm{D}}{\mathrm{D}t}\,\frac{\boldsymbol{\omega}_{\mathrm{a}}\nabla\Lambda}{\rho}=\frac{\boldsymbol{\omega}_{\mathrm{a}}\nabla(\mathrm{D}\Lambda/\mathrm{D}t)}{\rho}+\frac{\operatorname{helm}\boldsymbol{\omega}_{\mathrm{a}}\nabla\Lambda}{\rho}\,. \tag{2.1}$$

In this equation, $\boldsymbol{\omega}_{\mathrm{a}}=\nabla\times\mathbf{v}+2\Omega$ is the absolute vorticity vector, i.e., the vector of velocity curl in the absolute (inertial) reference frame. In (2.1), a transform is made to the reference frame rotating at constant angular speed Ω, where $\mathbf{v}$ is the velocity in the rotating reference frame; $\mathrm{D}/\mathrm{D}t$ is the total time derivative in the same frame of reference; $\Lambda(\mathbf{x},t)$ is an arbitrary function of coordinate and time; and the operator helm, following A A Friedman, is termed Helmholtzian (in recognition of Helmholtz),

$$\operatorname{helm}\boldsymbol{\omega}_{\mathrm{a}}\equiv\frac{\mathrm{D}\boldsymbol{\omega}_{\mathrm{a}}}{\mathrm{D}t}-(\boldsymbol{\omega}_{\mathrm{a}}\nabla)\mathbf{v}+\boldsymbol{\omega}_{\mathrm{a}}(\nabla\mathbf{v})\,.$$

A general theorem can be proven (see [24]) that the condition $\operatorname{helm}\mathbf{A}=0$ is the necessary and sufficient one for the preservation of vector lines and vector tubes of arbitrary vector field $\mathbf{A}(\mathbf{x},t)$. According to the Friedman equation,

$$\operatorname{helm}\boldsymbol{\omega}_{\mathrm{a}}=\rho^{-2}(\nabla\rho\times\nabla p)+\nabla\times\mathbf{F}\,,$$

or, alternatively (by virtue of the fundamental Clausius–Gibbs thermodynamical equation),

$$\operatorname{helm}\boldsymbol{\omega}_{\mathrm{a}}=\nabla T\times\nabla s+\nabla\times\mathbf{F}\,,$$

where $\mathbf{F}$ are nonpotential forces applied to the fluid, including the viscous force. Thus, if one takes $\Lambda\equiv s$ and considers an adiabatic and inviscid case when both terms on the right-hand side of (2.1) become zero, one arrives at Ertel's theorem [25] on potential vorticity conservation:

$$\frac{\mathrm{D}}{\mathrm{D}t}\,\Pi_s=0\,,\quad \Pi_s=\frac{\boldsymbol{\omega}_{\mathrm{a}}\nabla s}{\rho}\,.$$

In meteorology, instead of specific entropy, it is preferable to use the potential temperature θ (for air as the mixture of ideal gases), which is uniquely connected to it,

$$s=c_p\ln\theta+\text{const}\,,\quad \theta=T\left(\frac{p_{00}}{p}\right)^{R/c_p}\,,\quad p_{00}=10^3\ \text{GPa}\,.$$

Here, R is the gas constant for dry air, and c_p is the dry air specific heat at constant pressure. For Earth's atmosphere, consisting practically of diatomic gases, $R/c_p=2/7$. For the solar atmosphere, composed effectively from a monoatomic gas, $R/c_p=2/5$. Then, if we assume $\Lambda\equiv\theta$,

$$\frac{\mathrm{D}}{\mathrm{D}t}\,\Pi_\theta=0\,,\quad \Pi_\theta=\frac{\boldsymbol{\omega}_{\mathrm{a}}\nabla\theta}{\rho}\,.$$

In oceanography, as well as in studies of Earth's external liquid core, one can formally assume $s=-c_p\ln\rho+\text{const}$ and consider fluid motion to be incompressible, $\mathrm{D}\rho/\mathrm{D}t=0$, so that the law of potential vorticity conservation takes the form

$$\frac{\mathrm{D}}{\mathrm{D}t}\,\Pi_\rho=0\,,\quad \Pi_\rho=\frac{\boldsymbol{\omega}_{\mathrm{a}}\nabla\rho}{\rho}\,,$$

where, for convenience and consistency in notation, we preserve ρ in the denominator. In oceanography, a more rigorous problem formulation is used, which is based on the notion of potential density [2]. Note that we have presented a classical approach to the definition of potential vorticity. In contemporary research, it is shown that Kelvin's circulation theorem and conservation of potential vorticity (Ertel's invariant) follow from the relabeling symmetry for motion equations written in the Lagrangian variables [26, 27].

We discussed at length the definition of the potential vorticity, since this notion is central in this review and in essence permeates all its contents. Most sections of this review discuss traditional quasigeostrophic baroclinic instability with respect to wave perturbations that depend on the coordinate along the basic flow (such perturbations are commonly referred to as nonzonal or nonsymmetric). A key role in this case is played by the gradient of quasigeostrophic potential vorticity in the direction transverse to the unperturbed baroclinic flow [28] or the gradient of generalized quasigeostrophic vorticity [29] (see also [30]). In Section 8, we abandon the quasigeostrophic approximation and consider the so-called symmetric baroclinic, or simply symmetric, instability with respect to perturbations that do not depend on the coordinate along the basic flow. As we shall see, the criterion of symmetric baroclinic instability can be elegantly expressed in the most general form as the condition on sign preservation of the potential vorticity field (positiveness in the northern hemisphere and negativeness in the southern one) [31].

2.2 Quasigeostrophic model. Informal derivation of equations

In modern geophysical fluid dynamics, one can see a tendency to get rid of such factors, in a certain sense, of secondary importance, as a full account of air compressibility and Earth's sphericity, and distill dynamical effects of stratification and rotation in their most apparent and universal form applicable to all geophysical media, first and foremost, to the atmosphere, ocean, and Earth's liquid core. Such a possibility of sufficiently slow (with a speed much lower than the speed of sound) vertical processes at large and intermediate (meso)scales offer equations of motion in the Boussinesq approximation, written in a local Cartesian reference frame, where the only trace of Earth's sphericity is the assumed linear dependence of the Coriolis parameter on the latitudinal Cartesian coordinate (the Rossby beta plane model) (see, for example, [4]). It goes without saying that, in practical computations using modern numerical weather predictions and climate models, the air compressibility and Earth's sphericity are necessarily taken into account to the full degree, but, in this review, we will be discussing theoretical research, to which the tendency mentioned above applies in full measure.

To unify our presentation, having in mind its application to most geophysical media, we will rely on motion equations of a stratified fluid in the field of the Coriolis force (a) in the Boussinesq approximation and (b) in the so-called traditional approximation when the axis of common rotation is considered to be aligned with the local gravity force direction (vertical)

$$\frac{Du}{Dt} - fv = -\frac{\partial\phi}{\partial x}\,, \quad \frac{Dv}{Dt} + fu = -\frac{\partial\phi}{\partial y}\,,$$

$$\frac{Dw}{Dt} = -\frac{\partial\phi}{\partial z} + b\,, \quad \frac{Db}{Dt} = 0\,, \quad \frac{\partial u}{\partial x} + \frac{\partial v}{\partial y} + \frac{\partial w}{\partial z} = 0\,. \tag{2.2}$$

Fluid is considered to be in a homogeneous gravity field (Earth's surface is with a high degree of accuracy an equipotential surface, and the characteristic thickness of the atmosphere or ocean is much smaller that Earth's radius). Equations (2.2) correspond to those of free convection (in book [5]) and generalize them by taking into account general rotation, taking the Coriolis parameter as a linear function of the latitudinal coordinate, $f = f_0 + \beta y$, where f_0 and β are constants. It should be recalled that $\phi = \tilde{p}/\rho_0$, where ρ_0 is a constant (reference) value of density, $\tilde{p} = p - p_0(z)$, where $p_0(z) = \mathrm{const} - \rho_0 z$ is the hydrostatic pressure that corresponds to the reference state; the variable $b = -g(\rho - \rho_0)/\rho_0$ in contemporary literature on geophysical fluid dynamics is called buoyancy and is often denoted by the Greek letter θ or ϑ. In fact, it is the full buoyancy which can be conveniently written as a sum of buoyancy that corresponds to the mean stratified state, $\bar{b} = -g\bar{\rho}/\rho_0$, and the deviation thereof $b' = -g\rho'/\rho_0$, assuming that $\rho - \rho_0 = \bar{\rho}(z) + \rho'(x, y, z, t)$. Similarly, $\tilde{p} = \bar{p}(z) + p'(x, y, z, t)$, where $\bar{p}(z)$ and $\bar{\rho}(z)$ are linked by the hydrostatic relationship, and we present (2.2) in a more convenient form, separating out the stable state of fluid in an explicit form:

$$\frac{Du}{Dt} - fv = -\frac{\partial\phi'}{\partial x}\,, \quad \frac{Dv}{Dt} + fu = -\frac{\partial\phi'}{\partial y}\,, \quad \frac{Dw}{Dt} = -\frac{\partial\phi'}{\partial z} + b'\,,$$

$$\frac{Db'}{Dt} + N^2 w = 0\,, \quad \frac{\partial u}{\partial x} + \frac{\partial v}{\partial y} + \frac{\partial w}{\partial z} = 0\,. \tag{2.3}$$

In Eqns (2.3), $\phi' = p'/\rho_0$, and the buoyancy frequency squared (the Brunt–Váisálá frequency) $N^2 = -g(d\bar{\rho}/dz)/\rho_0$ is assumed to be constant.

Motions at a large scale, which are the main focus of this review in the context of baroclinic instability, are characterized with good accuracy by being in the geostrophic and hydrostatic balance. We present the field of horizontal velocity in the form $(u, v) = (-\partial\psi/\partial y, \partial\psi/\partial x)$, where $\psi = \phi'/f_0$ is the geostrophic streamfunction, and in the quasistatic approximation $b' = f_0(\partial\psi/\partial z)$. Now, we still need to take into account the smallness of the vertical velocity, since in the continuity equation the terms with $\partial u/\partial x$ and $\partial v/\partial y$ compensate each other with asymptotic accuracy, and in a good approximation

$$\frac{D}{Dt} = \frac{\partial}{\partial t} - \frac{\partial\psi}{\partial y}\frac{\partial}{\partial x} + \frac{\partial\psi}{\partial x}\frac{\partial}{\partial y}\,.$$

Thus, excluding ϕ' from equations of horizontal motion, we arrive at a system of two equations:

$$\frac{\partial}{\partial t}\,\Delta\psi + [\psi, \Delta\psi + \beta y] = f_0\,\frac{\partial w}{\partial z}\,,$$

$$\frac{\partial}{\partial t}\frac{\partial\psi}{\partial z} + \left[\psi, \frac{\partial\psi}{\partial z}\right] = -\frac{N^2}{f_0}\,w\,.$$

Differentiating both sides of the second equation by z and adding the result to the first equation after identity transformation, we arrive at Eqn (1.2) of potential vorticity conservation:

$$\frac{\partial}{\partial t}\,q + [\psi, q] = 0\,, \quad q = \Delta\psi + \frac{f_0^2}{N^2}\frac{\partial^2\psi}{\partial z^2} + f_0 + \beta y\,. \tag{2.4}$$

Equation (2.4) should be solved with boundary conditions of impermeability of the lower $z = z_-$ and upper $z = z_+$ fluid layer boundaries

$$\frac{\partial}{\partial t}\,b + [\psi, b] = 0\,, \quad b = f_0\,\frac{\partial\psi}{\partial z}\,, \quad z = z_\mp\,. \tag{2.5}$$

Taking into account $b = \theta$, conditions (2.5) coincide with conditions (1.3). The boundary conditions (2.5) reflect the main distinguishing features of the problem statement for the atmosphere and the ocean. In the atmosphere, Earth's surface is taken as the lower boundary $z = z_- = 0$, and the upper boundary is conditionally the height of the tropopause $z = z_+ = H$ (a surface separating the troposphere and stratosphere where the buoyancy frequency squared jumps toward higher values). In contrast, in the ocean, its surface can be naturally taken as the upper surface, $z = z_+ = 0$, and its bottom as the lower surface, $z = z_- = -D$. In the atmosphere, the variable b can be considered proportional to the deviation of potential temperature from its mean value.

Taking into account that the mean air density in the atmosphere $\rho_0 = \rho_0(z)$ strongly (nearly exponentially) decreases with height, and also that the buoyancy frequency may vary, the equation of potential vorticity conservation is frequently taken in a more general form [28]:

$$\frac{\partial}{\partial t} q + [\psi, q] = 0,$$
$$q = \Delta\psi + \frac{1}{\rho_0(z)} \frac{\partial}{\partial z} \rho_0(z) \frac{f_0^2}{N^2(z)} \frac{\partial\psi}{\partial z} + f_0 + \beta y .$$

A more rigorous account of compressibility of atmospheric air is achieved by the change to isobaric coordinates when pressure p plays the role of vertical coordinate [2, 19, 32–36], and the potential vorticity conservation law is expressed as

$$\frac{\partial}{\partial t} q + [\psi,\ q] = 0, \quad q = \Delta\psi + \frac{\partial}{\partial p} m^2 p^2 \frac{\partial\psi}{\partial p} + f_0 + \beta y ,$$

where $m^2 = f_0^2/(N^2 H_0^2)$, $H_0 = RT_0/g$ is the height of a homogeneous atmosphere which corresponds to the mean near-surface air temperature T_0, and partial derivatives over x, y, t are taken along isobaric surfaces. Conditions (2.5) are in this case also modified (see [35, 36]).

2.3 Energetic stability criteria

In the framework of Eqn (2.4) with conditions (2.5), the general problem of zonal flow nonlinear stability is considered. The beta-plane approximation is used. The flow is assumed to be periodic in the zonal direction with a period L, which is the mean length of the circle in the belt of latitudes. In the north and south, the flow is bounded by vertical walls going along fixed latitudes. These walls are considered to be impermeable to air:

$$\frac{\partial\psi}{\partial x} = 0, \quad y = y_*\,, \quad y^*\,,$$

and velocity circulation on them is assumed to be constant at each vertical level:

$$\int \frac{\partial\psi}{\partial y}\, dx = \text{const}, \quad y = y_*\,, \quad y^*\,.$$

In the last case, we rely on the fact that, taking into account periodicity with period L, the zonal channel is topologically equivalent to a circular channel with inner and outer walls. Since at each height level such a circular channel cannot be continuously deformed to a point, one needs to place conditions that the circulation be preserved on both the inner and outer walls (see Refs [20, 37]). We apply Arnold's method [37]. We rely on the existence of motion integrals in this problem: (a) energy

$$E = \frac{1}{2} \iiint \left\{ (\nabla\psi)^2 + \frac{f_0^2}{N^2} \left(\frac{\partial\psi}{\partial z} \right)^2 \right\} dx\, dy\, dz$$

as the sum of kinetic and available potential energies; (b) the zonal component of momentum

$$P = -\iiint \frac{\partial\psi}{\partial y}\, dx\, dy\, dz\,;$$

and (c) so-called Casimirs, the quantities that are conserved by virtue of (2.4) and (2.5),

$$F = \iiint \Phi(q, z)\, dx\, dy\, dz\,, \quad G = \iint_{\Sigma_-} \Gamma(\theta)\, dx\, dy\,,$$
$$H = \iint_{\Sigma_+} H(\theta)\, dx\, dy\,,$$

where Φ, Γ, and H are arbitrary continuously differentiable functions, and $\Sigma_\mp$ are the upper and lower boundaries for $z = z_\mp$, respectively. In our presentation, we follow mainly Ref. [35] and especially monographs [19, 36], although in these studies the quasigeostrophic motion of the atmosphere was considered in the isobaric coordinate system (see above). This problem was considered in the Boussinesq approximation in Ref. [38], but there is a certain caveat. The Casimir F features a function of two variables, i.e., the functional dependence on q is different at each level, varying from level to level. In [38], a function of single variable q is written, which is in all probability just a typo but worth mentioning nevertheless. We also mention (a note on terminology) that, in the expression for the full energy E, the second term is proportional to the square of the perturbation of potential temperature (buoyancy). Hence, the term — available potential energy.

A linear combination of motion integrals $I = E - UP + F + G + H$ is taken, where the constant U has the dimension of velocity. Let ψ_0 be the streamfunction of given stationary zonal flow, the stability of which is explored. The difference $I[\psi] - I[\psi_0]$ is a motion integral. Considering the deviation $\delta\psi = \psi - \psi_0$ to be small, we expand $I[\psi] - I[\psi_0]$ in a series in variations of subsequent orders,

$$I[\psi] - I[\psi_0] = \delta I + \frac{1}{2}\, \delta^2 I + \ldots\,.$$

The arbitrary functions Φ, Γ, and H can be selected so that, for the given zonal flow ψ_0 and for any arbitrarily taken U, the first variation δI becomes zero,

$$\Phi'_q\big|_{q=q_0} = \psi_0 + Uy, \quad z_- < z < z_+\,,$$
$$\Gamma'\big|_{\theta=\theta_0} = \frac{f_0^2}{N^2} (\psi_0 + Uy), \quad z = z_-\,,$$
$$H'\big|_{\theta=\theta_0} = -\frac{f_0^2}{N^2} (\psi_0 + Uy), \quad z = z_+\,.$$

The prime denotes differencing, and the subscript q means that the differencing was over the respective variable. If we assume that q_0 is monotonic with respect to latitude y for each z and that θ_0 is monotonic at $z = z_\mp$, respectively, then these conditions can always be satisfied. Computing the second variance, we find

$$\begin{aligned} \delta^2 I = \iiint \Bigg\{ &(\nabla\delta\psi)^2 + \frac{f_0^2}{N^2} \left(\frac{\partial\delta\psi}{\partial z} \right)^2 \\ &+ \frac{(\partial\psi_0/\partial y) + U}{\partial q_0/\partial y} (\delta q)^2 \Bigg\} dx\, dy\, dz \\ &+ \iint_{\Sigma_-} \frac{f_0^2}{N^2} \frac{(\partial\psi_0/\partial y) + U}{\partial\theta_0/\partial y} (\delta\theta)^2\, dx\, dy \\ &- \iint_{\Sigma_+} \frac{f_0^2}{N^2} \frac{(\partial\psi_0/\partial y) + U}{\partial\theta_0/\partial y} (\delta\theta)^2\, dx\, dy\,. \end{aligned} \tag{2.6}$$

If quadratic form (2.6) is positive definite, i.e., all the coefficients by squares of variables are positive, then the zonal flow ψ_0 is stable in the sense of Lyapunov. Note that quadratic form (2.6) is an exact motion integral for equations linearized with respect to perturbations superposed on the mean flow, and, in modern terminology, presents a combination of pseudoenergy and pseudomomentum.

What does this criterion offer in practice, i.e., which zonal flows can satisfy it? In order to satisfy the necessary condition $\delta I = 0$, we assumed that the potential vorticity of basic zonal flow is a monotonic function of latitude. It would be natural to suppose that it is a monotonically increasing function, by analogy with the Coriolis parameter f. Zonal flows in the midlatitude atmosphere are predominantly westerly, i.e., $\partial\psi_0/\partial y < 0$. Selecting the constant U, which was just arbitrary until now, such that it exceeds the maximum of the modulus of basic flow velocity, we see that all volume integrals in (2.6) become positive. This is formally analogous, if we take into account the Galilean invariance, to the change to the reference frame which moves such that winds become easterly and the condition of positive definiteness of the volume integral is valid (cf. [37]). In a subtropical ocean, zonal flows are directed to the east and the volume integral is positive definite for $U = 0$. There is a problem with surface integrals. The potential temperature on Earth's surface decreases monotonically toward the poles and the integral over Earth's surface in (2.6) is negative, so that the second variation is not sign definite. The situation is even worse because of the integral taken over the upper boundary, which is positive if the potential temperature decreases toward the poles and negative otherwise. In any case, the quadratic form (2.6) is not sign definite, and a necessary condition of baroclinic instability is fulfilled. When the potential temperature varies very little on the lower and upper boundary surfaces, the surface integrals in (2.6) can be omitted. Only the volume integral is left, and we arrive at the Charney–Stern criterion [28], which states that the zonal flow with a potential vorticity monotonically increasing (in absolute value) toward the poles is always stable.

The Charney–Stern criterion can be obtained from simpler considerations. Formally letting the constant U in (2.6) go to infinity, i.e., making it larger and larger, in the limit, we arrive at the quadratic form

$$\delta^2\hat{I} \equiv -\frac{\delta^2 I}{U} = -\iiint \frac{(\delta q)^2}{\partial q_0/\partial y}\,\mathrm{d}x\,\mathrm{d}y\,\mathrm{d}z - \iint_{\Sigma_-} \frac{f_0^2}{N^2}\frac{(\delta\theta)^2}{\partial\theta_0/\partial y}\,\mathrm{d}x\,\mathrm{d}y + \iint_{\Sigma_+} \frac{f_0^2}{N^2}\frac{(\delta\theta)^2}{\partial\theta_0/\partial y}\,\mathrm{d}x\,\mathrm{d}y\,, \quad (2.7)$$

which is the second variation of a simpler functional $\hat{I} = P + F + G + H$. Quadratic form (2.7) is once more a motion integral of linearized equations and is called pseudomomentum. Again, assuming that the upper and lower surfaces are isentropic, we can concentrate only on the volume integral in (2.7). For $\partial q_0/\partial y > 0$, the second variation $\delta^2\hat{I} < 0$. Hence, the zonal momentum takes the maximum value on the given flow ψ_0. According to (2.7), any perturbation of flow ψ_0 would lead to a reduction in zonal momentum, which is impossible because it is the motion integral. Hence, such a zonal flow is stable. If surface integrals are nonzero and their contribution is opposite in sign to the contribution from the volume integral, this limitation is relaxed, and the flow can be baroclinically unstable.

An interesting case is when the potential vorticity can be treated as constant at each altitude, which is an idealization, but an acceptable one for relatively narrow channels, when the Coriolis parameter can be considered approximately constant, with this constancy extended to the total quasigeostrophic potential vorticity. Now, the volume integral in (2.7) disappears, and if the potential temperature has the same sign of growth on the upper and lower boundaries, a baroclinic instability is possible (the momentum conservation law does not prohibit it). Linear analysis of instability of the Eady model [13] confirms this.

3. Surface quasigeostrophic model and stationary zonal flows

In Section 2, we formulated Eqns (2.4) and (2.5), which form the basis of the quasigeostrophic model of the atmosphere. In this section, a simplified variant of this model is considered, which will be further used to solve concrete problems of baroclinic instability theory. For a more compact presentation, partial derivatives will be denoted by subscript letters, and the buoyancy will be denoted by θ.

We will consider quasigeostrophic motions in a horizontal layer $0 < z < H$ with constant buoyancy frequency N and Coriolis parameter f. In the absence of the beta effect, it is convenient to use a dimensionless form of Eqns (2.4), (2.5):

$$\frac{\mathrm{D}q}{\mathrm{D}t} \equiv q_t + [\psi, q] = 0, \quad q = \psi_{xx} + \psi_{yy} + \psi_{zz}\,, \quad (3.1)$$

$$z = 0,\, 1: \qquad \psi_{zt} + [\psi, \psi_z] = 0\,. \quad (3.2)$$

Here, layer thickness H and baroclinic Rossby deformation radius $L_{\mathrm{R}} = NH/f$ [4] are taken as the vertical and horizontal scales, respectively. The scales of time, streamfunction, and velocity are, respectively, $T_* = L_{\mathrm{R}}/U_*$, $\Psi_* = U_* L_{\mathrm{R}}$, and $U_* = \Theta_*/N$, where Θ_* is a characteristic value of buoyancy change. Dimensionless horizontal components of velocity u, v and buoyancy θ are expressed through the streamfunction as $u = -\psi_y, v = \psi_x, \theta = \psi_z$.

Equation (3.1) is satisfied by flows with zero potential vorticity $q = 0$. The streamfunction of such flows, which are analogous to potential flows in classical fluid dynamics, can be found from the solution of the Laplace equation

$$\psi_{xx} + \psi_{yy} + \psi_{zz} = 0 \quad (3.3)$$

in the band $0 < z < 1$, subject to nonstationary boundary conditions (3.2). A dynamical model of flows based on Eqns (3.2), (3.3) was proposed in Refs [39, 40] and has a special name: the surface quasigeostrophic (SQG) model. A direct consequence of model equations is the conservation law for total energy

$$E_t = 0, \quad E = \int_0^1 \overline{(\psi_x^2 + \psi_y^2 + \psi_z^2)}\,\mathrm{d}z \quad (3.4)$$

and surface potential energy (for each of the boundaries)

$$V_t = 0, \quad V = \overline{\psi_z^2}\,, \quad (3.5)$$

where the bar denotes averaging over the horizontal coordinates. By virtue of the conservation laws, all the solutions to the SQG model are bounded in amplitude. Note that Eqns (3.2), (3.3) in fact define a boundary-value problem that is close to the problem on potential (with zero vorticity) surface gravity waves in a fluid. The velocity potential is found from the solution of the Laplace equation with nonstationary boundary conditions on the surface [5].

In applications, one often considers an SQG model with a single boundary (a model of a semi-infinite atmosphere or deep ocean). In such a model, only one condition (3.2) is imposed — on the underlying surface $z = 0$. Other scales are used to reduce model equations to a dimensionless form. For a given horizontal scale D, the vertical scale is defined as $H = fD/N$ (the vertical Rossby scale).

To solve the Laplace Eqn (3.3) and find harmonic functions, the two-dimensional velocity field $(u, v) = (-\psi_y, \psi_x)$ at boundaries is expressed in terms of the boundary buoyancy distribution $\theta = \psi_z$ (normal derivative) through nonlocal Hilbert transform-type operators. Thus, in the model with one boundary [41, 42],

$$(u, v) = \frac{1}{2\pi}\left(-\frac{\partial}{\partial y}, \frac{\partial}{\partial x}\right)\iint \frac{\theta(\mathbf{x}', t)}{|\mathbf{x} - \mathbf{x}'|}\,\mathrm{d}\mathbf{x}', \quad \mathbf{x} = (x, y)\,. \tag{3.6}$$

Taking into account (3.6), boundary condition (3.2) at $z = 0$ is reduced to a nonlinear integro-differential equation on the buoyancy $\theta = \theta(\mathbf{x}, t)$. The buoyancy on its own plays a role of an active scalar inducing the velocity field, by analogy with relative vorticity in two-dimensional fluid dynamics. The formation of singularities in the field of this scalar was explored in [41, 43]. The appearance of open-source numerical pseudospectral solvers for integro-differential equations (https://pyqg.readthedocs.io/en/latest/index.html) led to the growth in the number of publications on geophysical applications of the SQG model. The applications included an analysis of the dynamics of distributed and pointwise vortices [44–51], the dynamics of near-surface flows in the atmosphere and ocean [42, 47, 52], a description of surface fractal zone dynamics [53], and a comparison of energy cascades in models of SQG and QG turbulence [54–56]. A vast bibliography is given in review [57].

Further, an SQG model with two boundaries will be used to explore baroclinic instability of zonal flows. These flows are described by stationary solutions of Eqns (3.2) and (3.3), which do not depend on the coordinate x (in atmospheric models, axes x and y are traditionally directed to the east and north). The streamfunction $\Psi(y, z)$ of zonal flows (we use a capital letter for variables) is a solution of the boundary problem

$$\Psi_{yy} + \Psi_{zz} = 0\,, \quad \Psi_z(y, 0) = \Theta_{\mathrm{bott}}(y)\,,$$
$$\Psi_z(y, 1) = \Theta_{\mathrm{top}}(y) \tag{3.7}$$

for the two-dimensional Laplace equation in the belt $0 < z < 1$. Here, $\Theta_{\mathrm{bott}}(y)$, $\Theta_{\mathrm{top}}(y)$ are the given buoyancy distributions at the boundaries $z = 0$ and $z = 1$, respectively, with bounded derivatives at $|y| \to \infty$. The solution of (3.7) gives the distribution of velocity $U = -\Psi_y$ and buoyancy $\Theta = \Psi_z$.

By virtue of boundary conditions (conditions of the second kind), the solution $\Psi(y, z)$ of problem (3.7) can be found up to an arbitrary linear function of variable y. As a result, the velocity field $U = -\Psi_y$ is determined up to arbitrary constant U_{m}. Integrating the Laplace equation vertically and denoting the layer mean $\langle\Psi\rangle = \int_0^1 \Psi\,\mathrm{d}z$, we find $\langle\Psi\rangle_{yy} = \Theta_{\mathrm{bott}} - \Theta_{\mathrm{top}}$ or $\langle U\rangle_y = \Theta_{\mathrm{top}} - \Theta_{\mathrm{bott}}$. Hence, it follows that equal boundary distributions of buoyancy $\Theta_{\mathrm{top}} = \Theta_{\mathrm{bott}}$ induce zonal flows with mean velocity $\langle U\rangle = 0$ (an arbitrary constant is omitted). Such flows have a clearly expressed vertical shear and draw the most interest from the viewpoint of stability. We give some examples of exact solutions of (3.7) for various types of buoyancy distributions $\Theta_{\mathrm{top}} = \Theta_{\mathrm{bott}}$.

I. *Linear distribution.* For the distribution $\Theta_{\mathrm{bott}} = \Theta_{\mathrm{top}} = -y$, the exact solution of problem (3.7) takes the form

$$\Psi = -y\left(z - \frac{1}{2}\right), \quad U = -\Psi_y = z - \frac{1}{2}\,. \tag{3.8}$$

This solution describes a zonal flow with an antisymmetric velocity profile and constant vertical shear. The flow is maintained by the constant temperature gradient $\Theta = \Psi_z = -y$. An arbitrary linear distribution $\Psi_{\mathrm{m}} = -U_{\mathrm{m}}y$ can be added to the streamfunction; in this case, a uniform flow with velocity U_{m} will be added to the velocity field.

II. *Periodic distribution.* The distribution $\Theta_{\mathrm{top}} = \Theta_{\mathrm{bott}} = C\cos(ly)$ induces a spatially periodic flow with the velocity

$$U = C\,\frac{\sinh\left[l(z - 0.5)\right]\sin(ly)}{\cosh(0.5l)}\,. \tag{3.9}$$

The vertical flow profile is antisymmetric relative to the layer mid-depth $z = 1/2$.

III. *Frontal-type distribution.* The distribution $\Theta_{\mathrm{bott}} = \Theta_{\mathrm{top}} = -\tanh(\mu y)$ models a frontal zone (a smoothed step) with width μ^{-1}. An exact solution can be found for $\mu = \pi n$, $n = 1, 2, \ldots$, using either conformal mapping techniques (by mapping a horizontal band on a half-plane) or the Fourier transform over the horizontal coordinate with subsequent inversion. For $n = 1$, i.e., in the situation when the width of the transitional zone is about one third of the Rossby deformation radius, the solution for the streamfunction is

$$\Psi(y, z) = \frac{2}{\pi}\arctan\left[\frac{1 - \sin(\pi z)}{\cos(\pi z)}\tanh\left(\frac{\pi y}{2}\right)\right].$$

The respective expressions for velocity U and buoyancy Θ are

$$U(y, z) = -\frac{\cos(\pi z)}{\cosh(\pi y) + \sin(\pi z)}\,,$$
$$\Theta(y, z) = -\frac{\sinh(\pi y)}{\cosh(\pi y) + \sin(\pi z)}\,. \tag{3.10}$$

A shadow pattern of isolines of velocity distribution (3.10) in the lower half of the layer, shown in Fig. 2a, corresponds to an isolated jet flow. The upper half hosts an analogous flow, but in the opposite direction. Thus, equal frontal buoyancy distributions at the boundaries induce a system of two opposite jet flows located in the upper and lower halves of the atmospheric layer. In real conditions, because of surface drag, the lower flow will be less intense than the upper one, which can be viewed as a prototype of jet flow in Earth's atmosphere [58, 59].

IV. *Localized buoyancy distribution* $\Theta_{\mathrm{bott}} = \Theta_{\mathrm{top}} = 1/\cosh^2(\pi y)$. Exact solutions for the velocity and buoyancy fields are obtained from (3.10) by simple differentiation:

$$U(y, z) = -\frac{\cos(\pi z)\sinh(\pi y)}{\left[\cosh(\pi y) + \sin(\pi z)\right]^2}\,,$$
$$\Theta(y, z) = \frac{1 + \sinh(\pi y)\sin(\pi z)}{\left[\cosh(\pi y) + \sin(\pi z)\right]^2}\,. \tag{3.11}$$

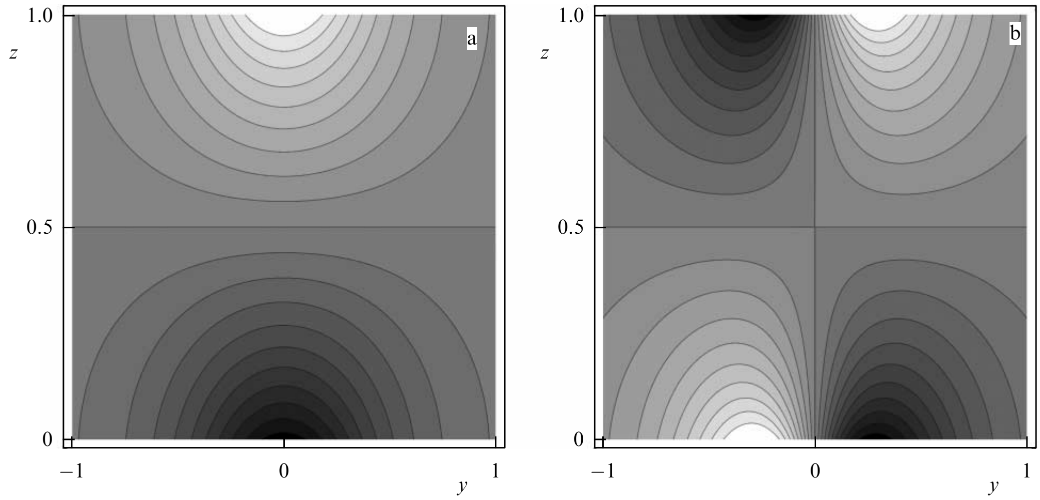

Figure 2. Isolines of zonal velocity in the plane y, z: (a) for flow (3.10) and (b) for flow (3.11).

A shadow pattern of isolines of velocity field (3.11) (Fig. 2b) shows a system of two opposite jets in the lower layer half. As in the earlier case, an analogous but opposite pattern will be seen in the upper layer half.

These examples indicate that the structure of stationary zonal SQG flows can be fairly nontrivial. The problem of linear stability for such flows reduces to solving the Laplace equation with linearized boundary conditions (3.2). For a flow with constant vertical shear (3.8), a solution can be found analytically (see Section 4). Approximate solutions for the problem of stability for analogs of flows (3.10) and (3.11) are given in Sections 5 and 6.

4. Baroclinic instability of a flow with uniform vertical shear (Eady problem)

4.1 Two approaches to solving the linear stability problem

Eady [13] (in 1949) considered a zonal flow with the velocity profile $U(z) = z$ and the streamfunction $\Psi = -yz$. This flow is a modified form of the SQG flow (3.8) obtained by adding a uniform flow with velocity $U_{\mathrm{m}} = 1/2$. Assuming $\psi = \Psi + \psi'$, we get the Laplace equation for the description of small flow perturbations $\psi_{xx} + \psi_{yy} + \psi_{zz} = 0$ (where the prime is omitted) with linearized conditions (3.2)

$$z = 0, 1: \quad \left(\frac{\partial}{\partial t} + z\,\frac{\partial}{\partial x}\right)\psi_z - \psi_x = 0\,. \tag{4.1}$$

If the flow is confined to a zonal channel with width L_*, conditions (4.1) are augmented by the requirement that the normal velocity component $v = \psi_x$ be vanishing on rigid lateral walls at $y = 0, L_*$.

Very often, the case of an unbounded flow (over the entire plane) is considered. Then, conditions of periodicity or boundedness at infinity are imposed on perturbations. These conditions are satisfied by two-dimensional perturbations without dependence on the meridional coordinate y, which, as follows from an analysis, also has the maximum growth rate.

There are two approaches to solving the linear stability problem. In the first of them (for a flow in the channel), perturbations are considered in the form of normal modes

$$\psi = \Phi(z)\exp\left[\mathrm{i}k(x - ct)\right]\sin(ly)\,, \quad l = \frac{\pi n}{L_*} \tag{4.2}$$

traveling in the zonal direction with a complex-valued phase velocity c. The following spectral problem is obtained after (4.2) is inserted into the Laplace equation and the boundary conditions:

$$\Phi_{zz} - \mu^2\Phi = 0, \quad z = 0, 1: \quad (z - c)\,\Phi_z - \Phi = 0\,,$$

where $\mu^2 = l^2 + k^2$ is the wave vector squared. Looking for a solution in the form $\Phi = a\cosh(\mu z) + b\sinh(\mu z)$, where a, b are arbitrary constants, leads to a quadratic equation on the spectral parameter which is the phase velocity $c = c_{\mathrm{r}} + \mathrm{i}c_{\mathrm{i}}$ [3],

$$c^2 - c + \mu^{-1}\coth\mu - \mu^{-2} = 0\,. \tag{4.3}$$

From (4.3), it follows the existence of two normal modes (a growing one and a decaying one) and the expression for the increment $s = kc_{\mathrm{i}}$ of the growing mode

$$s = kr\sqrt{1 - \alpha^2}, \quad \alpha = \cosh\mu - \frac{1}{2}\,\mu\sinh\mu\,, \tag{4.4}$$

where $r = (\mu\sinh\mu)^{-1}$. The real part of phase velocity $c_{\mathrm{r}} = 1/2$, i.e., the normal mode travels with the flow speed at the middle level.

According to (4.4), the instability ($s > 0$) takes place if $-1 < \alpha(\mu) < 1$ or, which is equivalent, $0 < \mu < \mu_{\mathrm{b}}$, where the bounding value $\mu_{\mathrm{b}} = 2.399$ is the root of equation $\coth(\mu/2) = \mu/2$ (the equation $\alpha(\mu) = -1$). Taking into account $\mu^2 = l^2 + k^2$, we get the long-wave interval of unstable wavenumbers $0 < k < k_{\mathrm{b}}$, where the interval right boundary $k_{\mathrm{b}} = (\mu_{\mathrm{b}}^2 - l^2)^{1/2}$ for the instability to exist. The condition $l < \mu_{\mathrm{b}}$ or, equivalently, the channel width $L > \pi n/\mu_{\mathrm{b}}$, should hold. If this condition is observed (a sufficiently wide channel), a numerical analysis of expression (4.4) gives the wavenumber $k = k_{\mathrm{m}}$ of the fastest growing mode with maximum increment $s = s_{\mathrm{m}}$.

For flows on the entire plane, the fastest growth is realized for two-dimensional perturbations with the streamfunction $\psi = \Phi(z)\exp\left[\mathrm{i}k(x - ct)\right]$. The increment of the two-dimensional normal mode is given by expression (4.4), in which we

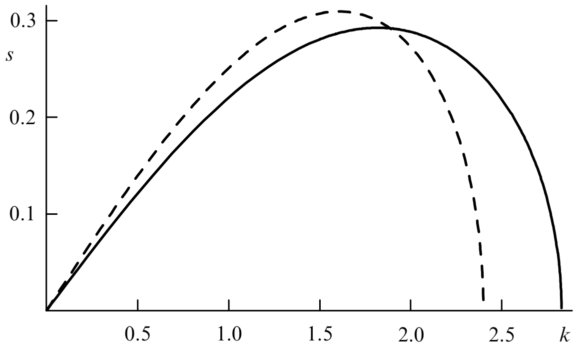

Figure 3. Dependence of instability increment on the wave number for discrete (solid line) and continuous (dashed line) Eady models.

set $\mu = k$ ($l = 0$). The dependence of the increment $s = s(k)$ on wavenumbers is plotted in Fig. 3. The fastest growth is achieved for the wavenumber $k = k_{\rm m} = 1.606$, with the increment $s = s_{\rm m} = 0.31$. For the parameters of the troposphere given above, the wavelength (in dimensional variables) $(2\pi/k_{\rm m})L_{\rm R} \sim 3600$ km (a quarter of a wavelength is the scale of a cyclone), and the e-folding time is about 4 days. These estimates are close to Eady's [13]. Note that a flow with a uniform vertical shear Λ has the dimensional velocity profile $U(z) = \Lambda z$ with the characteristic scale $U_* = \Lambda H$; an advective temporal scale $T_* = L_{\rm R}/U_* = (N/\Lambda)f^{-1}$. Thus, the dimensional value of the increment for the fastest growing mode is frequently written as [60] $s_{\rm m} = 0.31(f/N)\Lambda$. For $U_* = 10$ m s^{-1}, $H = 10$ km (atmosphere), the magnitude of vertical shear $\Lambda = U_*/H = 10^{-3}$ s^{-1}, and the advective time scale $T_* = 10^5$ s (about 1 day).

We stress that, in the development of baroclinic instability, a principal role is played by the vertical velocity shear, which is maintained by the horizontal gradient of temperature. This is a fundamental distinction from barotropic instability that evolves because of the horizontal velocity shear. Barotropic instability is in fact a classical shear instability complicated by the presence of the beta effect. In the development of barotropic instability, an important role is played by the barotropic Rossby radius mentioned earlier, which is substantially larger than the baroclinic deformation radius (for Earth's atmosphere at midlatitudes, the barotropic radius is about 3000 km). A detailed description of barotropic instability models can be found in monographs [2–4] and reviews [6–11].

Another approach to the solution to the linear baroclinic instability problem was proposed in Ref. [21] and later developed in Refs [61–63]. In this approach, a perturbation is taken as a real solution of the Laplace equation with periodic buoyancy distributions at the boundaries:

$$\psi_z\big|_{z=0,1} = \rho_{1,2}(t)\cos\left(kx + \varphi_{1,2}(t)\right)\sin(ly)\,. \tag{4.5}$$

Here, $\rho_{1,2}(t)$ and $\varphi_{1,2}(t)$ are real amplitudes and phases of boundary distributions. In the related solution of the Laplace equation

$$\psi = r\big\{\rho_2(t)\cosh(\mu z)\cos(kx+\varphi_2) - \rho_1(t)\cosh\left[\mu(z-1)\right]\cos(kx+\varphi_1)\big\}\sin(ly)\,, \tag{4.6}$$

the terms proportional to $\rho_1(t)$ and $\rho_2(t)$ correspond to the so-called edge Rossby waves localized, respectively, near the lower (upper) boundary [21]. The interaction of two such waves is described by the system of equations formulated in Ref. [21], which is obtained by inserting solution (4.6) into boundary conditions (4.1). The system consists of three nonlinear equations on amplitudes $\rho_1(t)$, and $\rho_2(t)$ and a phase shift between the boundary buoyancy distributions $\varphi(t) = \varphi_1(t) - \varphi_2(t)$,

$$\frac{d\rho_1}{dt} = kr\rho_2\sin\varphi,\quad \frac{d\rho_2}{dt} = kr\rho_1\sin\varphi\,, \tag{4.7}$$

$$\frac{d\varphi}{dt} = -2kr\left[\alpha - 0.5(d+d^{-1})\cos\varphi\right],\quad d = \frac{\rho_1}{\rho_2}\,. \tag{4.8}$$

This system is augmented by a separate equation

$$\frac{d\varphi_+}{dt} = -k - kr\,(d-d^{-1})\cos\varphi\,,\quad \varphi_+ = \varphi_1 + \varphi_2\,, \tag{4.9}$$

which, together with Eqn (4.8), allows us to find the phases proper. The expressions for the coefficients α, r entering this system are defined in (4.4)

It is important to stress that the use of complex amplitudes $a_{1,2}(t) = \rho_{1,2}(t)\exp(i\varphi_{1,2}(t))$ allows system (4.7)–(4.9) to be reduced to a system of two equations,

$$i\,\frac{da_1}{dt} - kpa_1 + kra_2 = 0\,,$$
$$i\,\frac{da_2}{dt} - k(1-p)a_2 - kra_1 = 0\,, \tag{4.10}$$

where $p = r\cosh\mu \equiv \coth\mu/\mu$. This system can be easily obtained directly by considering complex solutions of the Laplace equation

$$\psi = r\big\{a_2(t)\cosh(\mu z) - a_1(t)\cosh\left[\mu(z-1)\right]\big\}\exp(ikx)\sin(ly)\,, \tag{4.11}$$

which satisfy the conditions $\psi_z|_{z=0,1} = a_{1,2}(t)\exp(ikx)\sin(ly)$. An important feature of nonlinear system (4.7)–(4.9) is that, in contrast to linear system (4.10), it illustrates a principal role of the phase shift for the development of initial perturbation. Indeed, according to Eqns (4.7), the amplitudes grow if the phase shift $0 < \varphi < \pi$ ($\sin\varphi > 0$). Further, in an important special case of equal boundary amplitudes $\rho_1 = \rho_2 = \rho$, system (4.7), (4.8) is reduced to a system of two equations,

$$\frac{d\rho}{dt} = kr\rho\sin\varphi,\quad \frac{d\varphi}{dt} = -2kr(\alpha - \cos\varphi)\,. \tag{4.12}$$

For $\varphi = \varphi_{\rm n}$, $\cos\varphi_{\rm n} = \alpha(\mu)$, system (4.12) has an exact solution $\rho(t) = \rho(0)\exp(st)$ which corresponds to a growing normal mode with increment (4.4). The value $\varphi = \varphi_{\rm n}$ for this mode corresponds to a fixed point of the second Eqn (4.12) which exists only for the values $-1 < \alpha(\mu) < 1$, i.e., for the wavenumbers from the interval $0 < k < k_{\rm b}$ mentioned earlier. The increment and phase shift for two-dimensional normal modes are given by the expressions

$$s(k) = \frac{1}{\sinh k}\,(1-\alpha^2)^{1/2}\,,$$
$$\cos\varphi_{\rm n} = \alpha(k) \equiv \cosh k - 0.5\,k\sinh k\,. \tag{4.13}$$

The mode of fastest growth with the wavenumber $k = k_{\rm m} = 1.606$ corresponds to the phase shift $\cos\varphi_{\rm n} = \alpha = 0.672$ ($\varphi_{\rm n} = 47.8°$). We stress that the information about the phase shift is lost in the approach based on normal

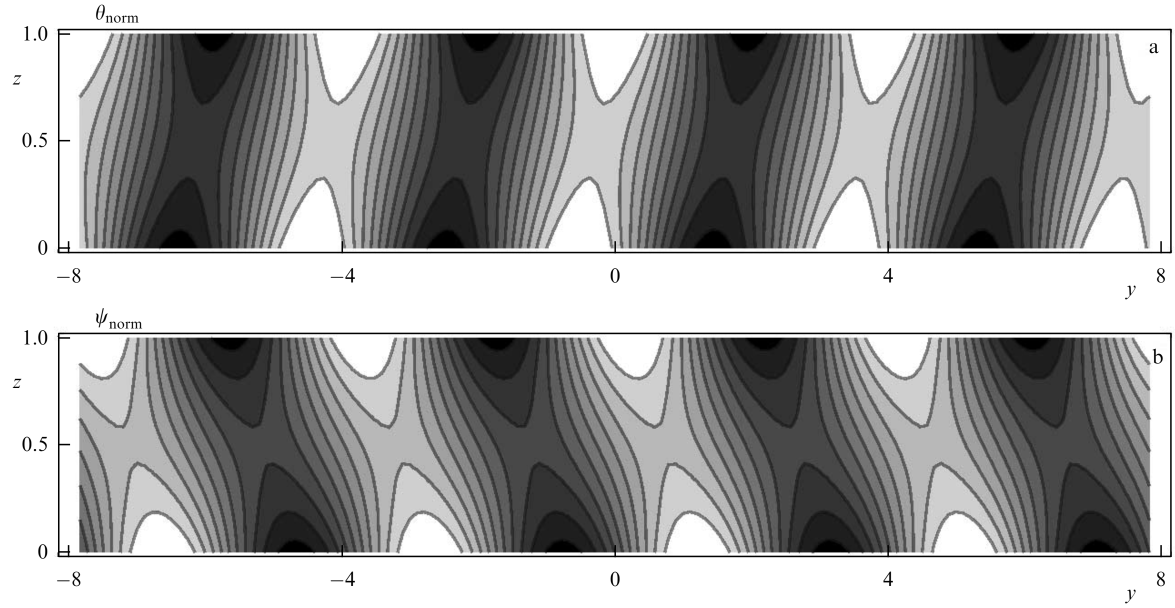

Figure 4. Isolines of buoyancy (a) and streamfunction (b) for the fastest-growing normal mode.

modes. The shadow patterns of isolines of buoyancy $\theta = \psi_z$ and streamfunction ψ (pressure perturbation) for the two-dimensional normal mode of fastest growth are given in Fig. 4. Because of the phase shift, the maxima in the field distribution on the upper and lower surfaces are displaced relative to each other. This feature is regularly found in meteorological observations [60].

For the full system (4.11), (4.12), Ref. [21] gives its first integrals $J_{1,2} = \text{const}$,

$$J_1 = \rho_2^2 - \rho_1^2\,, \quad J_2 = 0.5\,(\rho_1^2 + \rho_2^2) - \alpha^{-1}\,\rho_1\rho_2\cos\varphi\,, \tag{4.14}$$

which allow the integration of the system to be reduced to quadratures. Of interest is the simple exact solution $\rho_1(t) = \rho_2(0)(1-\alpha^2)^{-1/2}\sinh(st)$ which corresponds to the problem with the initial condition $\rho_1(0) = 0$. This solution describes the so-called type-B cyclogenesis, whereby near-surface vortical perturbations are generated by initial perturbations at higher levels [64, 65].

According to some existing studies [66], in up to 80% of cases the formation of near-surface cyclones in the midlatitude atmosphere is related to this mechanism. The shadow patterns of buoyancy isolines presented in Fig. 5 for three time moments provide a clear illustration of this mechanism.

4.2 Optimal perturbations in the linear Eady problem

In the linear theory of hydrodynamical instability, optimal perturbations are those with the maximum growth rate for energy or the ratio of final and initial energies. The search for optimal perturbations is stimulated by the understanding of the limitations of the classical approach that is based on finding exponentially growing normal modes. For example, it was shown that the growth rate of a superposition of growing and decaying normal modes can exceed the growth rate of the individual growing mode [67–69]. Even a superposition of two decaying modes can demonstrate an algebraic (nonmodal) energy growth at the initial stage. The mathematical reason for such behavior is related to the nonnormality of differential operators in problems of the stability theory, and hence the nonorthogonality of their eigenfunctions [68, 69].

Finding optimal perturbations is, as a rule, associated with solving a rather numerically complex problem on a conditional extremum of the full energy functional. For flows with vertical shear, the algorithm of the problem solution relies on the finite-difference approximation of the relevant differential operator in the vertical direction with subsequent singular value decomposition (SVD) of the operator matrix [70–74].

An important feature of the Eady problem is that it allows one to apply an analytical approach for finding optimal perturbations. The approach resorts to the energy balance equation and real-valued representation for the streamfunction of perturbations (3.6) (in terms of edge Rossby waves). Following Refs [75, 76], we will illustrate this approach considering (for brevity) the case of two-dimensional perturbations with equal boundary amplitudes.

Introducing the operations of horizontal and vertical averaging

$$\overline{\varphi}^{\,x} = \lim_{L\to\infty}\frac{1}{2L}\int_{-L}^{L}\varphi\,\mathrm{d}x\,, \quad \langle\varphi\rangle \equiv \int_0^1 \overline{\varphi}^{\,x}\,\mathrm{d}z\,,$$

we write the energy density and full energy of two-dimensional perturbation as

$$\varepsilon = 0.5\,(\psi_x^2 + \psi_z^2)\,, \quad E = \langle\varepsilon\rangle \equiv \int_0^1 \overline{\varepsilon}^{\,x}\,\mathrm{d}z\,.$$

From the definition of ε follows an identity $\varepsilon_t = (\psi\psi_{xt})_x + (\psi\psi_{zt})_z - \psi q_t$, where $q = \psi_{xx} + \psi_{zz}$. Horizontal averaging of this identity with subsequent integration over z and the use of conditions (4.1) leads to the equation of energy balance for perturbations with zero PV, $q = 0$,

$$\frac{\mathrm{d}E}{\mathrm{d}t} = \overline{\psi_x\psi_z}^{\,x}\Big|_{z=1}\,. \tag{4.15}$$

According to Eqn (4.15), a change in full energy is defined by the meridional buoyancy flux at the upper boundary.

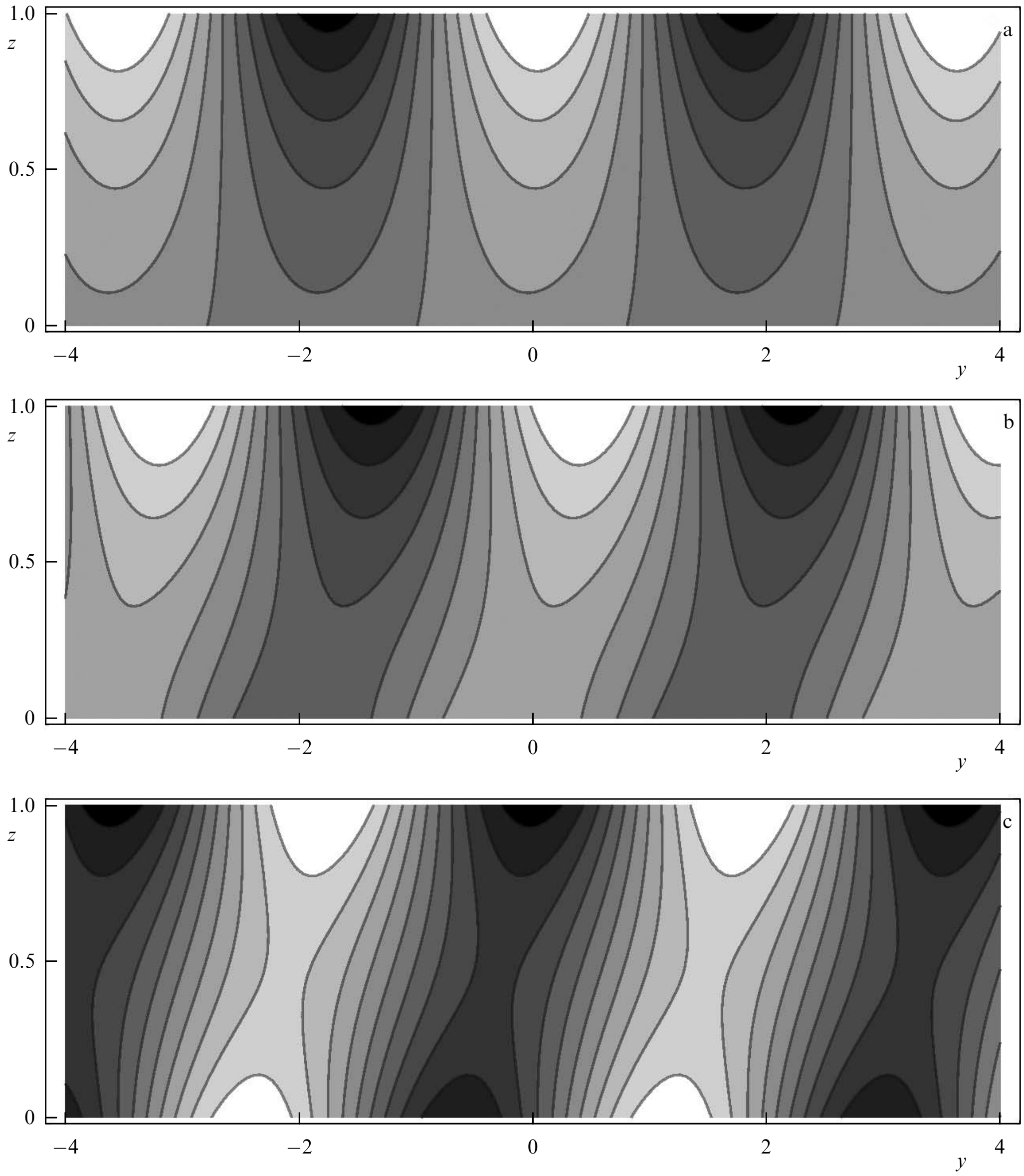

Figure 5. Isolines of the buoyancy field at time instants (a) $t = 0.1$, (b) $t = 1.0$, (c) $t = 4.0$. Case of initial perturbation confined near the upper boundary.

For two-dimensional perturbations with equal boundary amplitudes, the streamfunction is given by the expression

$$\psi = r\rho(t)\{\cosh(kz)\cos(kx+\varphi_2(t)) - \cosh[k(z-1)] \times \cos(kx+\varphi_1(t))\}, \quad r = (k\sinh k)^{-1}. \tag{4.16}$$

Making use of (4.16), direct integration and standard averaging rules for periodic functions result in the expression for the full energy and its derivative

$$\frac{dE}{dt} = \overline{\psi_x\psi_z}^{x}\Big|_{z=1} = \frac{1}{2}\frac{1}{\sinh k}\rho^2(t)\sin\varphi(t),$$
$$E(t) = \frac{1}{2}\langle\psi_x^2+\psi_z^2\rangle = \frac{1}{2}\frac{\coth k}{k}\rho^2(t) \times \left(1 - \frac{1}{\cosh k}\cos\varphi(t)\right). \tag{4.17}$$

According to the first expression, the full energy grows if the phase shift $0 < \theta < \pi$. Only for such a phase shift can the perturbation extract energy from the shear flow.

Expressions (4.17) allow one to obtain a simple solution to the problem of initial optimal perturbations characterized by maximum energy growth at the initial moment. For the energy growth rate, (4.17) leads to the expression

$$\gamma = \frac{1}{E}\frac{dE}{dt} = \frac{k\sin\varphi}{\cosh k - \cos\varphi}, \tag{4.18}$$

which depends only on the initial phase shift (for a fixed wavenumber). Since $\gamma > 0$ in the interval $0 < \varphi < \pi$ and turns to zero at the interval ends, $\varphi = \varphi_{opt}$ exists, such that the function $\gamma(k, \varphi)$ reaches an extremum. This value corresponds to the initial optimal perturbation. An elementary analysis of (4.18) for extrema leads to the expressions

$$\cos\varphi_{opt} = \frac{1}{\cosh k}, \quad \gamma_{opt} = \gamma(k, \varphi_{opt}) = \frac{k}{\sinh k}, \tag{4.19}$$

which define the dependences of phase shift and energy growth rate on the wavenumber of optimal perturbation.

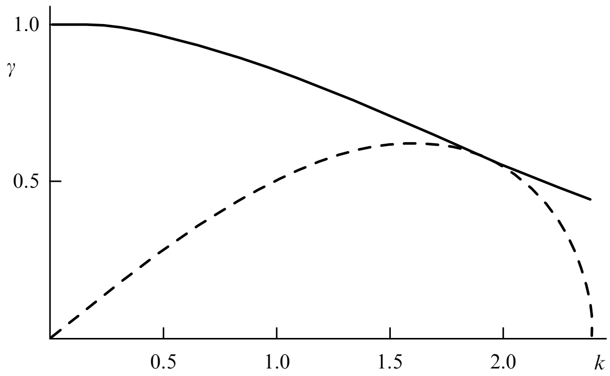

Figure 6. Dependences $\gamma_{\rm opt}$ (solid line) and $\gamma_{\rm n}$ (dashed line) on wavenumber k.

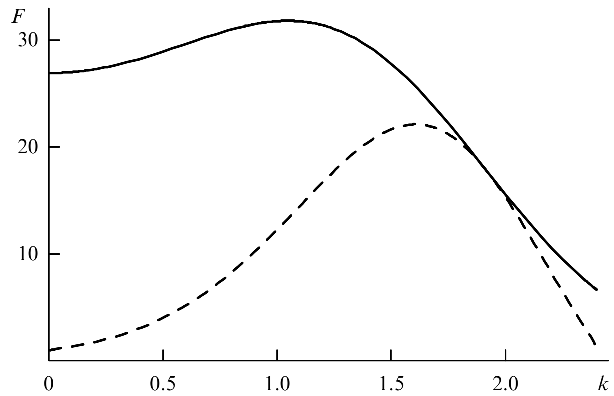

Figure 7. Dependence of $F_{\rm opt}$ (solid line) and $F_{\rm n}$ (dashed line) on wavenumber k for $t = 5$.

Since $\cos\varphi_{\rm n} = \alpha(k)$ for a growing normal mode, a comparison between (4.18) and (4.12) indicates that, in the general case, $\varphi_{\rm n} \neq \varphi_{\rm opt}$, i.e., exponentially growing normal modes are not optimal perturbations. The energy growth rate of growing normal mode $\gamma = \gamma_{\rm n}(k) = 2s(k)$ equals its doubled increment (4.13).

From the dependences $\gamma_{\rm opt}(k)$ and $\gamma_{\rm n}(k) = 2s(k)$ plotted in Fig. 6, it can be seen that there is only one wavenumber $k = k_1 = 1.915$ for which the normal mode is an optimal perturbation, i.e., $\cos\varphi_{\rm n} = \cos\varphi_{\rm opt}$ and $\gamma_{\rm opt} = \gamma_{\rm n}$. For this value (the root of the equation $\tanh k = k/2$), the phase shift is $\varphi_{\rm n} = \varphi_{\rm opt} = 73.22^\circ$. The value $k_1 \neq k_{\rm m}$, i.e., the normal mode of fastest growth, does not correspond to optimal perturbation. Patterns of isolines of buoyancy and streamfunction for optimal perturbations are qualitatively similar to the pattern for normal modes shown in Fig. 4. The difference lies in a more expressed slope of isolines. It is important to emphasize that, for initial optimal perturbations, the quantity $\gamma_{\rm opt}(k)$ reaches the maximum in the limit of long waves, $k \to 0$.

A more general problem on optimal perturbations is formulated in the following way. For a fixed moment t (optimization time), find an initial perturbation for which the functional $F = E(t)/E(0)$ reaches the maximum. Taking into account expansion $F = 1 + \gamma(0)\,t$, $\gamma(t) = E^{-1}\,{\rm d}E/{\rm d}t$, $t \ll 1$, the initial optimal perturbations considered above give the problem solution as $t \to 0$. For finite t, the solution requires integration of the system of dynamical Eqns (4.11).

Using (4.16) and the first integral J_2 (4.13), the ratio of final to initial energy can be reduced to

$$F = \frac{E(t)}{E(0)} = \frac{\alpha - \cos\varphi_0}{\cosh k - \cos\varphi_0}\,\frac{\cosh k - \cos\varphi(t)}{\alpha - \cos\varphi(t)}\,. \qquad (4.20)$$

In this expression, the phase shift $\varphi(t)$ is the solution to the Cauchy problem for the second Eqn (4.11)

$$\frac{{\rm d}\varphi}{{\rm d}t} = -2r(\alpha - \cos\varphi)\,, \quad \varphi(0) = \varphi_0\,, \qquad (4.21)$$

which depends on the initial value φ_0 and the wavenumber k as parameters $\varphi = \varphi(t, k, \varphi_0)$. Taking into account this dependence, the functional F becomes a function of three variables, $F = F(t, k, \varphi_0)$. Finding an optimal perturbation reduces to finding a maximum of this function for the first two arguments at fixed values. Let us keep in mind that φ_0 is the initial value of the phase shift.

An explicit expression for function $F = F(t, k, \varphi_0)$ is obtained by integrating Eqn (4.20). Standard separation of variables gives the exact solution $\varphi = \varphi(t, k, \varphi_0)$ in the form of the first integral

$$Y = \frac{X + c(t)}{c(t)X + 1}\,, \quad Y = \delta^{-1}\tan\left(\frac{\varphi(t)}{2}\right),$$
$$X = \delta^{-1}\tan\left(\frac{\varphi_0}{2}\right), \qquad (4.22)$$

where $c(t) = \tanh(s(k)t)$, $\delta = (k/2 - \tanh k/2)/(\coth k/2 - k/2)$. Expressing $\cos\varphi(t)$ in (4.20) through the tangent of the half angle and using the first integral (4.22), after some transformations, we get the relationship

$$F = \frac{1}{1 - c^2(t)}\,\frac{\big(X + c(t)\big)^2 + n\big(c(t)X + 1\big)^2}{X^2 + n}\,,$$
$$X = \delta^{-1}\tan\left(\frac{\varphi_0}{2}\right), \qquad (4.23)$$

which defines the function $F = F(t, k, \varphi_0)$, or equivalently, the function $F = F(t, k, X)$ in an explicit form. In expression (4.23), the parameter $n = \delta^{-2}\tanh^2(k/2)$ depends only on the wavenumber. The value of F for the normal mode $F = F_{\rm n} = \exp(2s(k)t)$ is found from (4.23) for $X = 1$.

For t, k fixed in the interval $0 < \varphi_0 < \pi$ $(0 < X < \delta^{-1})$, the function F (4.23) has a single maximum point $\varphi_0 = \varphi_{\rm opt}$ $(X = X_{\rm opt})$, which corresponds to the optimal perturbation. Differentiating (4.23) over X leads to a quadratic equation $X^2 - c(t)(n-1)X - n = 0$ determining this point. Hence,

$$X_{\rm opt} = \delta^{-1}\tan\left(\frac{\varphi_{\rm opt}}{2}\right) = \frac{1}{2}\bigg(c(t)(n-1)$$
$$+ \sqrt{c^2(t)(n-1)^2 + 4n}\bigg) \qquad (4.24)$$

and the respective maximum value

$$F_{\rm opt} = 1 + \frac{(n+1)c^2(t)}{1 - c^2(t)}\left(1 + \frac{1}{c(t)X_{\rm opt}}\right). \qquad (4.25)$$

Formulas (4.24) and (4.25) give an analytical solution to the optimal perturbation problem.

The dependences of $F_{\rm opt}$ and $F_{\rm n}$ on the wavenumber k that correspond to fixed optimization time $t = 5$ are given in Fig. 7. An important detail lies in the appearance in the curve $F_{\rm opt}(k)$

of a maximum point $k = k_{\max}(t)$ that corresponds to a preferred wavenumber with the maximum energy ratio. For $t = 5$ (with an optimization time of about 5 days), the value $k_{\max} \sim 1.2$. As in the case of initial optimal perturbations, at $k = k_1$, the curves touch each other (the normal mode is an optimal perturbation). For all other wavenumbers, $F_{\text{opt}} > F_{\text{n}}$. If for a fixed $k \neq k_1$ one plots the graphs of the dependences of F_{opt} and F_{n} on time on a logarithmic scale, they become two parallel lines, one above the other.

References [76, 78] also consider generalized problems that use other energetic characteristics (kinetic energy, potential energy at boundaries, and so on) for optimization. An analytical solution to the optimization problem for a free shear layer and jet flows in a rotating shallow water layer was obtained in recent Ref. [78].

4.3 Nonlinear dynamics of perturbations in the Eady problem

Two approaches are used in fluid dynamics and theoretical physics to describe the nonlinear dynamics of perturbations. The first of them is exemplified by the weakly nonlinear stability theory, including an analysis of different forms of amplitude equations [79]. This approach is asymptotically rigorous; however, its applicability requires the presence of the critical (threshold) parameter that controls the development of instability. The second approach consists in a reduction of the stability problem to finite-dimensional dynamical systems with the help of the Galerkin method [80]. The main requirement for such systems consists in preserving the conservation laws of the initial problem. The success of the approach depends in many respects on the appropriate choice of basis functions. Below, following recent Ref. [81], we present a brief analysis of the nonlinear dynamics of perturbations in the Eady problem using maximally truncated Galerkin approximations.

Nonlinear dynamics of flows with a constant vertical shear are described by a solution of the Laplace equation with nonlinear boundary conditions:

$$z = 0, 1: \quad \left(\frac{\partial}{\partial t} + z\frac{\partial}{\partial x}\right)\psi_z - \psi_x + [\psi, \psi_z] = 0\,. \qquad (4.26)$$

The flow is considered to occupy an infinite horizontal channel ($-\infty < x < \infty,\ 0 < y < \pi$) with dimensionless width $L = \pi$. To satisfy impermeability conditions on the channel lateral walls, the perturbation streamfunction can be taken as an expansion in a series of trigonometric basis functions $f_{\text{n}}(y) = \sin(ny)$. The fastest growing mode of linear theory for $n = 1$ is described by expression (4.6), which can be written as $\psi = A(x, z, t)\sin y$. In a nonlinear problem, this mode interacts with other modes that correspond to $n = 2, 3, \ldots$. We limit ourselves only to the interaction of the first two modes ($n = 1$, $n = 2$) and, in agreement with the Galerkin method, seek approximate solutions of the form

$$\psi = A(x, z, t)\sin y + C(z, t)\sin 2y\,. \qquad (4.27)$$

By virtue of the Laplace equation, the expansion coefficients satisfy the equations

$$A_{xx} + A_{zz} - A = 0\,, \qquad (4.28a)$$

$$C_{zz} - 4C = 0\,, \quad 0 < z < 1\,. \qquad (4.28b)$$

The equations connecting the distributions of A and C at the boundaries follow from boundary conditions (4.26). To obtain these equations, expansion (4.27) is inserted into conditions (4.26) and, further, the orthogonality conditions in the system of basis functions with $n = 1, 2$ are used. These conditions lead to the boundary equations

$$z = 0, 1: \quad A_{zt} + zA_{zx} - A_x + (CA_{xz} - A_xC_z) = 0\,, \qquad (4.29a)$$

$$C_{zt} + \frac{1}{2}(A_xA_z - AA_{xz}) = 0\,. \qquad (4.29b)$$

Thus, in the framework of the Galerkin method with two basis functions, the description of nonlinear perturbation dynamics is reduced to solving linear Eqns (4.28) with nonlinear boundary conditions (4.29).

The solution of Eqn (4.28a) is sought in a form that corresponds to the normal mode of linear theory,

$$A(x, z, t) = r\{\rho_2(t)\cosh(\mu z)\sin(kx + \varphi_2) - \rho_1(t)\cosh[\mu(z - 1)]\sin(kx + \varphi_1)\}\,. \qquad (4.30)$$

As a solution of Eqn (4.28b), we take the quantity

$$C = c(t)\,\frac{\cosh(2z) - \cosh[2(z - 1)]}{2\sinh 2}\,, \qquad (4.31)$$

which has equal values of the derivative at the boundaries $z = 0, 1$: $C_z = c(t)$. The boundary values of the function proper are $C = \mp mc(t)$, where the numerical constant is $m = (1/2)\tanh(1)$.

Inserting solutions (4.30) and (4.31) into boundary Eqns (4.29), one gets a closed system of four equations relative to $c(t)$, the amplitudes $\rho_1(t)$ and $\rho_2(t)$, and the phase shift between the distributions $\varphi(t) = \varphi_1(t) - \varphi_2(t)$,

$$\frac{\mathrm{d}c}{\mathrm{d}t} = -\frac{1}{2}kr\rho_1\rho_2\sin\varphi\,,$$

$$\frac{\mathrm{d}\rho_1}{\mathrm{d}t} = kr(1 + c)\rho_2\sin\varphi\,, \quad \frac{\mathrm{d}\rho_2}{\mathrm{d}t} = kr(1 + c)\rho_1\sin\varphi\,,$$

$$\frac{\mathrm{d}\varphi}{\mathrm{d}t} = -2kr[\alpha + \beta c - 0.5(1 + c)(d + d^{-1})\cos\varphi]\,,$$

$$d = \frac{\rho_1}{\rho_2}\,. \qquad (4.32)$$

Here, $\alpha = \cosh\mu - (1/2)\mu\sinh\mu$, $\beta = \cosh\mu - m\mu\sinh\mu$. System (4.32) is augmented by an isolated equation for the sum of phases $\varphi_+ = \varphi_1 + \varphi_2$, which is analogous to (4.9), and allows the phases to be found.

The dynamical system (4.32) generalizes system (4.7), (4.8) to a description of nonlinear perturbation dynamics. A principal difference from linear dynamics is the set of first integrals (conservation laws) $I_k = \text{const}$, $k = 1, 2, 3$ that follow from system (4.31),

$$I_1 = \rho_2^2 - \rho_1^2\,, \quad I_2 = \frac{1}{2}(\rho_1^2 + \rho_2^2) + 2c_1^2\,,$$

$$I_3 = \rho_1\rho_2\cos\varphi + 4(\alpha - \beta)c_1 + 2\beta c_1^2\,, \qquad (4.33)$$

where $c_1(t) = 1 + c(t)$. These integrals reflect the conservation laws for the full energy and surface potential energy at boundaries (3.3) and (3.4). From the first integral I_2, it follows that, as distinct from the solution to the linear system, all the solutions are bounded in amplitude. Thus, taking into

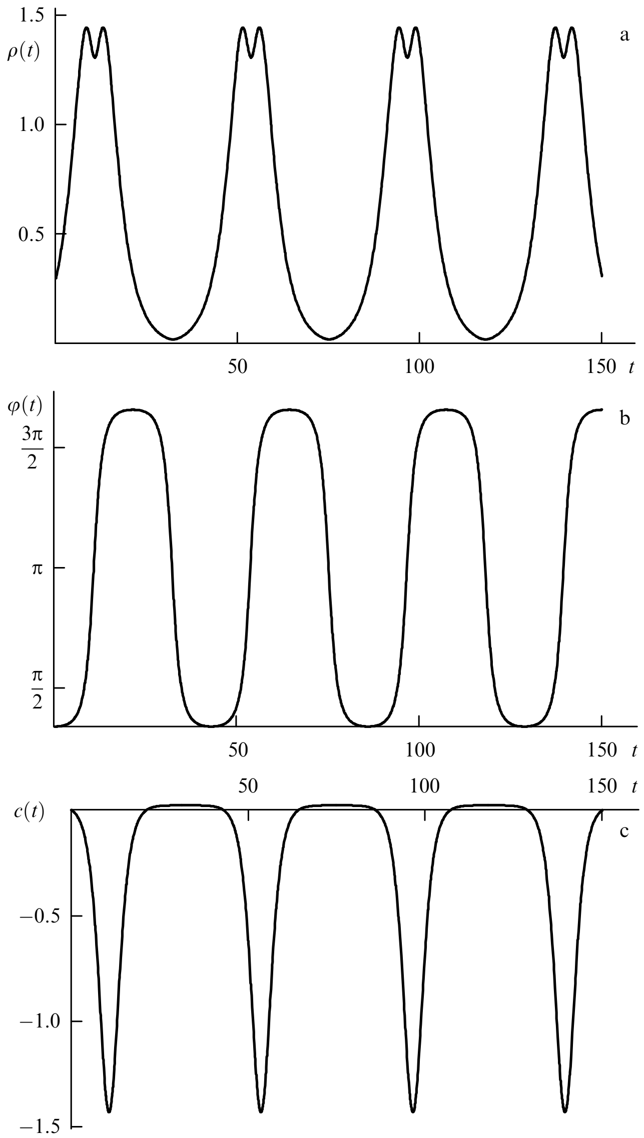

Figure 8. Time dependences of (a) $\rho(t)$, (b) $\varphi(t)$, (c) $c(t)$ for $k = 1.478$ and initial conditions $\rho(0) = 0.3$, $\varphi(0) = 1.07$, $c(0) = 0$.

account the interaction of two modes stabilizes the regime of infinite exponential perturbation growth in the linear theory. This regime is replaced with the one of stable regular oscillations.

In the case of equal boundary amplitudes $\rho_1 = \rho_2 = \rho$, system (4.33) is reduced to a system of three equations:

$$\frac{\mathrm{d}c_1}{\mathrm{d}t} = -\frac{1}{2}\,kr\rho^2 \sin\varphi\,, \quad \frac{\mathrm{d}\rho}{\mathrm{d}t} = kr_1\rho\sin\varphi\,,$$

$$\frac{\mathrm{d}\varphi}{\mathrm{d}t} = -2kr(\alpha - \beta + \beta c_1 - c_1\cos\varphi)\,. \tag{4.34}$$

Figure 8 plots the results of the numerical integration of system (4.34) with initial conditions $c(0) = 0$, $\rho(0) = 0.3$, $\varphi(0) = 1.07$. The value of $\varphi(0)$ corresponds to the phase shift of the fastest growing normal mode of linear theory with the wavenumber $k = k_{\mathrm{m}} = 1.478$. The computed behavior explicitly illustrates the presence of the oscillatory regime. As follows from the analysis, the oscillations take place in the vicinity of the equilibrium point for system (4.34), which corresponds to a secondary stationary flow. An expression

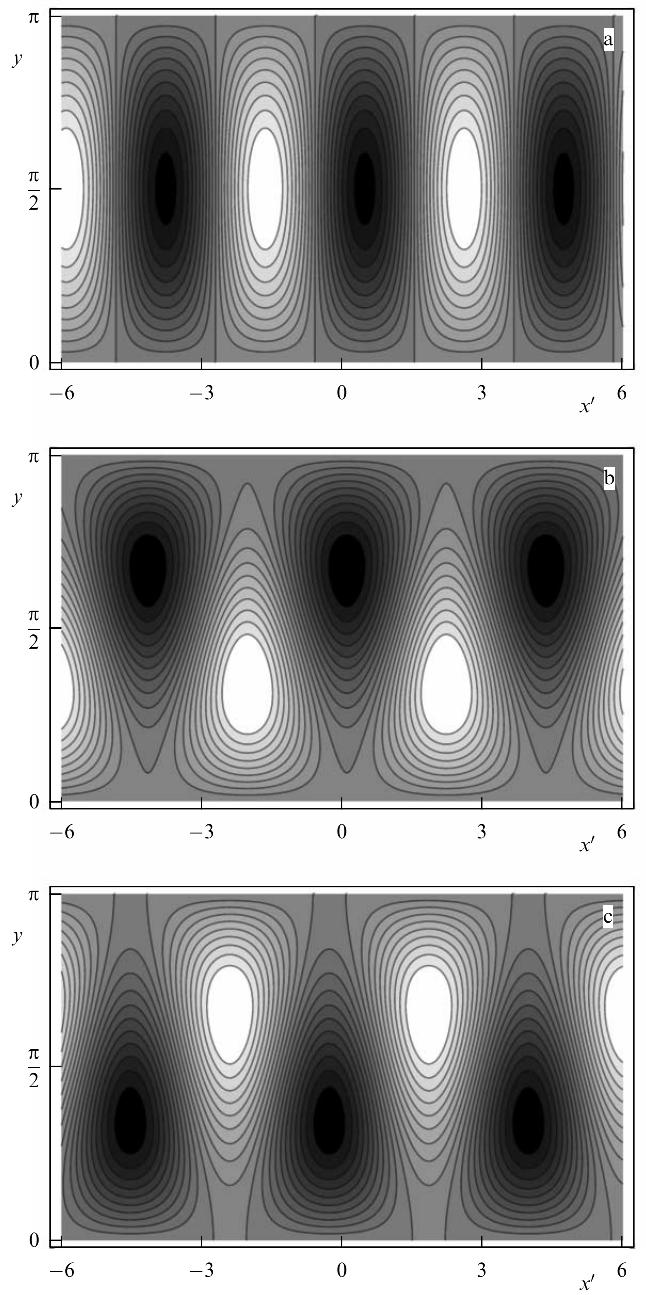

Figure 9. Isolines of a full streamfunction at the lower boundary at moments of time (a) $t = 0$, (b) $t = 10$, (c) $t = 30$. Parameters are $k = 1.478$, $\rho(0) = 0.3$, $\varphi(0) = 1.07$, $c(0) = 0$. Isolines are constructed in a moving reference frame, i.e., in the plane (x', y).

for the period of small oscillations in the vicinity of the equilibrium point obtained in Ref. [81] explicitly illustrates a strong dependence of the period on the initial conditions. For the parameters of the fastest growing mode of the linear theory, the period of small oscillations is $T = 40$ (about one month in dimensional units).

The full streamfunction ψ_* is the sum of perturbation streamfunction (4.27) and background flow $\Psi = -yz$. If the dependences $\rho(t)$, $c_1(t)$, $\varphi(t)$ are known, one can explore the structure of the full streamfunction at different moments of time at various vertical levels. Examples of isolines of ψ_* at the lower and upper boundaries at a moment of time that corresponds to a quarter of an oscillation period are given in Figs 9 and 10. As follows from the analysis, at the lower level,

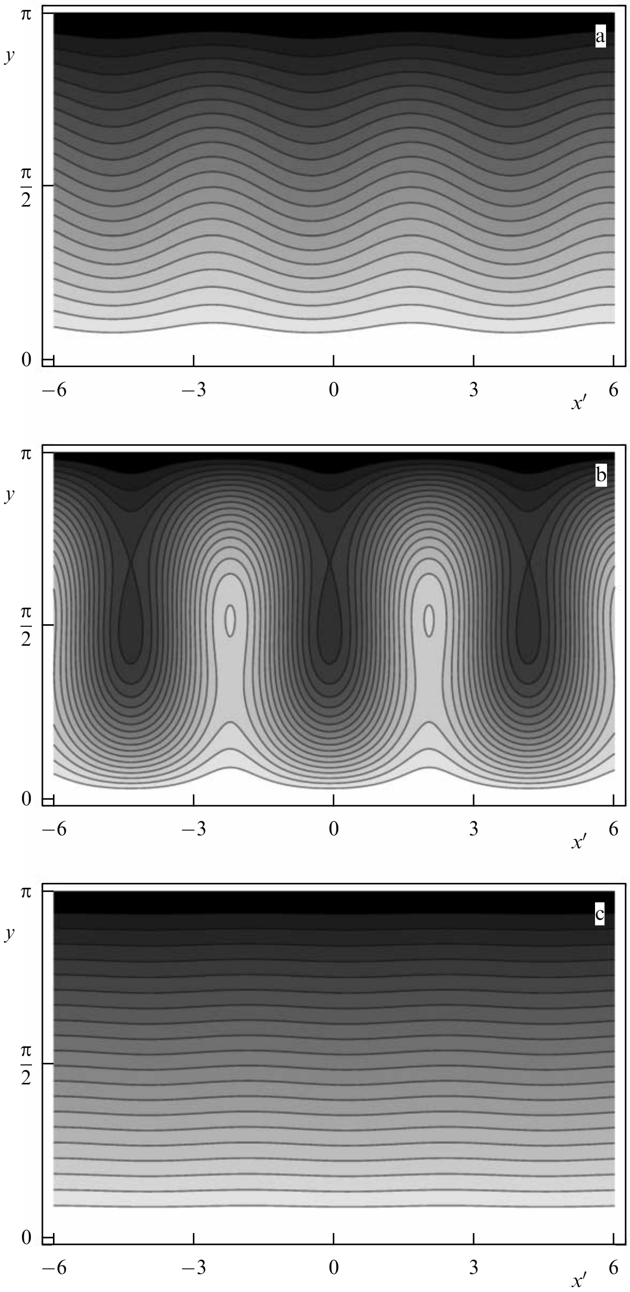

Figure 10. Same as in Fig. 9, but at the upper boundary.

there is a periodic process of intensification and decay of the system of cyclonic and anticyclonic vortices, the centers of which periodically displace toward either the right or left zonal channel boundaries. The evolution at the upper boundary reduces to a periodic process of meander formation in the zonal flow.

It should be mentioned that a regime with regular oscillations strictly periodic in time was discovered by Hide in a laboratory modeling of baroclinic instability in rotating cylindrical vessels [16, 22]. In the time that followed, attempts were made to discover a periodic regime in atmospheric observational data [82]. The observed oscillations of energy parameters in the atmosphere with a period of about 24 days and their connection to baroclinic instability are described in Ref. [83]. A theoretical description of nonlinear oscillations was first obtained by Pedlosky [3, 84–87], who considered an idealized geostrophic flow of two-layer fluid with a velocity jump between the layers. The existence of a threshold jump for the onset of instability enabled the development of a weakly nonlinear theory of baroclinic instability. According to this theory, a regime of nonlinear oscillations in flow parameters is established for small deviations from the critical value, which is associated with a periodic energy exchange between the flow and unstable baroclinic waves. Later, different theoretical aspects of baroclinic instability in two-layer flows were studied [3, 88–92]; however, it should be kept in mind that the two-layer structure is a very strong idealization if applied to Earth's atmosphere.

4.4 General linear problem statement for perturbations. Generation of baroclinic instability by vortical perturbations

Instability in the SQG model is linked to the growth of baroclinic waves — perturbations with zero PV distribution. In the general case, the generation of such waves can be associated with vortical perturbations with nonzero PV distribution. In this section, following Refs [77, 93], we briefly describe the mechanism of this generation.

For simplicity, we consider two-dimensional perturbations in the linear Eady problem. The streamfunction of such perturbations satisfies the PV conservation equation

$$\left(\frac{\partial}{\partial t} + z\,\frac{\partial}{\partial x}\right) q = 0\,, \quad q = \psi_{xx} + \psi_{zz} \tag{4.35}$$

with the boundary conditions at $z = 0,\ 1$: $(\partial/\partial t + z\partial/\partial x)\,\psi_z - \psi_x = 0$ (conditions (4.1)).

The general solution of conservation Eqn (4.35) is written in the form $q = q_{\rm i}(x - zt, z)$, where $q_{\rm i}(x, z)$ is the initial PV distribution. The description of perturbation dynamics in a flow with vertical shear is therefore reduced to solving the Poisson equation

$$\psi_{xx} + \psi_{zz} = q_{\rm i}(x - zt, z) \tag{4.36}$$

with boundary conditions (4.1). A solution of this problem is expressed as a sum of wave and vortex components

$$\psi = \psi^{(\rm v)}(x, z, t) + \psi^{(\rm w)}(x, z, t)\,. \tag{4.37}$$

Here, the vortex component $\psi^{(\rm v)}$ is defined as a solution of Eqn (4.36) with the conditions $\psi_z = 0$ at $z = 0,\ 1$ (ensuring no buoyancy at the boundaries). The wave component $\psi^{(\rm w)}$ is defined as a solution of the Laplace equation $\psi^{(\rm w)}_{xx} + \psi^{(\rm w)}_{zz} = 0$ with boundary conditions

$$z = 0,\ 1:\quad \left(\frac{\partial}{\partial t} + z\,\frac{\partial}{\partial x}\right)\psi^{(\rm w)}_z - \psi^{(\rm w)}_x = \psi^{(\rm v)}_x\,, \tag{4.38}$$

which are obtained by inserting (4.37) into the original conditions (4.1). The right-hand side of (4.38) presents a source enforcing the wave component (baroclinic waves).

An explicit expression for the vortex component can be obtained for the initial spatially periodic PV distribution

$$q_{\rm i}(x,\ z) = \Phi(z)\exp\left({\rm i}kx\right), \tag{4.39}$$

where $\Phi(z)$ describes the vertical structure. For such a distribution, the vortical component $\psi^{(\rm v)}(x,\ z,\ t) = \tilde{\psi}(z, t)\exp({\rm i}kx)$, where $\tilde{\psi}(z, t)$ is the solution to the boundary problem $\mathrm{d}^2\tilde{\psi}/\mathrm{d}z^2 - k^2\tilde{\psi} = \Phi(z)\exp(-{\rm i}kzt)$, $\tilde{\psi}_z|_{z=0,1} = 0$.

Using Green's function $G(z,\xi)$ of this problem, we get for the vortical component

$$\psi^{(\mathrm{v})} = \exp(\mathrm{i}kx)\int_0^1 G(z,\xi)\Phi(\xi)\exp(-\mathrm{i}k\xi t)\,\mathrm{d}\xi\,, \qquad (4.40)$$

$$G(z,\xi) = \frac{-1}{k\sinh k}\begin{cases}\cosh(kz)\cosh\left[k(\xi-1)\right]\,, & 0<z<\xi\,,\\ \cosh(k\xi)\cosh\left[k(z-1)\right]\,, & \xi<z<1\,.\end{cases}$$

Just as in the SQG model, the wave component with zero PV distribution is sought in the form of (4.11) that corresponds to two-dimensional perturbations ($\sin(ly)=1$). Finding from (4.40) values of $\psi^{(\mathrm{v})}$ at the boundaries, after inserting (4.11) into boundary conditions (4.38), we get an inhomogeneous variant of linear system (4.10):

$$\frac{\mathrm{i}\mathrm{d}a_1}{\mathrm{d}t} - kpa_1 + kra_2 = f_1(t)\,,$$

$$\frac{\mathrm{i}\mathrm{d}a_2}{\mathrm{d}t} - k(1-p)a_2 - kra_1 = f_2(t)\,,$$

$$f_1 = r\int_0^1 \cosh(k\xi)\Phi(\xi)\exp(-\mathrm{i}k\xi t)\,\mathrm{d}\xi\,,$$

$$f_2 = r\int_0^1 \cosh\left[k(\xi-1)\right]\Phi(\xi)\exp(-\mathrm{i}k\xi t)\,\mathrm{d}\xi\,, \qquad (4.41)$$

where $r=\sinh^{-1}k$. The right-hand sides of system (4.41) describe the sources of baroclinic wave generation by the vortical component.

An important particular case corresponds to a singular distribution $\Phi(z)=a_\mathrm{v}\delta(z-h)$, where $\delta(z)$ is the delta-function, and a_v is a real amplitude parameter. Taking into account (4.40), the vortical component for this distribution

$$\psi^{(\mathrm{v})} = a_\mathrm{v}G(z,h)\exp\left[\mathrm{i}(kx-\omega_\mathrm{v}t)\right],\quad \omega_\mathrm{v}=kh\,. \qquad (4.42)$$

Expression (4.42) (its real part) describes a neutral vortical wave with frequency ω_v and phase velocity $A_x=h$, which equals the flow velocity at $z=h$. In plasma physics, such waves are referred to as van Kampen–Case waves, or waves of continuous spectrum [94].

The propagation of vortical wave (4.42) leads to the excitation of baroclinic waves (the wave component of the solution). A description of the excitation can be found from the solution of system (4.41) with the right-hand sides $f_1=a_\mathrm{v}r\cosh(kh)\exp(-\mathrm{i}\omega_\mathrm{v}t)$, and $f_2=a_\mathrm{v}r\cosh\left[k(h-1)\right]\times\exp(-\mathrm{i}\omega_\mathrm{v}t)$. A general solution of inhomogeneous system (4.41) is the sum of the general solution of the homogeneous system (baroclinic component) and a particular solution of the inhomogeneous system (vortical component). It immediately follows that, for wavenumbers from the instability interval $0<k<k_\mathrm{b}$, the neutral vortical wave excites unstable baroclinic waves, i.e., catalyzes the development of instability.

An interesting detail is related to the dynamics of perturbations in the stable (neutral) case $k>k_\mathrm{b}$, where, in the absence of vortical perturbation, the streamfunction of the wave component represents a combination of two neutral edge Rossby waves with frequencies

$$\omega_{1,2} = \frac{k}{2}\pm\frac{1}{\sinh k}\sqrt{\alpha^2-1}\,,$$

$$\alpha=\alpha(k)=\cosh k-0.5\,k\sinh k\,. \qquad (4.43)$$

The propagation of vortical wave (4.42) can lead to the effect of resonance excitation of neutral baroclinic waves when their amplitudes grow linearly with time (in the absence of instability). This effect was described for the first time in Ref. [95], and it was studied later in Refs [73, 96, 97]. Below, we give an interpretation of resonance in terms of frequencies.

From system (4.41) taken with initial conditions $a_{1,2}(0)=0$, one finds the amplitudes $a_{1,2}(t)$ and then the streamfunctions of the wave component. The respective expression can be written as

$$\psi^{(\mathrm{w})} = a_\mathrm{v}\mu_1F_1(z)\,\frac{\exp\left[\mathrm{i}(kx-\omega_1t)\right]-\exp\left[\mathrm{i}(kx-\omega_\mathrm{v}t)\right]}{\omega_\mathrm{v}-\omega_1}$$

$$- a_\mathrm{v}\mu_2F_2(z)\,\frac{\exp\left[\mathrm{i}(kx-\omega_2t)\right]-\exp\left[\mathrm{i}(kx-\omega_\mathrm{v}t)\right]}{\omega_\mathrm{v}-\omega_2}\,, \qquad (4.44)$$

where the coefficients $\mu_{1,2}$ depend on the parameters k, h and the functions $F_{1,2}(z)$ are expressed through hyperbolic functions. Expression (4.44) is a superposition of two neutral baroclinic waves with frequencies ω_1 and ω_2 (respectively, the upper and lower edge Rossby waves) and the vortex wave with frequency ω_v.

The validity of solution (4.44) is violated in resonance cases when $\omega_\mathrm{v}=\omega_1$ or $\omega_\mathrm{v}=\omega_2$. The resonance wavenumber $k=k_\mathrm{r}$ at which the frequencies coincide is found from equations $\omega_\mathrm{v}(k)=\omega_{1,2}(k)$, which always have a solution. Taking the limit $\omega_1\to\omega_\mathrm{v}$ in (4.44), for the first resonance case we obtain the solution

$$\psi^{(\mathrm{w})} = \mathrm{i}a_\mathrm{v}\mu_1t\,F_1(z)\exp\left[\mathrm{i}(kx-\omega_\mathrm{v}t)\right]$$

$$- a_\mathrm{v}\mu_2F_2(z)\,\frac{\exp\left[\mathrm{i}(kx-\omega_2t)\right]-\exp\left[\mathrm{i}(kx-\omega_\mathrm{v}t)\right]}{\omega_\mathrm{v}-\omega_2}\,, \qquad (4.45)$$

which grows linearly with time. Thus, the resonance excitation is realized when the frequency of vortical waves (4.42) coincides with one of the frequencies of the edge Rossby waves (4.43).

It should be stressed that the effect of resonance is realized in the case of singular distribution $\Phi(z)$ of initial vorticity in the vertical direction. As shown in Ref. [93], in the case of discontinuous function $\Phi(z)$, there can be a quasi-resonance excitation of baroclinic waves with a logarithmic growth in amplitudes. The problem of optimal perturbations with nonzero initial vorticity was considered in Ref. [77].

5. Baroclinic instability of zonal periodic flow

Following Ref. [98], we consider one more example in which the development of baroclinic instability leads to the establishment of an oscillatory-in-time regime. In this example, a spatially periodic flow is considered in the framework of the SQG model with one horizontal boundary $z=0$ (the underlying surface). The streamfunction and flow velocity profile are described by the exact two-dimensional solution of the Laplace equation

$$\Psi = -\exp(-z)\cos y,\quad U=\exp(-z)\sin y\,. \qquad (5.1)$$

The dimensional form of velocity profile $U=U_0\exp(-z/H)\sin(y/L)$, $H=Lf/N$, where L is the given horizontal scale. Writing $\psi=\Psi+\psi'$ and omitting the prime further, we arrive at the Laplace equation for perturbations with the boundary condition

$$z=0:\qquad \psi_{zt}+\sin y(\psi_{xz}+\psi_x)+[\psi,\psi_z]=0\,. \qquad (5.2)$$

Two approaches were used in Ref. [98] to explore the linear stability of flows with one boundary. In the first approach, perturbations harmonic in the coordinate x with a period of $2\pi/k$ and with a period of 2π (the period of background flow) over the transverse coordinate y are considered. Such perturbations satisfying the Laplace equation can be presented as a trigonometric series

$$\psi = \exp(st)\exp(\mathrm{i}kx)\sum_{n=-\infty}^{n=+\infty}\exp(-k_n z)\exp(\mathrm{i}ny)\varphi_n\,,$$
$$k_n = \sqrt{k^2+n^2}\,,$$

where s is the increment of perturbations. Inserting this representation into the linearized form of boundary condition (5.2), one gets a dispersion relation to determine s, which contains an infinite continued fraction. Its truncation at a finite step leads to successive approximations for the increment. This approach was first proposed in Ref. [99] for exploring the stability of the Kolmogorov flow.

In the second approach, low-mode approximations of the solution are constructed using the Galerkin method. As shown in Ref. [98], both approaches lead to the same approximations for the increment. The first approximation has the form

$$s^2 = \frac{k(1-k)(k_1-1)}{2k_1}\,,\quad k_1 = \sqrt{k^2+1}\,. \tag{5.3}$$

Formula (5.3) describes the dependence of the increment squared on the wavenumber. According to (5.3), the instability takes place at $0<k<1$, and the fastest growth occurs for $k = k_{\mathrm{m}} \sim 0.7$ (Fig. 11). Thus, there exists a long-wave instability of the periodic flow with a preferred horizontal scale (in the zonal direction) about the wavelength of the background flow.

The Galerkin method can also be conveniently applied to describe the nonlinear dynamics of perturbations. The maximally truncated approximation of the nonlinear solution, which consist of the expansion in three basis functions, $f_1 = \sin y, f_2 = \cos y, f_3 = 1$, has the following form:

$$\psi = A(x,z,t)\sin y + B(z,t)\cos y + C(x,z,t)\,. \tag{5.4}$$

By virtue of the Laplace equation, the coefficients of expansion satisfy the equations

$$A_{xx}+A_{zz}-A=0\,,\quad B_{zz}-B=0\,,\quad C_{xx}+C_{zz}=0\,. \tag{5.5}$$

Inserting (5.4) into boundary condition (5.2) and subsequently taking account of orthogonality to the basis functions leads to the nonlinear system of equations at the boundary

$$z=0:\quad A_{zt}+(B+1)C_{xz}+(1-B_z)C_x=0\,, \tag{5.6a}$$
$$C_{zt}+\frac{1}{2}\left[(B+1)A_z+(1-B_z)A_x\right]=0\,, \tag{5.6b}$$
$$B_{zt}+C_xA_z-AC_{xz}=0\,. \tag{5.6c}$$

A linearized variant of system (5.6) reduces to a system of equations that corresponds to the linear stability theory.

To construct solutions to the nonlinear problem which are periodic in coordinate x, one also uses a variant of the Galerkin method. Approximate solutions of Eqns (5.5) and

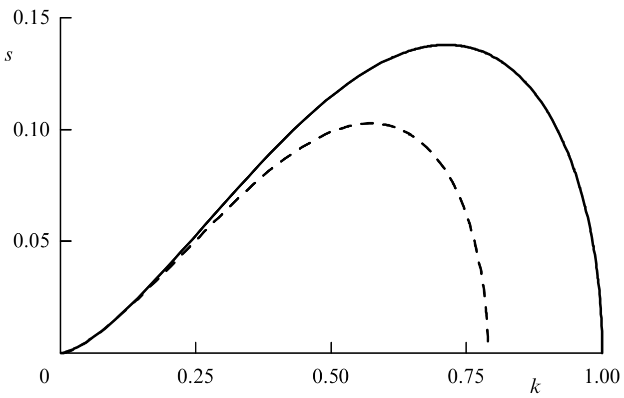

Figure 11. Dependence of instability increment on wavenumber for the first (solid line) and second (dashed line) approximations of the Galerkin method.

(5.6) are sought in the form

$$A=a(t)\exp(-kz)\sin(kx)\,,\quad C=c(t)\exp(-kz)\cos(kx)\,,$$
$$B=b(t)\exp(-z)\,. \tag{5.7}$$

For the selected form of the solution, Eqn (5.5) is exactly satisfied, and boundary conditions (5.6a) and (5.6b) are reduced to a nonlinear ordinary differential equation without any approximation. Further, the operation of horizontal averaging over the horizontal coordinate

$$\overline{\varphi}^{\,x} = \lim \frac{1}{L}\int_0^L \varphi\,\mathrm{d}x\,,\quad L=\frac{2\pi}{k}$$

is introduced and, for the selected form of the solution, one computes the averaged nonlinear term of equation (5.6c) $\overline{(C_xA_z - AC_{xz})}^{\,x} = (1/2)k(k_1-k)ac$. From the last expression, it follows that an approximate solution for the coefficient B should depend only on time and the vertical coordinate, which is taken into account in expansion (5.4). Denoting $\tilde{b} = b+1$, we obtain a system of ordinary differential equations for the description of nonlinear dynamics of perturbation:

$$\frac{\mathrm{d}a}{\mathrm{d}t}+\alpha\tilde{b}c=0\,,\quad \frac{\mathrm{d}c}{\mathrm{d}t}+\gamma\tilde{b}a=0\,,\quad \frac{\mathrm{d}\tilde{b}}{\mathrm{d}t}-\beta ac=0\,. \tag{5.8}$$

The coefficients of the system

$$\alpha=\frac{k(1-k)}{k_1}\,,\quad \gamma=\frac{k_1-1}{2}\,,\quad \beta=\frac{k(k_1-k)}{2} \tag{5.9}$$

depend on the perturbation wavenumber k. For the interval $0<k<1$ of unstable wavenumbers, $\alpha,\ \beta, \gamma > 0$.

Nonlinear system (5.8) is analogous to the system describing the motion of a symmetric top in mechanics (or fluid motion in an ellipsoidal cavity). The respective theory is presented in detail in Ref. [80]. Formally mathematically, with respect to $a, \tilde{b}, c$, system (5.8) has two stable equilibrium states $(a,0,0)$, and $(0,0,c)$ and one unstable state $(0,\tilde{b},0)$. An important role belongs to the conservation laws following from (5.8),

$$\gamma a^2-\alpha c^2=I_1=\mathrm{const}\,,\quad \beta a^2+\alpha\tilde{b}^2=I_2=\mathrm{const}\,. \tag{5.10}$$

From the second law, it directly follows that, in contrast to the solution to the linear problem, all solutions are bounded with respect to time.

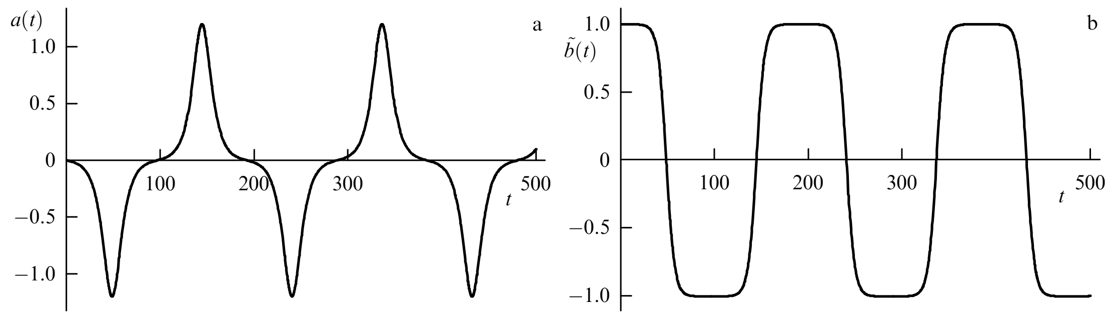

Figure 12. Results of numerical integration of system (5.8) for variables $a(t)$ (a) and $\tilde{b}(t)$ (b).

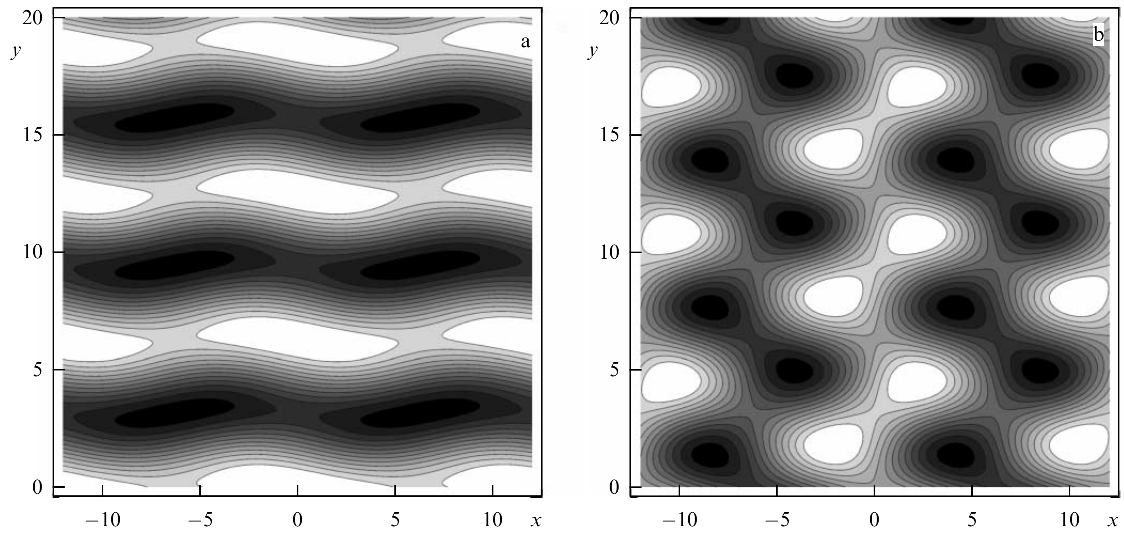

Figure 13. Isolines of full streamfunction (5.12) for moments of time (a) $t = 30$ and (b) $t = 50$.

Taking account of first integrals (5.10), solutions of system (5.8) can be expressed in terms of elliptical functions. These solutions describe nonlinear oscillations with a period depending on the initial amplitude (nonisochrone oscillations). For the problem with initial conditions $a(0) = 0$, $b(0) = 0$, $c(0) = c_0$, the period of oscillations is given by the formula

$$T = \frac{4}{n} K(m), \quad n^2 = \alpha(\gamma + \beta c_0^2), \quad m^2 = \left(1 + \frac{\beta}{\gamma} c_0^2\right)^{-1}, \tag{5.11}$$

where $K(m)$ is a complete elliptic integral of the first kind,

$$K(m) = \int_0^{\pi/2} \frac{\mathrm{d}\theta}{\sqrt{1 - m^2 \sin^2\theta}}.$$

From (5.11), it follows that the period of oscillations increases if the initial amplitude c_0 is reduced. Results of a numerical integration of system (5.8) for the value $c_0 = 0.01$ (Fig. 12) clearly illustrate how the stage of initial exponential perturbation growth is replaced by the stage of stable nondecaying oscillations.

Using numerical computations, one can construct contour plots of full streamfunction $\psi_* = \Psi + \psi'$ at different moments of time:

$$\psi_* = \big(b(t) + 1\big) \exp(-z) \cos y + a(t) \exp(-k_1 z) \times \sin(kx) \sin y + c(t) \exp(-kz) \cos(kx). \tag{5.12}$$

The respective patterns are repeated with period $T_1 = T/2$. As an example, Fig. 13 shows the streamlines at the level $z = 0$ at the dimensionless moments of time $t = 30$ and $t = 50$ for the parameters $c_0 = 0.01$ and $k = 0.5$. As can be seen, when the instability is evolving, a system of isolated vortex structures is formed in the periodic flow. It is most clearly seen at the moment $t = 50$, which corresponds to half the period $T_1 \sim 100$. At this moment, a vortex ensemble forms, which fully destroys the zonal structure of primary flow. As time progresses, the flow returns to its unperturbed zonal state (at moment $t = 100$), and this process is repeated periodically. The life cycle of nonlinear perturbations presents a periodic process of birth and decay of a system of closed vortical structures in the flow.

It is important that approximate solution (5.12) exactly satisfies the energy conservation laws of SQG model (3.4) and (3.5). Indeed, direct computation of energies (taking squares, integration, and averaging) for solution (5.12) gives

$$V = \frac{1}{2}\,\overline{\psi_z^2} = \frac{1}{4}\left(\tilde{b}^2 + k^2 c^2 + \frac{1}{2} k_1^2 a^2\right),$$

$$E = \frac{1}{2}\int_0^\infty \overline{(\psi_x^2 + \psi_y^2 + \psi_z^2)}\,\mathrm{d}z = \frac{1}{4}\left(\tilde{b}^2 + kc^2 + \frac{1}{2} k_1 a^2\right)$$

(the star is omitted). Taking into account expressions for coefficients (5.9) and first integrals (5.10), it can be directly seen that

$$V = \frac{I_2 - k^2 I_1}{2\alpha}, \quad E = \frac{I_2 - kI_1}{2\alpha}. \tag{5.13}$$

Since an arbitrary function of independent first integrals I_1 and I_2 is also a first integral, (5.13) implies the conservation of energies V and E, and clarifies the physical sense of integrals I_1 and I_2, which (more precisely their linear combinations) reflect the conservation of surface potential and full energies. Namely these conservation laws are responsible for the onset of oscillations in a system without dissipation. We note that numerical integration of the full system of equations of the SQG model carried out in Ref. [98] confirmed the existence of the oscillatory regime in the stability problem.

We also stress that the periodic flow considered here can be seen as a geophysical prototype of periodical flows in atmospheres of giant planets [100] or the multiple jets recently discovered in the southern ocean [101,102].

Observational data show that multiple jets meander, coalesce, depart from each other, and vary in intensity. This testifies to the internal dynamical instability of such flows and agrees with the results of the analysis performed here.

6. Discrete variant of SQG model and baroclinic instability of jet flows

Exploring baroclinic instability becomes much simpler in a discrete SQG model with two vertical internal levels. Zonal flows in this model are initiated by given distributions of buoyancy at the boundaries of the atmospheric layer (the underlying surface and tropopause). Piecewise-constant buoyancy distributions in the form of a step or localized rectangle (analogs of frontal zones) induce, respectively, an isolated jet or a system of two oppositely directed jets in the upper half of the atmospheric layer, with an oppositely directed flow in the lower half. These flows are analogs of jet flows (3.10) and (3.11) in the continuous model. In Sections 6.1–6.3, the linear stability theory for such flows is presented, the interval of unstable wavenumbers is given, and analytic expressions for instability increments are found.

6.1 Discrete model with two vertical levels and the statement of stability problems

To construct an SQG model with two levels in the vertical direction, Laplace Eqn (3.3) is written in the form $\Delta\psi + \theta_z = 0$, where $\theta = \psi_z$, $\Delta\psi = \psi_{xx} + \psi_{yy}$. Interval $[0, 1]$ of the z-axis is split into four equal intervals with length $h = 1/4$. The notation $\psi_1 = \psi|_{z=h}$, $\psi_2 = \psi|_{z=3h}$, $\theta_{\rm m} = \theta|_{z=2h}$ is introduced, and central differences are used to approximate the derivative θ_z. Then, for levels $z = h$ and $z = 3h$, the Laplace equation leads to the respective equations

$$\Delta\psi_1 + \frac{\theta_{\rm m} - \theta_{\rm bott}}{2h} = 0, \quad \Delta\psi_2 + \frac{\theta_{\rm top} - \theta_{\rm m}}{2h} = 0, \tag{6.1}$$

where $\theta_{\rm top}$ and $\theta_{\rm bott}$ are the values of buoyancy at the upper and lower boundaries. Assuming further $\theta_{\rm m} = (\psi_2 - \psi_1)/(2h)$, from (6.1) we get

$$\Delta\psi_1 + \frac{\lambda^2}{2}(\psi_2 - \psi_1) = \frac{\theta_{\rm bott}}{2h}, \qquad \Delta\psi_2 - \frac{\lambda^2}{2}(\psi_2 - \psi_1) = -\frac{\theta_{\rm top}}{2h}, \tag{6.2}$$

which connect the distributions of the streamfunction with boundary buoyancy distributions. Here and below, we denote $\lambda^2 = 1/(2h^2) = 8$.

In the framework of the SQG model, conditions (3.2) should hold at the horizontal boundaries $z = 0$ and $z = 1$: $D\theta_{\rm bott}/Dt = 0$, $D\theta_{\rm top}/Dt = 0$. We carry these conditions on the levels $z = h$ and $z = 3h$, and, taking account of (6.2), obtain the equations

$$q_{1t} + [\psi_1, q_1] = 0, \quad q_{2t} + [\psi_2, q_2] = 0, \qquad q_{1,2} = \Delta\psi_{1,2} \pm \frac{\lambda^2}{2}(\psi_2 - \psi_1), \tag{6.3}$$

which formally coincide with equations of the two-level quasigeostrophic Phillips model [103] obtained by discretizing the general PV conservation Eqn (3.1). Its difference from the classical Phillips model lies in the physical interpretation of variables. The distributions of PV at the upper and lower model levels of model (6.3) now have the sense of doubled buoyancy distributions at the upper and lower boundaries of the atmospheric layer.

The streamfunction of stationary zonal flows (depending on coordinate y) is found from Eqns (6.2). These equations are reduced to two isolated equations,

$$\tilde{\Psi}_{yy} - \lambda^2\tilde{\Psi} = -(\Theta_{\rm bott} + \Theta_{\rm top}), \quad \bar{\Psi}_{yy} = \Theta_{\rm bott} - \Theta_{\rm top}, \tag{6.4}$$

on the barotropic $\bar{\Psi} = (\Psi_1 + \Psi_2)/2$ and baroclinic $\tilde{\Psi} = (\Psi_2 - \Psi_1)/2$ streamfunction components. Here, $\Theta_{\rm bott}(y)$, $\Theta_{\rm top}(y)$ are the given buoyancy distributions at boundaries $z = 0$, $z = 1$, and all variables of zonal flows are denoted with capital letters. In the case $\Theta_{\rm top} = \Theta_{\rm bott}$, the barotropic component $\bar{\Psi} = 0$, and the velocity field at two levels $(U_1, U_2) = (-U, U)$, $U = -\tilde{\Psi}_y$, where $U_{yy} - \lambda^2 U = 2{\rm d}\Theta_{\rm bott}/{\rm d}y$. Thus, just as in the continuous model, equal boundary buoyancy distributions induce oppositely directed flows at the upper and lower levels. Such flows have a well expressed velocity shear and are therefore the most interesting from the viewpoint of stability.

To explore the stability of zonal flows, we assume $\psi_1 = \Psi_1 + \psi_1'$, $\psi_2 = \Psi_2 + \psi_2'$ and study the linearized Eqns (6.3):

$$\left(\frac{\partial}{\partial t} + U_1\frac{\partial}{\partial x}\right)q_1' + 2\frac{{\rm d}\Theta_{\rm bott}}{{\rm d}y}\frac{\partial\psi_1'}{\partial x} = 0,$$

$$\left(\frac{\partial}{\partial t} + U_2\frac{\partial}{\partial x}\right)q_2' - 2\frac{{\rm d}\Theta_{\rm top}}{{\rm d}y}\frac{\partial\psi_2'}{\partial x} = 0.$$

If $\Theta_{\rm top} = \Theta_{\rm bott}$, this system transforms into the following:

$$\frac{\partial}{\partial t}(\Delta\theta - \lambda^2\theta) + U\frac{\partial}{\partial x}\Delta\sigma - 2\frac{{\rm d}\Theta_{\rm bott}}{{\rm d}y}\frac{\partial\sigma}{\partial x} = 0, \qquad \frac{\partial}{\partial t}\Delta\sigma + U\frac{\partial}{\partial x}(\Delta\theta - \lambda^2\theta) - 2\frac{{\rm d}\Theta_{\rm bott}}{{\rm d}y}\frac{\partial\theta}{\partial x} = 0. \tag{6.5}$$

Here, we introduced variables $\sigma = (1/2)(\psi_1' + \psi_2')$, $\theta = (1/2)(\psi_2' - \psi_1')$ in terms of which the streamfunctions of perturbations $\psi_{1,2}' = \sigma \mp \theta$ at different levels are easily expressed.

In the framework of system (6.5), it is straightforward to obtain a solution to the discrete variant of the Eady problem that corresponds to linear distributions $\Theta_{\rm bott} = \Theta_{\rm top} = -y$, and the velocity field at two levels is $(U_1, U_2) = (-U, U)$, where $U = 1/4$. In this case, system (6.5) is reduced to a single equation

$$\frac{\partial^2}{\partial t^2}(\Delta\theta - 8\theta) - \frac{1}{16}\frac{\partial^2}{\partial x^2}(\Delta\theta + 8\theta) = 0\,,$$

which has exponentially growing solutions $\theta = \theta_0 \exp(st) \times \exp\left[i(kx + ly)\right]$ with the squared increment

$$s^2 = \frac{k^2}{16}\frac{8 - \mu^2}{8 + \mu^2}\,, \quad \mu^2 = k^2 + l^2\,. \tag{6.6}$$

A comparison of increment (6.6) with that of the continuous model (see Fig. 3) shows that the error in finding the right boundary of the interval of unstable wavenumbers does not exceed 16%, i.e., the two-level model turns out to be quite accurate. We note that, in our recent study [104], a general method for constructing multi-level difference approximations of the SQG model equation is developed. As applied to the Eady problem, it is shown that, as the number of levels is increased, the relative errors rapidly decrease, in particular, the error of the four-level model no longer exceeds 3.6%

6.2 Instability of an isolated jet flow

This flow is induced by a piecewise-constant distribution of buoyancy $\Theta_{\rm bott}(y) = a/2$, $y < 0$, $\Theta_{\rm bott}(y) = -a/2$, $y > 0$, or $\Theta_{\rm bott}(y) = a(1/2 - H(y))$, where $H(y)$ is the Heaviside function. To construct this distribution from the first Eqn (6.4), one finds the profile of jet flow velocity at the upper level (Fig. 14)

$$U_2 = U = U_0 \exp\left(-\lambda|y|\right), \quad U_0 = \frac{a}{\lambda}\,. \tag{6.7}$$

At the lower level, there is an oppositely directed flow. Note that profile (6.7) is close to the observed profile of upper tropospheric jet flows [58].

The linear stability of flow (6.7) is studied in the framework of system of equations (6.5). Since, for this flow, $d\Theta_{\rm bott}/dy = -a\delta(y)$, where $\delta(y)$ is the delta function, this system is satisfied by solutions for which at $y \neq 0$

$$\Delta\theta - \lambda^2\theta = 0\,, \quad \Delta\sigma = 0\,. \tag{6.8}$$

Solutions of Eqns (6.8) periodic over the coordinate x which decay at $|y| \to \infty$ can be written in the form

$$\theta = -\frac{1}{2k_1} A(t) \exp\left(-k_1|y|\right)\cos(kx)\,,$$
$$\sigma = \frac{1}{2k} B(t) \exp\left(-k|y|\right)\sin(kx)\,, \tag{6.9}$$

where k is the wavenumber; here and below, we use the notation $k_1 = (k^2 + \lambda^2)^{1/2}$. The amplitude functions $A(t)$, $B(t)$ entering (6.9) are found from the conditions on jumps of normal derivatives at $y = 0$. Taking into account $d\Theta_{\rm bott}/dy = -a\delta(y)$, after integration of Eqns (6.5) over a small vicinity of $y = 0$, we obtain

$$\frac{\partial}{\partial t}\{\theta_y\} + U_0\frac{\partial}{\partial x}\{\sigma_y\} + 2a\frac{\partial\sigma}{\partial x} = 0\,,$$
$$\frac{\partial}{\partial t}\{\sigma_y\} + U_0\frac{\partial}{\partial x}\{\theta_y\} + 2a\frac{\partial\theta}{\partial x} = 0\,. \tag{6.10}$$

Here, curly brackets denote the jump of derivative $\{\theta_y\} = \theta_y(y + 0) - \theta_y(y - 0)$.

It can be easily verified that, for solution (6.9), $\{\theta_y\} = A(t)\cos(kx)$, $\{\sigma_y\} = B(t)\sin(kx)$. Inserting these last expressions into (6.10), taking account of $a = \lambda U_0$, we obtain a system of linear differential equations for the amplitudes $A_t = U_0(\lambda - k)B$, $B_t = (k/k_1)U_0(k_1 - \lambda)A$. This system has solutions of the form $A = A_0\exp(st)$, $B = B_0\exp(st)$, where the increment squared

$$s^2 = U_0^2\left(\frac{k}{k_1}\right)(\lambda - k)(k_1 - \lambda)\,. \tag{6.11}$$

Since $k_1 = \sqrt{k^2 + \lambda^2} > \lambda$, from (6.11) it follows that, for wavenumbers from the interval $0 < k < \lambda$, $\lambda = \sqrt{8} = 2\sqrt{2}$, an unstable perturbation exists, i.e., flow (6.7) is unstable. In dimensional variables, the right boundary of the instability interval corresponds to the wavelength $(2\pi/\lambda)L_R = 2221.4$ km (for $L_R = 1000$ km). The maximum increment (Fig. 15) occurs for the wavenumber $k = k_m = 2.01$ and the wavelength $(2\pi/k_m)L_R = 3118.2$ km, and the characteristic e-folding time for $U_0 = 1$ is $T_0/\gamma_{\max} = 50.45$ h (about two days).

Taking (6.9) into account, one can obtain an expression for the streamfunction of growing perturbation at the upper level $\psi_2' = \theta + \sigma$. This expression is transformed into the following one:

$$\psi_2' = -\frac{A_0\exp(\gamma t)}{2k_1}\left[\exp\left(-k_1|y|\right)\cos(kx) + \beta\exp\left(-k|y|\right)\sin(kx)\right]\,, \tag{6.12}$$

where $\beta = \sqrt{k_1(k_1 - \lambda)/k(\lambda - k)}$. The contour plot of streamfunction (6.12) for $k = k_m$ (the fastest growing mode) is given in Fig. 16a.

We note that the isolines are sloping against the direction of flow. Only for such a slope can a growing perturbation

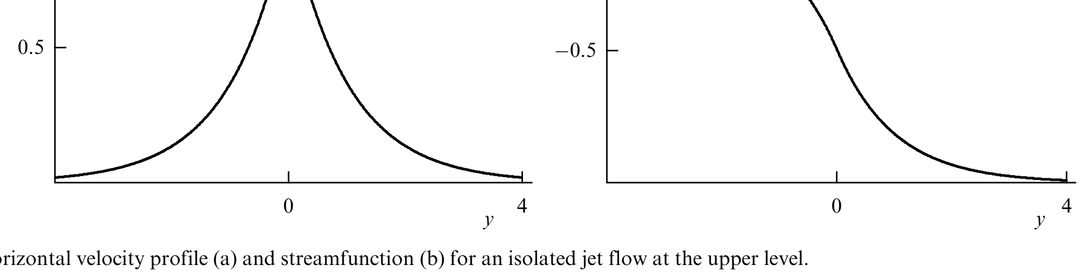

Figure 14. Horizontal velocity profile (a) and streamfunction (b) for an isolated jet flow at the upper level.

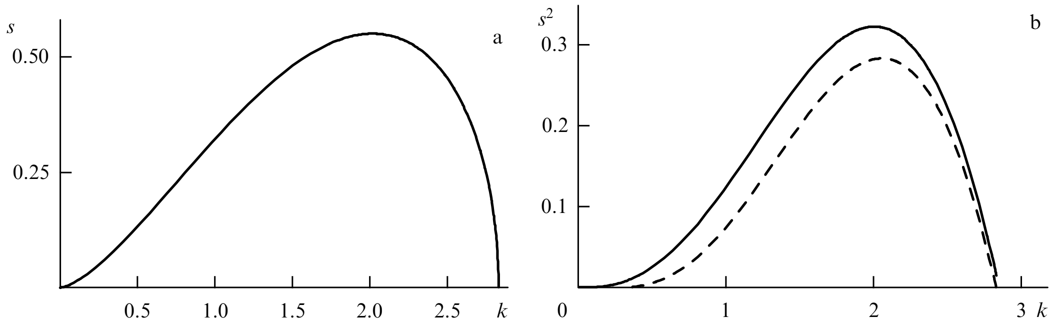

Figure 15. Dependence of instability increment on wavenumber for an isolated jet flow (a) and a system of two opposite jet flows (b).

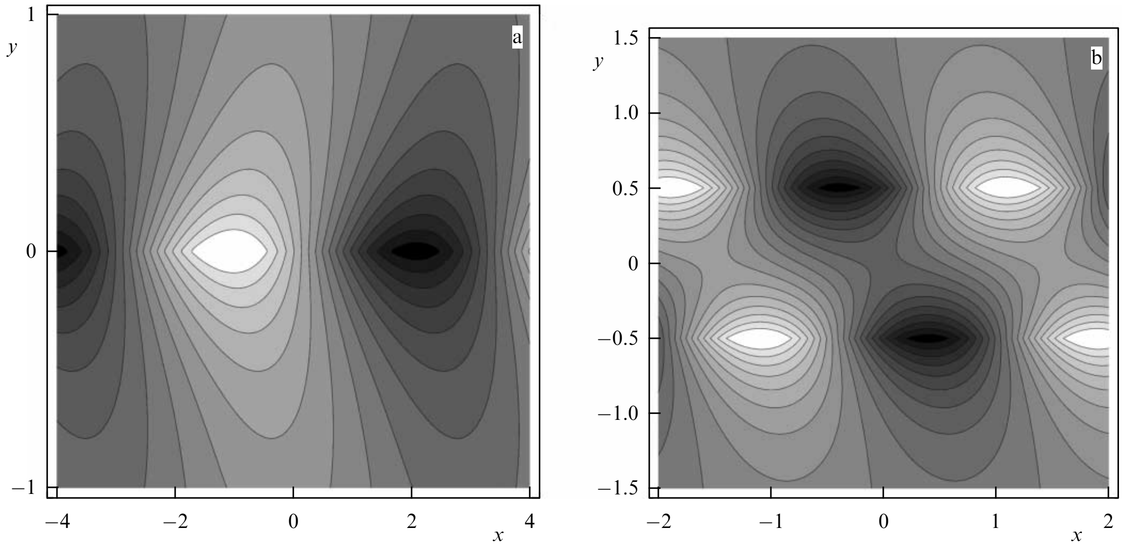

Figure 16. Perturbation streamfunction at the upper level for an isolated jet flow (a) and a system of two opposite jets (b).

extract energy from the energy of the jet flow. The perturbation streamfunction at the lower level has a similar shape, but with an opposite slope of isolines.

6.3 Instability of a system of two opposite jets

A system of two opposite jets is induced by a piecewise-constant buoyancy distribution $\Theta_{\text{bott}} = a$, $|y| < b$, $\Theta_{\text{bott}} = 0$, $|y| > b$. For this distribution, from the first equation in (6.4), we find the upper level velocity profile

$$U_2 = -\Psi_{2y} = U_0 \begin{cases} \dfrac{\sinh(\lambda y)}{\sinh(\lambda b)}\,, & |y| < b\,, \\ \operatorname{sgn} y \exp\left[-\lambda\big(|y| - b\big)\right], & |y| > b\,, \end{cases}$$

$$U_0 = \frac{a}{\varphi(b)}\,, \quad \varphi(b) = \frac{1}{2}\,\lambda\left[1 + \coth(\lambda b)\right], \tag{6.13}$$

which describes a system of two opposite jets with distance $2b$ between their axes and axial velocity U_0 (Fig. 17). An analogous system of jets is formed at the lower level, but it has the opposite direction.

The stability of flow (6.13) is explored in the framework of system (6.5). Taking account of $\mathrm{d}\Theta_{\text{bott}}/\mathrm{d}y = a[\delta(y+b) - \delta(y-b)]$, system (6.5) is satisfied by perturbations for which Eqns (6.8) are valid at $y \neq \pm b$. Solutions of these equations, which are periodic over the coordinate x and decay at $|y| \to \infty$, can be written in the real form as

$$\begin{aligned} \theta = &-\frac{1}{2}\,k_1\left[A_1(t)\exp\big(-k_1|y-b|\big)\right. \\ &\left. + A_2(t)\exp\big(-k_1|y+b|\big)\right]\cos(kx)\,, \\ \sigma = &-\frac{1}{2k}\left[B_1(t)\exp\big(-k|y-b|\big)\right. \\ &\left. + B_2(t)\exp\big(-k|y+b|\big)\right]\sin(kx)\,, \end{aligned} \tag{6.14}$$

where $k_1^2 = k^2 + \lambda^2$. Amplitudes $A_{1,2}(t)$ and $B_{1,2}(t)$ entering (6.14) are found from the system of equations on jumps of normal derivatives at $y = \pm b$. For solutions (6.14), the jumps of derivatives are $y = \pm b$: $\{\theta_y\} = A_{1,2}\sin(kx)$, $\{\sigma_y\} = B_{1,2}\cos(kx)$. Inserting these expressions into the system of equations for the jumps leads to a system of four linear differential equations for the amplitudes. Taking into account $a = U_0\varphi(b)$, system (6.14) can be cast into a matrix form,

$$\frac{\mathrm{d}\mathbf{a}}{\mathrm{d}t} = -U_0 P_1 \mathbf{b}\,, \quad \frac{\mathrm{d}\mathbf{b}}{\mathrm{d}t} = U_0\,\frac{k}{k_1}\,P_2\mathbf{a}\,. \tag{6.15}$$

Here, we use the column vectors $\mathbf{a} = (A_1, A_2)^{\mathrm{T}}$ and $\mathbf{b} = (B_1, B_2)^{\mathrm{T}}$ and the matrices

$$P_1 = \begin{pmatrix} k - \varphi(b) & -\varphi(b)\exp(-2kb) \\ \varphi(b)\exp(-2kb) & \varphi(b) - k \end{pmatrix},$$
$$P_2 = \begin{pmatrix} k_1 - \varphi(b) & -\varphi(b)\exp(-2k_1 b) \\ \varphi(b)\exp(-2k_1 b) & \varphi(b) - k_1 \end{pmatrix}. \tag{6.16}$$

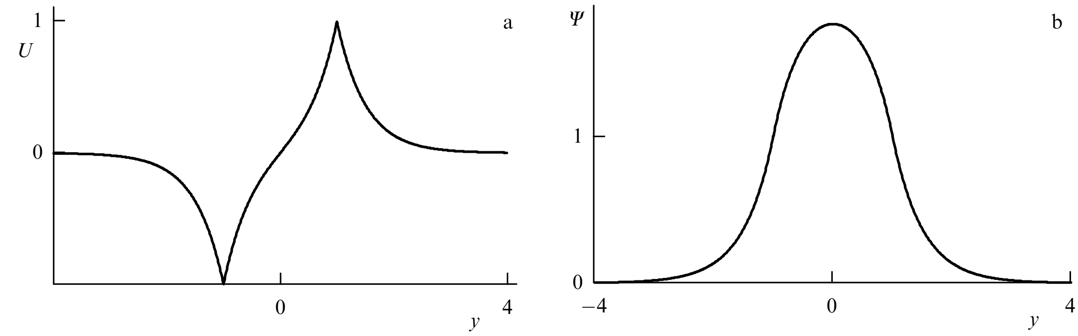

Figure 17. Horizontal profiles of velocity (a) and streamfunction (b) at the upper level for a system of jet flows.

The study of stability is therefore reduced to an analysis of the behavior of system (6.15).

System (6.15) has solutions in the form $\mathbf{a} = \exp(st)\,\mathbf{a}_0$, $\mathbf{b} = \exp(st)\,\mathbf{b}_0$, where the vectors $\mathbf{a}_0$, $\mathbf{b}_0$ satisfy a homogeneous system of algebraic equations $s\mathbf{a}_0 = -U_0 P_1 \mathbf{b}_0$, $s\mathbf{b}_0 = U_0(k/k_1)P_2\mathbf{a}_0$. Denoting $\tilde{s}^2 = (s/U_0)^2(k_1/k)$, one can reduce this system to one vector equation $(P_1P_2 + \tilde{s}^2E)\,\mathbf{a}_0 = 0$, where E is an identity matrix. The solvability condition for the last equation gives an equation on the square of the normalized increment $\tilde{s}^2$,

$$\det(P_1P_2 + \tilde{s}^2E) = 0\,. \tag{6.17}$$

Equation (6.17) is an analog of the problem dealing with the eigenvalues of matrix P_1P_2 and its eigenvector $\mathbf{a}_0$.

As follows from an analysis of the roots of Eqn (6.17), there are two growing eigenmodes. The squares of increments for these modes are given by the expressions

$$\begin{aligned} s^2 &= U_0^2\left(\frac{k}{k_1}\right)\eta_1(k)\eta_2(k)\,,\\ s^2 &= U_0^2\left(\frac{k}{k_1}\right)\mu_1(k)\mu_2(k)\,. \end{aligned} \tag{6.18}$$

For the first mode, $\eta_1(k) = \varphi(b)[1+\exp(-2kb)] - k$, $\eta_2(k) = k_1 - \varphi(b)[1-\exp(-2k_1b)]$. For the second one, $\mu_1(k) = \varphi(b)[1+\exp(-2k_1b)] - k_1$, $\mu_2(k) = k - \varphi(b)[1-\exp(-2kb)]$. The first mode grows for the wavenumber values $0 < k < k_b$, where k_b is the root of the equation $\eta_1(k) = 0$, i.e., the equation $k = \varphi(b)[1+\exp(-2kb)]$. The last equation has the structure of the equation that arises in the classical Rayleigh problem on the instability of a free shear layer. The expression $k_b = \varphi(b)[1+\exp(-2b\varphi(b))]$ provides a good approximation of the root in a wide range of parameter b. For large values of b, the second mode is a growing one for $0 < k < \lambda$. As follows from Fig. 15, which plots the dependence of the increment on the wave number, the first mode (solid line) grows faster than the second one (dashed line).

Using (6.14) and the expressions for eigenvectors $\mathbf{a}_0$, one can obtain expressions for the perturbation of streamfunction $\psi_2' = \theta + \sigma$ at the upper level. The main difference for the modes is related to the slope of isolines of ψ_2' in the region $|y| > b$. While the first mode has an optimal slope against the flow (Fig. 16b), the isolines slope along the flow for the second mode. Note that the first and second modes are analogs of sinusoidal and varicose modes of instability for two-dimensional flows of a homogeneous fluid [105].

7. Baroclinic instability in the presence of the beta effect

Everywhere above, we dealt with baroclinic instability without accounting for the variable Coriolis parameter (beta effect). This effect was taken into account by Charney [12], who considered the stability of a flow with constant vertical shear Λ in a semi-infinite atmosphere (the Charney problem). The stability is explored in the framework of linearized PV Eqn (2.4), the solution of which is sought in the form of normal mode $\psi = \Phi(z)\exp[ik(x-ct)]\sin(ly)$, $l = \pi n/L_*$. In dimensionless variables, the complex phase velocity $c = c_r + ic_i$ is found from the solution to the spectral problem ($\kappa^2 = k^2 + l^2$)

$$\begin{aligned} &(z-c)(\Phi_{yy} - \kappa^2\Phi) + \Pi_y\Phi = 0\,,\\ &z = 0:\; c\Phi_z + \Phi = 0\,, \end{aligned} \tag{7.1}$$

complemented by the condition that $\Phi(z)$ be finite as $z \to \infty$. Compared to the Eady problem, the presence of the background gradient of potential vorticity $\Pi_y = \beta$ in (7.1) substantially complicates the spectral problem analysis because of the appearance of critical levels (singular points) that correspond to $z = c$. The representation of the exact solution to (7.1) in terms of hypergeometrical functions shows that there is a countable number of neutral modes that are regular at critical levels. These modes correspond to some values of wavenumbers $k = k_i$. In a classical situation (for two-dimensional shear flows), the values $k = k_i$ separate intervals of stable and unstable wavenumbers. Miles established a subtle result [106] that unstable modes ($c_i > 0$) of problem (7.1) are present both left and right of each $k = k_i$. Taking into account the beta effect, therefore, leads to the appearance of a countable set of unstable normal modes. This is the main distinction from the Eady problem which has only two modes (growth and decay).

A numerical analysis of the spectrum of (7.1), together with an analysis of the structure of the fastest growing mode, was carried out in Refs [107, 108]. The increment of such a two-dimensional mode ($l = 0$) is given by the expression $s_m = 0.286(f/N)\Lambda$, which is practically very close to the analogous expression for the Eady problem $s_m = 0.31(f/N)\Lambda$ (see Section 3). Constants entering these expressions differ by less than 8%. The wavelength of the most unstable mode in the Charney problem is also close to that in the Eady problem (even though the latter has no specific vertical scale). A detailed comparison of solutions to the two problems is given by Gill [60].

Studying the beta effect influence on stability becomes substantially simpler in the framework of quasigeostrophic models which are discrete in the vertical direction. Such models filter weakly unstable modes with small vertical scales and allow an explicit description of the role of the nonzero PV gradient induced by the beta effect. In the framework of the two-level model, this was done for the first time in Ref. [103], which triggered numerous publications on studies of baroclinic instability in the presence of the beta effect (a review was proposed by Pedlosky [3]). Below, we will explore the influence of the beta effect in the framework of the SQG model from Section 6 with two discrete vertical levels. Taking into account this effect, the dimensionless expression for the quasigeostrophic potential vorticity can be written as (omitting the constant f_0) $q = \psi_{zz} + \psi_{xx} + \psi_{yy} + \beta y$, where the parameters $\beta = \beta_0 L_R^2/U$ and (in the beta-plane approximation) $\beta_0 = (2\Omega/R)\cos\varphi_0$. The streamfunction of motions with $q = 0$ satisfies the equation

$$\Delta\psi + \beta y + \theta_z = 0\,, \tag{7.2}$$

where, as earlier, $\theta = \psi_z$, $\Delta\psi = \psi_{xx} + \psi_{yy}$. Just as in Section 6, the interval $[0, 1]$ of the z-axis is divided into four equal intervals with length $h = 1/4$, the notation $\psi_1 = \psi|_{z=h}$, $\psi_2 = \psi|_{z=3h}$, $\theta_m = \theta|_{z=2h}$ is introduced, and central differences are used to approximate the derivative θ_z. From the related differential form of Eqn (7.2), we follow the relationships

$$\begin{aligned} &\Delta\psi_1 + \beta y + \frac{\lambda^2}{2}(\psi_2 - \psi_1) = \frac{\theta_{\rm bott}}{2h}\,,\\ &\Delta\psi_2 + \beta y - \frac{\lambda^2}{2}(\psi_2 - \psi_1) = -\frac{\theta_{\rm top}}{2h}\,, \end{aligned} \tag{7.3}$$

where $\theta_{\rm top}$ and $\theta_{\rm bott}$ are the distributions of buoyancy at the upper and lower boundaries. Inserting (7.3) into boundary conditions $D\theta_{\rm bott}/Dt = 0$, $D\theta_{\rm top}/Dt = 0$, we obtain Eqns (6.3) of the two-level model:

$$q_{1t} + [\psi_1, q_1] = 0\,, \quad q_{2t} + [\psi_2, q_2] = 0\,, \tag{7.4}$$

where now

$$q_{1,2} = \Delta\psi_{1,2} + \beta y \pm \frac{F}{2}(\psi_2 - \psi_1)\,. \tag{7.5}$$

Here, $F = \lambda^2$. Except for the physical interpretation of variables mentioned earlier, Eqns (7.4) and (7.5) coincide with the equations of the two-level or two-layer model with the beta effect. The value of parameter F, in contrast to that in a two-layer model, does not depend on the density difference between the two layers, but on the step of the vertical subdivision, $F = \lambda^2 = 1/(2h^2) = 8$.

The streamfunction of stationary zonal flows (depending on coordinate y) is found from Eqns (7.3). As earlier, these equations are reduced to two isolated equations,

$$\tilde{\Psi}_{yy} - F\tilde{\Psi} = -(\Theta_{\rm bott} + \Theta_{\rm top})\,, \quad \bar{\Psi}_{yy} + \beta y = \Theta_{\rm bott} - \Theta_{\rm top}\,, \tag{7.6}$$

on the barotropic $\bar{\Psi} = (\Psi_1 + \Psi_2)/2$ and baroclinic $\tilde{\Psi} = (\Psi_2 - \Psi_1)/2$ streamfunction components. Here, $\Theta_{\rm bott}(y)$ and $\Theta_{\rm top}(y)$ are the given distribution of buoyancy on the boundaries $z = 0$, $z = 1$, and all variables for zonal flows are denoted by capital letters. Further, we will consider distributions which induce a flow with equal and oppositely directed constant velocities at two levels $U_{1,2} = \pm U$. According to Eqns (7.6), such distributions should satisfy the conditions

$$\Theta_{\rm bott} + \Theta_{\rm top} = -FUy\,, \quad \Theta_{\rm top} - \Theta_{\rm bott} = \beta y\,. \tag{7.7}$$

The second condition of (7.7) corresponds to the zero barotropic component of the streamfunction. From conditions (7.7), it follows that

$$\Theta_{\rm top,\,bott} = \frac{1}{2}\,y(UF \pm \beta)\,, \tag{7.8}$$

i.e., to excite flows with opposite velocity directions at two levels (such a flow is considered most frequently), one needs special linear distributions of buoyancy at the boundaries, which include the beta effect.

The analysis of flow stability is carried out in the framework of linearized system of Eqns (7.4). According to (7.8), the derivatives $d(\Theta_{\rm top,\,bott})/dy = -(1/2)(UF \pm \beta)$ entering the system and playing the role of PV gradient in each layer are nonzero: they are defined by β and velocity U. For the variables $\theta = (1/2)(\psi_2' - \psi_1')$ and $\sigma = (1/2)(\psi_1' + \psi_2')$, system (7.4) is reduced to the following:

$$\begin{aligned} &\frac{\partial}{\partial t}(\Delta\theta - F\theta) + U\frac{\partial}{\partial x}\Delta\sigma + UF\frac{\partial\sigma}{\partial x} + \beta\frac{\partial\theta}{\partial x} = 0\,,\\ &\frac{\partial}{\partial t}\Delta\sigma + U\frac{\partial}{\partial x}(\Delta\theta) - \beta\frac{\partial\sigma}{\partial x} = 0\,. \end{aligned} \tag{7.9}$$

Looking for wave solutions of Eqns (7.9) of the form $\theta = a_0\exp(\kappa t)\exp[i(kx + ly)]$, $\sigma = b_0\exp(\gamma t)\exp[i(kx + ly)]$ and denoting $\gamma^2 = k^2 + l^2$, we arrive at the quadratic equations

$$\begin{aligned} \kappa^2(\kappa^2 + F)\gamma^2 - i\beta(2\kappa^2 + F)\gamma - \beta^2 k^2&\\ - k^2U^2\kappa^2(F - \kappa^2) = 0& \end{aligned} \tag{7.10}$$

on the complex increment γ. The real part of this increment $s = \operatorname{Re}\gamma$ characterizes the growth of perturbations. From (7.10), it follows that, at $\beta = 0$, the increment squared is given by the expression

$$\gamma^2 = s^2 = \frac{U^2(F - \kappa^2)}{F + \kappa^2}\,, \tag{7.11}$$

which coincides with (6.6) (for $F = 8$, $U = 1/4$). Instability takes place for $\kappa^2 < F$. For $\beta \neq 0$, the complex increment

$$\begin{aligned} &\gamma = \frac{1}{2\kappa^2(\kappa^2 + F)}\left(i\beta(2\kappa^2 + F) \pm \sqrt{D}\right),\\ &D = k^2\left(U^2\kappa^4(F^2 - \kappa^4) - 4\beta^2F^2\right). \end{aligned} \tag{7.12}$$

According to (7.12), instability occurs if $\kappa^2 < F$ and

$$U^2 > U_c^2(\kappa) = \frac{\beta^2}{\kappa^4(F^2 - \kappa^4)}\,, \tag{7.13}$$

i.e., the flow velocity at the upper level U must exceed the critical value $U_c(\kappa)$ (7.13). The last condition is obviously equivalent to the bound on the vertical velocity shear $U_1 - U_2 = 2U$. The existence of the threshold velocity is the main feature introduced by the beta effect. The equation $U = U_c(k)$ describes the neutral stability curve in the parameter plane (U, κ^2). For $\kappa^2 = F/\sqrt{2} = 4\sqrt{2}$, this curve has a minimum point, the minimum value $U_{c\,\min} = 2\beta$. Thus, for any $U > 2\beta$, there exists an interval of unstable κ^2 containing the minimum point.

Note that, for $U = 0$ (no vertical shear), $\gamma = i\omega_{1,2}$ and the wave solutions present barotropic and baroclinic Rossby waves $\sigma = C\exp[i(kx + ly - \omega_{1,2}t)]$ with frequencies $\omega_1 = -\beta k/\kappa^2$, $\omega_2 = -\beta k/(\kappa^2 + F)$.

The existence of a neutral curve allows developing a weakly nonlinear theory for the velocities $U = U_c + \Delta$, $\Delta \ll U_c$ in terms of the slow time $T = \Delta^{1/2} t$ [85]. Taking account of $D = 4\beta^2 F^2 (U^2/U_c^2 - 1)$, the increment for linear perturbations $\gamma = r\Delta^{1/2}$, where $r = \beta F/U_c^{1/2} \kappa^2 (\kappa^2 + F)$. The amplitude of linear perturbations satisfies the equation $A_{TT} - rA = 0$. In the weakly nonlinear theory, this linear second-order equation is replaced by the equation containing a cubic nonlinearity,

$$A_{TT} - rA = NA|A|^2 . \tag{7.14}$$

A principal role is played by the constant N, more precisely, by its sign. If $N < 0$, then, in the supercritical case $(U > U_c)$, there are oscillations with respect to some equilibrium state (soft stability loss). For positive N, the solutions of Eqn (7.14) grow unboundedly, i.e., nonlinearity fails to stabilize the exponential growth of linear perturbations. In the context of the two-layer model, the author of Ref. [85] carried out a rather cumbersome computation of the constant N and established that the complex amplitude satisfies Eqn (7.14) with $N < 0$. It was also shown that the absolute value of complex amplitude $R = |A|$ satisfies the equation that describes particle motion in a field with potential

$$V(R) = -a^2 R^2 + bNR^4 + c^2 R^{-2} . \tag{7.15}$$

For $N < 0$, the potential $V(R)$ has a minimum point, and the time dependence $R(T)$ corresponds to periodic (oscillatory) particle motion in the potential well. These oscillations are analogous to the ones explored in Section 3 by the Galerkin method.

8. Symmetric baroclinic instability

Symmetric baroclinic instability, the study of which was initiated by the classical papers by Rayleigh [109] and Solberg [110] (see also [111]), occurs in problems formulated in a cylindrical or spherical geometry where initially there is zonal (azimuthal) symmetry. An approximate analysis can be carried out in local Cartesian coordinates ignoring the curvature of coordinate lines, which is appropriate when the respective centrifugal forces are much smaller than the Coriolis force (cf. [112]). In the atmosphere, such symmetric baroclinic instability may unfold and be noticeable in jet streams (on their subtropical side), atmospheric fronts, tropical hurricanes, and the near-equatorial atmosphere in general [113]. Symmetric baroclinic instability has great (if not even greater than for the atmosphere) significance in the ocean (see, for example, [114]).

Consider an f-plane and a circular vortex on it. The 'f-plane' concept implies that the Coriolis parameter f is approximately constant, which is true when the meridional scale of motion is not very large. Strictly speaking, the problem should be treated in cylindrical coordinates r, λ, z, where r is the radial coordinate, λ the azimuthal (zonal) coordinate, and z is the axial (vertical) coordinate. However, for simplicity, in places where the curvature radius of coordinate surfaces is already large and the centrifugal inertia force related to this curvature is small compared with the Coriolis force, one introduces the local Cartesian coordinates x, y, z: the x-axis is directed radially, the y-axis is azimuthal, and the z-axis is directed upward. The respective velocity components are u, v, w. We assume that hydrodynamical fields vary much more strongly in the radial direction than in the azimuthal one and write Eqns (2.2) in the form

$$\frac{\mathrm{D}u}{\mathrm{D}t} - fv = -\frac{\partial \phi}{\partial x} , \quad \frac{\mathrm{D}v}{\mathrm{D}t} + fu = 0 , \quad \frac{\mathrm{D}w}{\mathrm{D}t} = -\frac{\partial \phi}{\partial z} + b ,$$
$$\frac{\mathrm{D}b}{\mathrm{D}t} = 0 , \quad \frac{\partial u}{\partial x} + \frac{\partial w}{\partial z} = 0 . \tag{8.1}$$

The stability of stationary zonal velocity field $V(x, z)$, which is linked to the buoyancy field $B(x, z)$ by the thermal wind equation $f(\partial V/\partial z) = \partial B/\partial x$, is explored. We impose small perturbations $(u', v', w', \phi', b') = (-\partial\psi'/\partial z, v', \partial\psi'/\partial x, \phi', b')$ on this state, such that the continuity equation is satisfied identically, linearize (8.1) with respect to the primed quantities, and, by excluding ϕ, arrive at the equations on perturbations of the streamfunction (cf. [31])

$$\frac{\partial^2}{\partial t^2}\left(\frac{\partial^2 \psi'}{\partial x^2} + \frac{\partial^2 \psi'}{\partial z^2}\right) + \left[\frac{\partial B}{\partial z}\frac{\partial^2 \psi'}{\partial x^2} - 2\frac{\partial B}{\partial x}\frac{\partial^2 \psi'}{\partial x \partial z} + f\left(\frac{\partial V}{\partial x} + f\right)\frac{\partial^2 \psi'}{\partial z^2}\right] = 0 . \tag{8.2}$$

The coefficients in (8.2) are treated as nearly constant, i.e., the spatial scale of perturbations is supposed to be much smaller than the scale of basic flow. Equation (8.2) is strict when $V(x, z)$ and $B(x, z)$ are linear functions of coordinates x and z. Multiplying both sides of (8.2) by $\partial\psi'/\partial t$ and integrating over the entire flow domain with periodic boundary conditions at its boundaries, we obtain the conservation law

$$\frac{\mathrm{d}H}{\mathrm{d}t} = 0 , \quad H = \frac{1}{2}\iint \left[\psi'^2_{xt} + \psi'^2_{zt} + \frac{\partial B}{\partial z}\psi'^2_x - 2\frac{\partial B}{\partial x}\psi'_x\psi'_z + f\left(\frac{\partial V}{\partial x} + f\right)\psi'^2_z\right] \mathrm{d}x\,\mathrm{d}z . \tag{8.3}$$

Subscript letters denote derivatives over respective coordinates. In order that Eqn (8.2) have a solution which is bounded in time and regular in the entire infinite plane (or satisfying given conditions at the boundary of finite spatial domain), the linear operator in square brackets in (8.2) should be elliptic [115] or the quadratic form in the integrand in (8.3) should be positive definite, which is the same thing. Thus, the following conditions should be observed: (a) static stability $\partial B/\partial z > 0$, (b) inertial stability $f(f + \partial V/\partial x) > 0$, and (c) the discriminant of the quadratic form matrix should be positive, i.e.,

$$\frac{\partial B}{\partial z} f\left(f + \frac{\partial V}{\partial x}\right) - \left(\frac{\partial B}{\partial x}\right)^2 > 0 . \tag{8.4}$$

Condition (8.4) of symmetric baroclinic instability can be written in an elegant form if we introduce the potential vorticity

$$\Pi = \frac{\partial(m, B)}{\partial(x, z)} = \frac{\partial m}{\partial x}\frac{\partial B}{\partial z} - \frac{\partial m}{\partial z}\frac{\partial B}{\partial x} ,$$

where $m = V + fx$, and use the thermal wind equation. Obviously, (8.4) is reduced to the condition of positivity (in the northern hemisphere, where $f > 0$) of potential vorticity

$$f\Pi > 0 .$$

Using the thermal wind equation, for $f > 0$ and for valid condition a) of static stability, stability condition (8.4) can be presented as

$$1+\frac{1}{f}\frac{\partial V}{\partial x}-\mathrm{Ri}^{-1}>0\,, \tag{8.5}$$

where $\mathrm{Ri}=(\partial B/\partial z)/(\partial V/\partial z)^2$ is the gradient Richardson number. When $\mathrm{Ri}<1$, i.e., the influence of baroclinicity (vertical velocity shear) is large, the horizontal velocity shear ceases to be an essential ingredient of instability. Note that in this case criterion (8.5) looks very essential, because the related criterion of wave shear instability $\mathrm{Ri}<1/4$ (Miles–Howard criterion [106, 116]) is more limiting. Possibly, this is also the reason why symmetric instability is rather important in studies of organized mesoscale vortex structures. Thus, the traditional baroclinic instability that was considered in Sections 2–7 (let us recall that it is the instability with respect to perturbations which depend on the along-flow coordinate) is realized for Richardson numbers which are much larger than one. Symmetric baroclinic instability with respect to perturbations that depend on the coordinate perpendicular to the basic flow is realized for the Richardson numbers in the interval $1/4<\mathrm{Ri}<1$. Finally, vertical shear instability occurs for $\mathrm{Ri}<1/4$. We note that symmetric baroclinic instability is a form of slantwise convection and is realized in cases when particle motion occurs in a narrow wedge formed by isentropic surfaces and surfaces of constant absolute momentum $m=\mathrm{const}$. In this case, the isentropic surfaces should be at a larger angle to the horizontal plane than surfaces $m=\mathrm{const}$.

The second and historically more traditional way of deriving the criterion of symmetric instability consists in exploring the instability by the 'parcel' method when the pressure field ϕ is 'frozen' and considered to be fully specified by the functions $V(x,z)$ and $B(x,z)$. No limitation on the perturbation scale is imposed. Then, the following system of equations, written in the matrix form, is valid for perturbations:

$$\frac{\partial^2}{\partial t^2}\begin{Vmatrix} v' \\ b' \end{Vmatrix}+\begin{Vmatrix} f(f+\partial V/\partial x) & \partial V/\partial z \\ f^2\,\partial V/\partial z & \partial B/\partial z \end{Vmatrix}\begin{Vmatrix} v' \\ b' \end{Vmatrix}=0\,.$$

This matrix equation leads to the conservation law

$$\frac{1}{2}\left[\left(\frac{\partial v'}{\partial t}\right)^2+\frac{1}{f^2}\left(\frac{\partial b'}{\partial t}\right)^2\right]+f\left(f+\frac{\partial V}{\partial x}\right)\frac{v'^2}{2}+\frac{\partial V}{\partial z}v'b'+\frac{1}{f^2}\frac{\partial B}{\partial z}\frac{b'^2}{2}=\mathrm{const}\,, \tag{8.6}$$

which ensures stability if the quadratic form in (8.6) is positive definite, i.e., the conditions of static and inertial stability are observed, as is the condition coinciding with (8.5) by virtue of the thermal wind equation.

Thus, general rotation and stable stratification are stabilizing factors, whereas baroclinicity, expressed through the respective component in the vorticity equation, destabilizes the flow, and symmetric stability is ensured only if this destabilizing factor is sufficiently small. If this last condition is violated, then necessary conditions for instability are fulfilled. K Ooyama [117] proved that violation of (8.4) is also a sufficient condition for instability. Indeed, multiplying (8.2) by ψ' and introducing the functionals

$$K=\frac{1}{2}\iint\{\psi_x'^2+\psi_z'^2\}\,\mathrm{d}x\,\mathrm{d}z\,,$$

$$I=\frac{1}{2}\iint\{\psi_{xt}'^2+\psi_{zt}'^2\}\,\mathrm{d}x\,\mathrm{d}z\,,$$

after several integrations by parts we obtain the relationship (cf. [118])

$$\frac{\mathrm{d}^2K}{\mathrm{d}t^2}=4I-2H\,. \tag{8.7}$$

Assume that the conditions of symmetric stability are violated in some flow domain. Then, it is always possible to select an initial perturbation with $H(0)<0$. For such a perturbation from (8.7), it follows that $\mathrm{d}^2K/\mathrm{d}t^2\geqslant 2|H|$ from here by conservation of H $K(t)\geqslant|H|t^2+\dot{K}(0)t+K(0)$ (the upper dot implies a time derivative). It is now clear that, however small the initial value $K(0)$, as time progresses, $K(t)$ will exceed any value $\varepsilon>0$ specified before, which implies instability. This agrees with general theorems by N G Chetaev [119] on instability. In meteorology, a similar analysis method for baroclinic instability of zonal flows, based on computing the second time derivative of perturbation kinetic energy, was already used in Ref. [120]. As applied to the effect of spontaneous helicity amplification in a humid atmosphere, a like approach was used in Ref. [121].

As sufficient conditions, one also takes the condition of positivity of the matrix trace

$$f\left(f+\frac{\partial V}{\partial x}\right)+\frac{\partial B}{\partial z}>0$$

and condition (8.4) of matrix discriminant positivity in the matrix equation written above (cf. [117]), which are equivalent to the conditions (a), (b), and (c) formulated above. In astrophysical fluid dynamics, conditions of symmetric stability of zonal flows on rotating stars and disks, analogous in essence but more complicated in their presentation, are known as Solberg–Høiland [122, 123] (see below for details).

Note that in the literature such a right-hand coordinate system (x,y,z) is frequently taken in which the basic flow $U(y,z)$ is directed along the x-axis and does not depend on x. In this case, the buoyancy field of the basic flow takes the form $B(y,z)$, the thermal wind equation is written as $f(\partial U/\partial z)=-\partial B/\partial y$, and the conditions of symmetric stability become

$$f\left(f-\frac{\partial U}{\partial y}\right)+\frac{\partial B}{\partial z}>0\,,\quad \frac{\partial B}{\partial z}f\left(f-\frac{\partial U}{\partial y}\right)-\left(\frac{\partial B}{\partial y}\right)^2>0\,.$$

An elegant way of deriving the sufficient conditions of linear symmetric instability consists in using the Arnold method [37] (see Refs [124, 125], where the case of incompressible layered fluid was considered, but without the Boussinesq approximation). We depart from (8.1) and take into account that $(u,w)=(-\partial\psi/\partial z,\partial\psi/\partial x)$. A fluid layer is considered which is bounded at the top and the bottom by impermeable surfaces; periodic boundary conditions are imposed in the horizontal plane. We use the existence of motion integrals in this problem: the energy

$$E=\iint\left\{\frac{(\nabla\psi)^2}{2}+\frac{(m-fx)^2}{2}-zb\right\}\mathrm{d}x\,\mathrm{d}z$$

as the sum of kinetic and potential energies, as well as Casimirs, quantities whose conservation directly (trivially) follows from motion equations,

$$F=\iint\left\{\Phi(m,\,b)-\frac{m^2}{2}\right\}\mathrm{d}x\,\mathrm{d}z\,.$$

Here, $m=v+fx$, and Φ is an arbitrary continuously differentiable function. A linear combination of motion integrals is taken: $I = E + F$. Let (V, B) be a given stationary zonal flow, whose stability is explored. Vertical circulation is absent, $\Psi = 0$, and for this solution geostrophic balance is observed in the radial direction, and hydrostatic balance is observed vertically, so that the thermal wind relation $f(\partial V/\partial z) = \partial B/\partial x$ is valid. The difference $I[m, b, \psi] - I[V + fx, B, \Psi]$ is a motion integral. Assuming that perturbations $\delta m = v - V$, $\delta b = b - B$, $\delta\psi = \psi - \Psi$ are small, we expand $I[m, b, \psi] - I[V + fx, B, \Psi]$ in series in variations of increasing orders

$$I[m, b, \psi] - I[V + fx, B, \Psi] = \delta I + \frac{1}{2}\delta^2 I + \ldots .$$

The arbitrary function Φ can be selected such that, for the given zonal flow $(V, B, \Psi = 0)$, the first variation δI is zero:

$$\Phi'_m\big|_{m=V+fx,\,b=B} = fx\,, \quad \Phi'_b\big|_{m=V+fx,\,b=B} = z\,.$$

The prime means partial differentiation over the respective variable. Computing the second variation, we find

$$\delta^2 I = \iint \left\{ (\nabla\delta\psi)^2 + \Phi''_{mm}(\delta m)^2 + 2\Phi''_{mb}\delta m\,\delta b + \Phi''_{bb}(\delta b)^2 \right\} \mathrm{d}x\,\mathrm{d}z \qquad (8.8)$$

and, omitting intermediate steps, we point out that $\Phi''_{mm} = f^2(\partial B/\partial z)/\Delta$, $\Phi''_{bb} = f[(\partial V/\partial x) + f]/\Delta$, $\Phi''_{mb} = \Phi''_{bm} = -f(\partial B/\partial x)/\Delta$, where

$$\Delta = f\left(\frac{\partial V}{\partial x} + f\right)\frac{\partial B}{\partial z} - \left(\frac{\partial B}{\partial x}\right)^2.$$

According to the Silvester criterion, the condition of positive definiteness of quadratic form in the integrand of (8.8) consists in conditions $\partial B/\partial z > 0$ and $\Delta > 0$. This necessitates the validity of inertial stability condition $f[(\partial V/\partial x) + f] > 0$ and consequently the positivity of the trace of the quadratic form matrix, $(\partial B/\partial z) + f[(\partial V/\partial x) + f] > 0$. If these inequalities hold, the zonal flow (V, B) is stable in the Lyapunov sense.

The stability of geostrophic states was also explored using the direct Lyapunov method in Refs [126, 127]. Reference [126], published simultaneously with Ref. [124], was based on a set of simplifying assumptions (in particular, the Boussinesq approximation). Reference [127] gives a series of strict a priori estimates for norms of perturbations which follow from the conditions $\partial B/\partial z > 0$ and $\Delta > 0$.

Thus far, we have been considering criteria of symmetric baroclinic stability in an ideal fluid. M McIntyre [112] showed that, in the case of viscous heat conducting fluid, for Prandtl numbers that differ from one, an additional symmetric instability is possible, which can be both monotonic and oscillating, even if the criteria mentioned above are valid (see also [113]).

The method applied above can be generalized to the case of baroclinic circular vortices, in which case it is necessary to treat the streamline curvature. For such vortices in the cylindrical reference frame (r, λ, z), the equations of motion have the form

$$\frac{\mathrm{D}u}{\mathrm{D}t} - \frac{v^2}{r} = -\frac{\partial\phi}{\partial r}\,, \quad \frac{\mathrm{D}v}{\mathrm{D}t} + \frac{uv}{r} = 0\,, \quad \frac{\mathrm{D}w}{\mathrm{D}t} = -\frac{\partial\phi}{\partial z} + b\,,$$

$$\frac{\mathrm{D}b}{\mathrm{D}t} = 0\,, \quad \frac{\partial}{\partial r}(ur) + \frac{\partial}{\partial z}(wr) = 0\,,$$

and the unperturbed flow satisfies the thermal wind equation

$$\frac{\partial}{\partial z}\frac{V^2}{r} = \frac{\partial B}{\partial r}\,.$$

Studying stability with respect to azimuthally-symmetric perturbations $(u', v', w', \phi', b') = (-r^{-1}\,\partial\psi'/\partial z, v', r^{-1}\,\partial\psi'/\partial r, \phi', b')$, where u, v, w correspond to the radial, azimuthal, and axial velocity components and ψ is the Stokes streamfunction, is more involved technically but remains the same in essence as in the simple case considered above. Denoting the specific angular momentum as $m = Vr$ and a convenient shortcut $x = r^2/2$ for the radial coordinate, the stability conditions take the form (a) $\partial m^2/\partial x > 0$, the condition of centrifugal stability (the Rayleigh criterion [109]); (b) $\partial B/\partial z > 0$, the condition of static stability; (c) the condition of symmetric baroclinic stability,

$$\frac{1}{4x^2}\frac{\partial m^2}{\partial x}\frac{\partial B}{\partial z} - \left(\frac{\partial B}{\partial x}\right)^2 \equiv \frac{1}{2x^2}\, m\Pi > 0\,,$$

where Π is the potential vorticity

$$\Pi = \frac{\partial(m, B)}{\partial(x, z)} = \frac{\partial m}{\partial x}\frac{\partial B}{\partial z} - \frac{\partial m}{\partial z}\frac{\partial B}{\partial x}\,.$$

Generalization to the case of general rotation consists in a formal change $m \to M = m + fr^2/2 \equiv m + fx$ in the stability criteria written above, where M is the absolute specific angular momentum; the Coriolis parameter f is assumed to be constant.

These considerations can be, for example, applied to the central part of intense tropical cyclones (see also [128] and references therein); these publications maintain that, when the conditions of symmetric instability are fulfilled, one can correctly pose the problem of finding the meridional circulation created by sources of momentum and buoyancy which supports cyclostrophically and hydrostatically balanced vortical motion [129], as well as, under certain assumptions, the motion in accretion disks in astrophysics. In the first case, we are dealing in a very good approximation with motion in a homogeneous gravity field, while in the second (ignoring the effect of self-gravity), with rotation in the gravity field of a point massive object at a disk center. We begin with the equations in cylindrical coordinates

$$\frac{\mathrm{D}u}{\mathrm{D}t} - \frac{m^2}{r^3} = -\frac{1}{\rho}\frac{\partial p}{\partial r} - \frac{\partial\varphi}{\partial r}\,, \quad \frac{\mathrm{D}w}{\mathrm{D}t} = -\frac{1}{\rho}\frac{\partial p}{\partial z} - \frac{\partial\varphi}{\partial z}\,,$$

$$\frac{\mathrm{D}m}{\mathrm{D}t} = 0\,, \quad \frac{\mathrm{D}\rho}{\mathrm{D}t} = 0\,, \qquad (8.9)$$

$$\frac{\partial}{\partial r}(ur) + \frac{\partial}{\partial z}(wr) = 0\,, \quad \varphi = -\frac{GM_0}{\sqrt{r^2 + z^2}}\,,$$

where $m = vr$ is the specific angular momentum, G is the Newtonian constant of gravitation, and M_0 is the mass of a central gravitating body at the origin of coordinates $(r, z) = (0, 0)$. The z-axis is directed along the disk rotation. The disk is symmetric with respect to the plane $z = 0$, i.e., the upper half-space is considered $z \geqslant 0$, and, without loss of generality, thin, i.e., $z \ll r$. The flow is density stratified, incompressible, but free from the Boussinesq approximation. For convenience, the notation $x = r^2/2$ is introduced, as is, following Ref. [124], a new sought-after function $\mu = (1/4)\rho m^2$. Equations (8.9) allow stationary fluid rotation, which satisfies conditions of cyclostrophic and hydrostatic balances,

$$-\frac{\mu}{x^2} = -\frac{\partial p}{\partial x} - \rho\,\frac{\partial \varphi}{\partial x}\,, \quad 0 = -\,\frac{\partial p}{\partial z} - \rho\,\frac{\partial \varphi}{\partial z}\,,$$

and, as a consequence, the thermal wind equation

$$\frac{1}{x^2}\frac{\partial \mu}{\partial z} = -\,\frac{\partial(\rho, \varphi)}{\partial(x, z)}\,. \tag{8.10}$$

Let us explore the stability of this stationary rotation with the help of the Arnold method. We rely on the existence of two motion integrals: the energy

$$E = \iint \left\{ \frac{\rho u^2}{2} + \frac{\mu}{x} + \rho\varphi \right\} \mathrm{d}x\,\mathrm{d}z, \;\; \mathbf{u} = (u, w)$$

and the Casimir

$$F = \iint \Phi(\mu, \rho)\,\mathrm{d}x\,\mathrm{d}z\,,$$

where Φ is an arbitrary continuously differentiable function. We compose the functional $I = E + F$ and explore it on the absolute extremum, assuming the variations $\delta u, \delta\mu, \delta\rho$ to be small. The necessary condition that the first variation equal zero, $\delta I = 0$, is $u = 0$, $\Phi'_\mu = -x^{-1}$, $\Phi'_\rho = \varphi(x, z)$. Now, the second variation takes the form

$$\delta^2 I = \iint \Big(\rho(\delta u)^2 + \Phi''_{\mu\mu}(\delta\mu)^2 + 2\Phi''_{\mu\rho}\,\delta\mu\,\delta\rho + \Phi''_{\rho\rho}(\delta\rho)^2\Big)\,\mathrm{d}x\,\mathrm{d}z\,,$$

where $\Phi''_{\mu\mu} = x^{-2}(\partial\rho/\partial z)/\varDelta$, $\Phi''_{\rho\rho} = (1/\varDelta)\,(\partial(\mu, \varphi)/\partial(x, z))$, $\Phi''_{\mu\rho} = \Phi''_{\rho\mu} = -(1/\varDelta)\partial(\rho, \varphi)/\partial(x, z)$, $\varDelta = \partial(\mu, \rho)/\partial(x, z)$.

Using the thermal wind Eqn (8.10), it can be shown that the conditions of stability are expressed as

$$\frac{1}{\varDelta}\frac{\partial \rho}{\partial z} > 0\,,$$
$$\frac{1}{\varDelta^2}\left[\frac{\partial(\mu, \varphi)}{\partial(x, z)}\left(-\,\frac{\partial \rho}{\partial z}\right) + \frac{\partial(\rho, \varphi)}{\partial(x, z)}\left(-\,\frac{\partial \mu}{\partial z}\right)\right] > 0\,. \tag{8.11}$$

It can be readily seen that the second condition (8.11) has the form

$$-\,\frac{1}{\varDelta}\frac{\partial \varphi}{\partial z} = \frac{1}{\rho\varDelta}\frac{\partial p}{\partial z} > 0\,.$$

Since we are limited to the upper half-space $z \geqslant 0$,

$$\frac{\partial \varphi}{\partial z} = \frac{GM_0 z}{(r^2 + z^2)^{3/2}} \cong \frac{GM_0 z}{r^3} > 0\,,$$

where the approximate equality is valid because of the condition on disk thickness $z \ll r$ and, respectively, the pressure decreases with increasing distance to the symmetry plane, conditions (8.11) take the form

$$-\,\frac{\partial \ln\rho}{\partial z} > 0\,, \;\; -\varDelta = \frac{\partial(\rho, \mu)}{\partial(x, z)} \equiv \frac{\rho^2}{4}\,\frac{\partial(m^2, -\ln\rho)}{\partial(x, z)} > 0\,, \tag{8.12}$$

and we arrive at the Solberg stability criterion (cf. [130], where, instead of $-\ln\rho$, the specific entropy s is used; for incompressible fluid, $s \cong -c_p \ln\rho + \text{const}$).

An essential problem is the generation of turbulence and the creation of turbulent viscosity, which is needed to maintain the disk accretion in a quasi-stationary state [131]. The point is that, if the velocity profile is Keplerian, $v(r) \propto r^{-1/2}$, the Rayleigh criterion $\partial m^2/\partial x > 0$ of centrifugal stability is fulfilled, and if additionally $-\partial \ln\rho/\partial z > 0$ (static stability in the axial direction), the second condition (8.12) is fulfilled as well. For the second condition (8.12) to be violated and instability to occur, one needs to account for deviations in the velocity profile from the Keplerian one, which depend on the axial coordinate z (the effect of baroclinicity expressed by the thermal wind equation [127]).

We note that, to explain the generation of turbulence in the disk, staying in the framework of the Kepler velocity profile, we resort to more complex mechanisms, for example, related to magneto–rotational instability (MRI), discovered in [132] (see also [133]), when electro-conducting fluid rotates around an axis parallel to a magnetic field, and angular rotation speed $\Omega(r) \equiv v(r)/r$ decreases with increasing radius r [134] (see also [135]). One new research avenue is explicitly taking account of stable matter stratification in the disk in the direction perpendicular to its plane, which can lead to instability of the Kepler velocity profile (which is certainly stable for neutral stratification), but this time with respect to azimuthally nonsymmetric perturbations, first and foremost, with the wavenumber equal to one (the so-called spiral instability mode). We are dealing with stratorotational instability (SRI), which at present is studied most thoroughly using model fluid dynamical problem statements (stratified Taylor–Couette flow and others) [136–140].

9. Baroclinic instability in astrophysics

Baroclinic (wave) instability is natural for astrophysical objects, and similar problems were considered beginning in the 1960s. A set of connected questions was addressed in Section 8. A detailed review of work from the 1960–1970s is presented in Refs [122, 141]. In particular, the following problems could be specially mentioned: (a) stability of differential rotation as applied to stars in general and solar tachocline in particular; (b) development of turbulence in astrophysical disk systems. In the latter case, there are some distinctions between accretion disks and protoplanetary systems. Also of interest are problems of baroclinic instability in planetary atmospheres — from the planets of the Earth group and giant planets of the solar system to exoplanets [142–144]. It is noted that the instability is either badly reproduced or is not reproduced at all in modeling with low resolution and/or large artificial viscosity.

In the study by Goldreich and Schubert [145], where a local (shortwave) stability analysis was used, it is shown that a necessary condition of stability for zones of radiative transfer on a rotating star is an increase in angular momentum for increasing distance from the center and the absence of the dependence of rotation speed on the vertical coordinate. The role of baroclinicity in the stability of differential rotation was analyzed in Ref. [146], which, like many other studies, considered motions in cylindrical coordinates r, ϕ, z and the main unperturbed state in the form $\mathbf{v}_0 = \mathbf{r} \times \boldsymbol{\Omega} = r\Omega(r, z)\mathbf{e}_\phi$ (here, Ω is the angular rotation velocity and $\mathbf{e}_\phi$ is the unit vector in the azimuthal direction). The equilibrium position satisfies the equation $\nabla P = \rho\widetilde{\mathbf{g}}$, where $\widetilde{\mathbf{g}} = \mathbf{g} + r\Omega^2\mathbf{e}_\phi = \nabla\Phi + r\Omega^2\mathbf{e}_\phi$ is the effective gravity force and Φ is the gravitational potential. A sufficient stability condition is the fulfillment of the conditions $\widetilde{\mathbf{g}}\widetilde{\boldsymbol{\beta}} > 0$ and $\widetilde{\mathbf{g}} \times \widetilde{\boldsymbol{\beta}} = 0$, where $\widetilde{\boldsymbol{\beta}} = \nabla_{\rm ad}\nabla\ln P - \nabla\ln T$ ($\nabla_{\rm ad} = {\rm d}\ln T/{\rm d}\ln P$ for adiabatic variations). The stability condition, as in Ref. [145], holds for $\partial\Omega/\partial z = 0$. If there is a vertical inhomogeneity in rotation, $\partial\Omega/\partial z \neq 0$, surfaces orthogonal to the direction of the effective gravity force and entropy $\widetilde{\boldsymbol{\beta}}$ gradient are already at an angle to each other, as shown in Fig. 1. Perturbations that get wedged between these surfaces become unstable. In dynamical meteorology, baroclinic instability means an instability of adiabatic wave motions in a baroclinic atmosphere, and it is considered through a global analysis of perturbations. A physical mechanism of baroclinic instability is very similar to thermal convection, although rotation makes the resulting instability oscillating. On the other hand, the instability at hand is accompanied by nonadiabatic effects. The physical cause of this instability is obvious: radiative heat exchange between a perturbed fluid element and its surroundings introduces asymmetry into the oscillatory motion, such that an oscillating element passes its equilibrium position as velocity increases.

A specific feature of baroclinic instability in astrophysical fluid dynamics is that the hydrostatic balance and conditions of geostrophic balance are not necessarily valid.

Analytical estimates of the stability of the linear velocity profile, which depends on both vertical z and transverse x coordinates (nonseparable profile) for the barotropic and baroclinic cases, were obtained in Ref. [147],

$$\mathbf{V}_0 = (0, \delta x + \varepsilon z, 0)\,. \tag{9.1}$$

Here, δ, ε are the horizontal and vertical shears, respectively. A local coordinate system is used, where x corresponds to the radial direction, and y, to the azimuthal one. The method of variable separation is not applicable for the linearized problem, and the solution here can be presented as a nonmodal wave with time-dependent wavenumbers [148]

$$f(x,y,z,t) = \exp\left[{\rm i}(k - m\delta t)x + {\rm i}my + {\rm i}(l - m\varepsilon t)z\right] f(t)\,. \tag{9.2}$$

For perturbations with $m = 0$ in the rotating reference frame under conditions of thermal (azimuthal) wind $2\Omega\,\partial V_0/\partial z = \beta g\,\partial T/\partial x$, one obtains oscillatory solutions with frequency $\overline{N}$,

$$\overline{N}^2 = \frac{k^2N^2 - 4\varepsilon kl + 2(2+\delta)l^2}{k^2 + l^2}\,.$$

The case $\varepsilon = \delta = 0$ corresponds to neutrally stable inertia-gravity waves. However, for nonzero shears, these waves can lose stability. For $\varepsilon = 0$ and $\delta < -2$, the modes with $k = 0$ ($l \neq 0$) are unstable. In this case, vertical stratification fails to maintain the returning force, and the specific angular moment decreases outside (i.e., in the positive x direction).

If $\varepsilon(\delta) \neq 0$, exponentially growing solutions exist for ${\rm Ri} < 2/(2+\delta)$, where ${\rm Ri} \equiv N^2/\varepsilon^2$. For $\delta = 0$, one gets the usual criterion for symmetric instability (${\rm Ri} < 1$) of baroclinic flows. However, for $-2 < \delta < 0$, the range of unstable Richardson numbers is larger. In fact, flows with arbitrarily large Richardson numbers can be unstable in the presence of certain horizontal (latitudinal) shear; if $\delta < -2$, all flows are unstable. It is noteworthy that, for $N^2 = 0$, any flow with nonzero baroclinicity ($\varepsilon \neq 0$) will be unstable.

For the maximum instability increment $\sigma_{\max}$, we have

$$\sigma^2_{\max}\big|_{m=0} = -N^2 + \frac{8\varepsilon^2}{\sqrt{v^2 + 16\varepsilon^2} - v}\,, \tag{9.3}$$

where $v = N^2 - 2(2+\delta)$. If $\varepsilon \to 0$, the instability condition $\delta < -2$ appears once again. The condition of exponential growth ${\rm Ri} < 2/(2+\delta)$ follows for $\sigma^2_{\max}|_{m=0} > 0$.

If $\delta = 0$, $\varepsilon \neq 0$, the dimensionless asymptotic solution contains branches $\sim t^{-1\pm{\rm i}\alpha}\exp(\pm 2{\rm i}t)$ ($\alpha = (k - m\delta t)/m$) and $\sim t^{-4}$. We can mention that the frequency of oscillations (in dimensional units) is the rotation frequency 2Ω instead of the Brunt–Váisálá frequency. In other words, the returning force in this case is the Coriolis one, which makes nonaxisymmetric perturbations stable even in the case of unstable temperature stratification of the main state. Thus, the stability of baroclinic flow with a vertical shear is fully dissimilar to the stability in the barotropic case.

In a general nonaxisymmetric case with $\varepsilon(\delta) \neq 0$, $k(l,m) \neq 0$, an asymptotic solution to the problem has two modes: one decaying as $\sim t^{-3}$ and the other one growing or oscillating as $\sim t^{\pm{\rm i}\overline{N}' d}\exp(\pm{\rm i}\overline{N}' t)$. The dependences of $\overline{N}'$, d on the parameters N, δ, ε, k, l, m are given in Ref. [147]. For $\delta^2{\rm Ri} + 4 - 2\delta < 0$, the value of $\overline{N}'^2$ turns out to be negative; hence, a sufficient instability condition is ${\rm Ri} < 1/4$. Let us note that the growth of axisymmetric perturbations always prevails over the growth of nonaxisymmetric ones.

Large horizontal shears are possible in accretion disks. The buoyancy frequency can be very small (as, for example, in the vicinity of the convective zones, close to the star center or in the mid-plane of the accretion disk). The Kepler (horizontal) shear dominates over the vertical shear related to the baroclinicity of the basic state, and its influence cannot be neglected. In particular, for long-wave perturbations, the hydrostatic balance in the vertical direction is preserved even if geostrophic balance is modified.

In rapidly rotating stars, baroclinic instability may occur in the entire volume. In slowly rotating stars, it may occur only in very narrow regions located in the vicinity of (a) the star's center, (b) the boundary of the convective zone, or (c) a jump in the gradient of rotation speed [149].

Reference [150] mentions that deviations from the barotropic or baroclinic regime define the level of turbulence in disks. References [151, 152] carry out a linear analysis of baroclinic instability in the radiative transfer zone of a star with radially inhomogeneous rotation. Global perturbations are considered, i.e., their scale is not assumed to be small compared to the star radius. The radial scale of perturbation is still assumed to be small. The unperturbed state is axisymmetric. The main flow component here is rotation, which is assumed to be sufficiently slow so that the deviation of stratification from spherical symmetry is small. Stratification proper in radiating zones of stars is stable, i.e., the specific entropy $s = c_v\ln P - c_p\ln\rho$ increases with radius. The main cause of instability is an inhomogeneity of rotation. There are two families of unstable perturbations, which correspond to Rossby waves and internal gravity waves. The instability is a dynamical one: its growth time, comprising several thousand rotation periods, is small compared to the time of star evolution. A reduction in heat conductivity strengthens the instability. Unstable perturbations are characterized by kinetic helicity. As a result, a magnetic field can be generated by turbulence that evolves during instability. The instability manifests itself for a very small inhomogeneity of rotation, $\Delta\Omega \sim 10^{-3}\Omega$, and this is the distinction from barotropic instabilities which arise for relatively large rotation inhomogeneity.

Differential rotation is not the only possible cause of baroclinicity. In addition to the nonconservative centrifugal force, a magnetic field can also lead to baroclinicity. As a consequence, a question arises as to whether the baroclinic instability induced by a magnetic field is possible.

Reference [153] considers baroclinic instability in a two-level model on a β-plane in the presence of a zonal magnetic field. In this case, the potential vorticity is no longer preserved. The minimum vertical shear needed for instability does not depend on the β-effect, but is defined by the magnetic field intensity. Short waves become unstable, whereas long-wave perturbations become stabilized. Unstable waves transform the available potential energy into the energy of magnetic field perturbations. The changes in nonmagnetic components are similar to those in the Phillips model. A vertical and single-cell meridional magnetic field is generated.

In Refs [154, 155], with the use of the magnetohydrodynamical (MHD) generalization of the two-level hydrostatic (but nongeostrophic) model, it is shown that the toroidal field tends to stabilize baroclinically unstable regimes in the solar tachocline. Respectively, baroclinic instability should occur in the tachocline at latitudes where the toroidal field is weak or changes sign, but not where the field is strong. Reference [154] mentions that the solar tachocline is likely to be close to the state of the geostrophic thermal wind for which the Coriolis force related to the differential rotation is equilibrated by the gradient of latitudinal pressure, which leads to a link between the vertical gradient of rotation and the latitudinal gradient of entropy. The growth rate of unstable perturbations is approximately five times higher at middle and high latitudes than at low latitudes.

At all latitudes and for all stratifications, the longitudinal scale of most unstable perturbations compares to the Rossby deformation radius, while the growth rate is defined by the gradient of local latitudinal entropy.

Baroclinic instability in the tachocline, competing with the instability due to the gradient of angular velocity of latitudinal rotation, which was found in earlier research, is important for the functioning of the solar dynamo, and it should be found in the majority of stars that contain a boundary between the radiative and convective regions.

In Ref. [156], the baroclinicity is explored namely in the context of nonzero vertical shear. In a more general sense, a flow is baroclinic if its isobaric surfaces do not coincide with its isopycnal surfaces. Such flows become baroclinic because of molecular-mass gradients: the addition of dust influences the density, but not the pressure. Baroclinic instability develops even for large Richardson numbers.

As follows from analytical estimates and three-dimensional modeling, in particular, protoplanetary disks have a negative gradient of radial entropy, which makes them baroclinic [157]. Such a baroclinic flow turns out to be unstable and generates turbulence. The instability is related to the development of transient (nonmodal) perturbations [158, 159]. Note that under barotropic initial conditions turbulence rapidly degrades. Pressure waves, Rossby waves, and vortices evolve in the disk plane. Most interestingly, these super-dense anticyclonic vortices form from a low background noise and become long-lived, which is assumed to lead to planet formation [160]. Clusters of protoplanetary matter have a surface density that is up to four times larger than in the surroundings. Furthermore, they accumulate dust in their centers, which strengthens their role in processes of planet formation [161]. Similar results were also obtained in Refs [162, 163].

Turbulence developing in baroclinic disks carries angular momentum outside and initiates the transport of matter directed radially inside. Potential energy is released, and the excess kinetic energy is scattered. Thermal convection in the vertical disk direction is not needed for this effect. Convection creates negative Reynolds stresses, but they prove to be several orders of magnitude weaker than those created by baroclinic instability.

In the protoplanetary disk geometry, density becomes stratified in the radial direction, in contrast to that in planetary atmospheres; therefore, azimuthal pressure fluctuations lead to a vortical state. A number of numerical models of protoplanetary disks did not take into account the effects of baroclinicity and were therefore only able to simulate a decaying turbulence from some initial distribution of vortical flows. Reference [164] revealed a new hydrodynamical instability of protoplanetary disks which can occur through a change in the dust-to-gas ratio and lead to dust accumulation inside the disk. The instability causes the appearance of a vertical entropy gradient, which in turn leads to baroclinic instability capable of generating toroidal gas vortices accumulating dust in rings.

References [165, 166] found that baroclinic instability with thermal relaxation leads to the formation of large elliptically unstable vortices. Initially, hollow vortices are formed which evolve into vortex structures with a turbulent core. Internal vortical layers evolve over the entire disk along critical surfaces of the layer and form new vortices in the upper disk part. Such baroclinic vortices can play an essential role in the evolution of a global disk and take part in separating solid bodies from the gas component and also foster the formation of new vortices outside the disk plane via the critical layer excitation mechanism.

10. Conclusions

Although the authors have tried to review what is currently the most interesting work on baroclinic instability in geophysical flows as fully as possible, the review in many respects reflects their personal preferences and working experience. A partial justification for the incompleteness of the results presented in this review, especially those concerning applications to the real atmosphere and ocean, is our intention to highlight in the main part of the review modern tendencies and 'points of growth' in the theory of baroclinic instability in the framework of geophysical fluid dynamics. In particular, this concerns the focus on systematic use of motion equations in the Boussinesq approximation (the approximation of weak fluid compressibility — in the dynamical sense), which allows one to eliminate factors secondary for the baroclinic instability theory, but strongly complicating formal analysis, such as a full account for fluid (atmospheric air) compressibility. The tendencies and 'growth points' presented in this review, in our view, characteristic namely of the last decade of the 20th century and the beginning of the 21st century, and understandably missing from reviews from the earlier period touching on baroclinic instability, including the brilliant reviews by A S Monin et al., could be of interest for a wide physics audience, including specialists in fluid dynamics and its applications in geophysics and astrophysics.

The authors hope that the present review will inform the reader about the present state of the baroclinic instability theory in geophysical fluid dynamics and will attract readers' interest in the problems outlined here, assuming also the possibility of transfer of the described methods to adjacent branches of physical science.

The work on writing this review was supported by a grant from the Russian Foundation for Basic Research, no. 20-15-50175-expansion. The results in Section 6 were obtained with support from the Russian Science Foundation (project no. 19-17-00248).

References

1. Wallace J M, Hobbs P V *Atmospheric Science: an Introductory Survey* (New York: Academic Press, 1977)
2. Monin A S *Theoretical Geophysical Fluid Dynamics* (Dordrecht: Kluwer Acad. Publ., 1990); Translated from Russian: Monin A S *Teoreticheskie Osnovy Geofizicheskoi Gidrodinamiki* (Leningrad: Gidrometeoizdat, 1988)
3. Pedlosky J *Geophysical Fluid Dynamics* (Berlin: Springer-Verlag, 1987)
4. Vallis G K *Atmospheric and Oceanic Fluid Dynamics: Fundamentals and Large-Scale Circulation* (Cambridge: Cambridge Univ. Press, 2006)
5. Landau L D, Lifshitz E M *Fluid Mechanics* (Oxford: Pergamon Press, 1987); Translated from Russian: *Gidrodinamika* (Moscow: Nauka, 1988)
6. Nezlin M V *Sov. Phys. Usp.* **29** 807 (1986); *Usp. Fiz. Nauk* **150** 3 (1986)
7. Dolzhanskii F V, Krymov V A, Manin D Yu *Sov. Phys. Usp.* **33** 495 (1990); *Usp. Fiz. Nauk* **160** (7) 1 (1990)
8. Monin A S *Sov. Phys. Usp.* **29** 843 (1986); *Usp. Fiz. Nauk* **150** 61 (1986)
9. Monin A S, Zhikharev G M *Sov. Phys. Usp.* **33** 313 (1990); *Usp. Fiz. Nauk* **160** (5) 1 (1990)
10. Onishchenko O G, Pokhotelov O A, Astaf'eva N M *Phys. Usp.* **51** 577 (2008); *Usp. Fiz. Nauk* **178** 605 (2008)
11. Fridman A M *Phys. Usp.* **51** 213 (2008); *Usp. Fiz. Nauk* **178** 225 (2008)
12. Charney J G *J. Meteorology* **4** (5) 135 (1947)
13. Eady E T *Tellus* **1** (3) 33 (1949)
14. Dymnikov V P, Filatov A N *Ustoichivost' Krupnomasshtabnykh Atmosfernykh Protsessov* (Stability of Large-scale Atmospheric Processes) (Leningrad: Gidrometeoizdat, 1990)
15. Shakina N P *Gidrodinamicheskaya Neustoichivost' v Atmosfere* (Hydrodynamical Instability in the Atmosphere) (Leningrad: Gidrometeoizdat, 1990)
16. Hide R, Mason P J *Adv. Phys.* **24** 47 (1975)
17. Obukhov A M *Izv. Akad. Nauk SSSR, Ser. Geofiz. Geograf.* **13** (4) 281 (1949)
18. Lindzen R S *Dynamics in Atmospheric Physics: Lecture Notes for an Introductory Graduate-Level Course* (Cambridge: Cambridge Univ. Press, 1990)
19. Kurgansky M V *Vvedenie v Krupnomasshtabnuyu Dinamiku Atmosfery: Adiabaticheskie Invarianty i ikh Primenenie* (Introduction to Large-scale Dynamics of the Atmosphere: Adiabatic Invariants and their Applications) (St. Petersburg.: Gidrometeoizdat, 1993)
20. Dikiy L A *Gigrodinamicheskaya Ustoichivost' i Dinamika Atmosfery* (Hydrodynamical Stability and Dynamics of the Atmosphere) (Leningrad: Gidrometeoizdat, 1976)
21. Davies H C, Bishop C H *J. Atmos. Sci.* **51** 1930 (1994)
22. Hide R *Quart. J. R. Meteor. Soc.* **79** 161 (1953)
23. Hide R *Philos. Trans. R. Soc. Lond. A* **250** 441 (1958)
24. Fridman A A *Izbrannye Trudy* (Selected Papers) (Moscow: Nauka, 1966)
25. Ertel H *Naturwissenschaften* **30** 543 (1942)
26. Svirkunov P N *Trudy Inst. Eksp. Meteorol. Ross. Akad. Nauk* **27** 88 (1996)
27. Zakharov V E, Kuznetsov E A *Phys. Usp.* **40** 1087 (1997); *Usp. Fiz. Nauk* **167** 1137 (1997)
28. Charney J G, Stern M E *J. Atmos. Sci.* **19** 159 (1962)
29. Bretherton F P *Quart. J. R. Meteor. Soc.* **92** 325 (1966)
30. Montgomery M T, Shapiro L J *J. Atmos. Sci.* **52** 1829 (1995)
31. Hoskins B J *Quart. J. R. Meteor. Soc.* **100** 480 (1974)
32. Buleev N I, Marchuk G I, in *Raboty po Dinamicheskoi Meteorologii: za 1951–1954 gg.* (Works on Dynamical Meteorology: 1951–1954) (Trudy Inst. Fiziki Atmosfery Akad. Nauk SSSR, No. 2, Exec. Ed. I A Kibel) (Moscow: Izd. AN SSSR, 1958) p. 66
33. Monin A S *Izv. Akad. Nauk SSSR, Ser. Geofiz.* (4) 497 (1958)
34. Monin A S *Weather Forecasting as a Problem in Physics* (Cambridge, MA: MIT Press, 1972); Translated from Russian: Monin A S *Prognoz Pogody kak Zadacha Fiziki* (Moscow: Nauka, 1969)
35. Diky L A, Kurgansky M V *Izv. Atmos. Ocean. Phys.* **7** 623 (1971); *Izv. Akad. Nauk SSSR Fiz. Atm. Okeana* **7** 939 (1971)
36. Kurgansky M V *Adiabatic Invariants in Large-Scale Atmospheric Dynamics* (Boca Raton, FL: CRC Press, 2002)
37. Arnold V I, in *Vladimir I. Arnold — Collected Works: Hydrodynamics, Bifurcation Theory, and Algebraic Geometry 1965–1972* (Eds A B Givental et al.) (Berlin: Springer, 2014) p. 19; Translated from Russian: *Dokl. Akad. Nauk SSSR* **162** 975 (1965)
38. Blumen W *J. Atmos. Sci.* **25** 929 (1968)
39. Blumen W *J. Atmos. Sci.* **35** 774 (1978)
40. Held I M et al. *J. Fluid Mech.* **282** 1 (1995)
41. Majda A J, Tabak E G *Physica D* **98** 515 (1996)
42. Harvey B J, Ambaum M H P *Quart. J. R. Meteor. Soc.* **136** 1506 (2010)
43. Constantin P, Majda A J, Tabak E *Nonlinearity* **7** 1495 (1994)
44. Muraki D J, Snyder C *J. Atmos. Sci.* **64** 2961 (2007)
45. Carton X *J. Atmos. Sci.* **66** 1051 (2009)
46. Dritschel D G *Geophys. Astrophys. Fluid Dyn.* **105** 368 (2011)
47. Harvey B J, Ambaum M H P *Geophys. Astrophys. Fluid Dyn.* **105** 377 (2011)
48. Harvey B J, Ambaum M H P, Carton X J *J. Atmos. Sci.* **68** 964 (2011)
49. Lim C C, Majda A J *Geophys. Astrophys. Fluid Dyn.* **94** 177 (2001)
50. Reinaud J N, Dritschel D G, Carton X *Geophys. Astrophys. Fluid Dyn.* **110** 461 (2016)
51. Reinaud J N, Dritschel D G, Carton X *Phys. Fluids* **29** 086603 (2017)
52. Juckes M *J. Atmos. Sci.* **51** 2756 (1994)
53. Hakim G J, Snyder C, Muraki D J *J. Atmos. Sci.* **59** 2405 (2002)
54. Capet X et al. *J. Fluid Mech.* **604** 165 (2008)
55. Tulloch R, Smith K S *J. Atmos. Sci.* **66** 450 (2009)
56. Ragone F, Badin G *J. Fluid Mech.* **792** 740 (2016)
57. Lapeyre G *Fluids* **2** 7 (2017)
58. Palmén E, Newton C W *Atmospheric Circulation Systems: Their Structure, Physical Interpretation* (New York: Academic Press, 1968); Translated into Russian: *Tsirkulyatsionnye Sistemy Atmosfery* (Leningrad: Gidrometeoizdat, 1973)
59. Kalashnik M V, Nerushev A F, Ivangorodsky R V *Izv. Atmos. Ocean. Phys.* **53** 156 (2017); *Izv. Ross. Akad. Nauk. Fiz. Atm. Okeana* **53** 179 (2017)
60. Gill A E *Atmosphere-Ocean Dynamics* (New York: Academic Press, 1982)
61. Heifetz E et al. *Quart. J. R. Meteor. Soc.* **130** 233 (2004)
62. Heifetz E et al. *Quart. J. R. Meteor. Soc.* **130** 211 (2004)
63. Heifetz E, Methven J *Phys. Fluids* **17** 064107 (2005)
64. Petterssen S, Smebye S J *Quart. J. R. Meteor. Soc.* **97** 457 (1971)
65. Rotunno R, Fantini M *J. Atmos. Sci.* **46** 3599 (1989)
66. Mitsudera H *J. Atmos. Sci.* **51** 3137 (1994)
67. Farrell B F, Ioannou P J *J. Atmos. Sci.* **53** 2025 (1996)
68. Drazin P G *Introduction to Hydrodynamic Stability* (Cambridge: Cambridge Univ. Press, 2002); Translated into Russian: *Vvedenie v Teoriyu Gidrodinamicheskoi Ustoichivosti* (Moscow: Fizmatlit, 2005)
69. Charru F *Instabilités Hydrodynamiques* (Paris: EDP Sciences, 2007); Translated into English: *Hydrodynamic Instabilities* (Cambridge: Cambridge Univ. Press, 2011); Translated into Russian: *Neustoichivost' v Gidrodinamike* (Moscow–Izhevsk: Inst. Komp'yut. Issled., 2015)

70. Diaconescu E P, Laprise R *Earth Sci. Rev.* **113** 161 (2012)
71. Morgan M C *J. Atmos. Sci.* **58** 2518 (2001)
72. Morgan M C, Chen C C *J. Atmos. Sci.* **59** 169 (2002)
73. de Vries H, Opsteegh J D *J. Atmos. Sci.* **64** 673 (2007)
74. de Vries H, Opsteegh J D *J. Atmos. Sci.* **64** 695 (2007)
75. Kalashnik M V, Chkhetiani O *J. Atmos. Sci.* **75** 2741 (2018)
76. Kalashnik M V, Chkhetiani O G *Izv. Atmos. Ocean. Phys.* **54** 415 (2018); *Izv. Ross. Akad. Nauk. Fiz. Atm. Okeana* **54** 487 (2018)
77. Kalashnik M V, Chkhetiani O *J. Atmos. Sci.* **74** 293 (2017)
78. Kalashnik M V, Chkhetiani O G *Fluid Dyn.* **55** 171 (2020); *Izv. Ross. Akad. Nauk. Mekh. Zhidk. Gaza* (2) 28 (2020)
79. Dodd R K et al. *Solitons and Nonlinear Wave Equations* (London: Academic Press, 1982)
80. Gledzer E B, Dolzhanskii F V, Obukhov A M *Sistemy Gidrodinamicheskogo Tipa i Ikh Primenenie* (Systems of Hydrodynamic Type and Their Applications) (Moscow: Nauka, 1981)
81. Kalashnik M V, Kurgansky M V *Fluid Dyn.* **55** 554 (2020); *Izv. Ross. Akad. Nauk. Mekh. Zhidk. Gaza* (4) 126 (2020)
82. Hunt B G *J. Atmos. Sci.* **35** 1133 (1978)
83. McGuirk J P, Reiter E R *J. Atmos. Sci.* **33** 2079 (1976)
84. Pedlosky J *Tellus* **15** 20 (1963)
85. Pedlosky J *J. Atmos. Sci.* **27** 15 (1970)
86. Pedlosky J *J. Atmos. Sci.* **29** 53 (1972)
87. Pedlosky J, Polvani L M *J. Atmos. Sci.* **44** 631 (1987)
88. Hart J E *Annu. Rev. Fluid Mech.* **11** 147 (1979)
89. Hart J E *J. Atmos. Sci.* **38** 400 (1981)
90. Barcilon A, Drazin P G *J. Atmos. Sci.* **41** 3314 (1984)
91. Wang B, Barcilon A *J. Atmos. Sci.* **43** 1275 (1986)
92. Klein P, Pedlosky J *J. Atmos. Sci.* **43** 1243 (1986)
93. Kalashnik M V, Chkhetiani O G *Fluid Dyn.* **51** 606 (2016); *Izv. Ross. Akad. Nauk. Mekh. Zhidk. Gaza* (5) 29 (2016)
94. Timofeev A V *Sov. Phys. Usp.* **13** 632 (1971); *Usp. Fiz. Nauk* **102** 185 (1970)
95. Thorncroft C D, Hoskins B J *J. Atmos. Sci.* **47** 2317 (1990)
96. Chang E K *J. Atmos. Sci.* **49** 2452 (1992)
97. Kalashnik M V *Izv. Atmos. Ocean. Phys.* **51** 576 (2015); *Izv. Ross. Akad. Nauk Fiz. Atm. Okeana* **51** 648 (2015)
98. Kalashnik M V, Kurgansky M V, Kostrykin S V *J. Atmos. Sci.* **77** 239 (2020)
99. Meshalkin L D, Sinai Ia G *J. Appl. Math. Mech.* **25** 1700 (1961); *Priklad. Mat. Mekh.* **25** 1140 (1961)
100. Vasavada A R, Showman A P *Rep. Prog. Phys.* **68** 1935 (2005)
101. Maximenko N A, Bang B, Sasaki H *Geophys. Res. Lett.* **32** L12607 (2005)
102. Sokolov S, Rintoul S R *J. Phys. Oceanogr.* **37** 1394 (2007)
103. Phillips N A *Tellus* **6** 274 (1954)
104. Kalashnik M V, Kurgansky M V, Chkhetiani O G *Phys. Fluids* **33** 076608 (2021)
105. Drazin P G, Reid W H *Hydrodynamic Stability* (Cambridge: Cambridge Univ. Press, 2004)
106. Miles J W *J. Fluid Mech.* **10** 496 (1961)
107. Kuo H L *J. Meteor.* **6** 105 (1949)
108. Kuo H L *J. Atmos. Sci.* **35** 1840 (1978)
109. Rayleigh Lord *Philos. Trans. R. Soc. Lond. A* **93** 148 (1917)
110. Solberg H *Proces-verbaux Del'assoc. de Meteor., Un. Geod. Geophys. Int., Edimbourg* **33** 66 (1933)
111. Emanuel K A *J. Atmos. Sci.* **36** 2425 (1979)
112. McIntyre M E *Geophys. Fluid Dyn.* **1** 19 (1970)
113. Dunkerton T J *J. Atmos. Sci.* **38** 2354 (1981)
114. Thomas L N et al. *Deep Sea Res. Pt. II Topical Stud. Oceanogr.* **91** 96 (2013)
115. Courant R, Gilbert D *Methods of Mathematical Physics* Vol. 2 (New York: Interscience Publ., 1962); Translated into Russian: *Metody Matematicheskoi Fiziki* Vol. 2 (Moscow: Mir, 1964)
116. Howard L N *J. Fluid Mech.* **10** 509 (1961)
117. Ooyama K *J. Atmos. Sci.* **23** 43 (1966)
118. Kalashnik M V *Izv. Atmos. Ocean. Phys.* **44** 787 (2008); *Izv. Ross. Akad. Nauk Fiz. Atm. Okeana* **44** 848 (2008)
119. Chetaev N G *The Stability of Motion* 1st ed. (New York: Pergamon Press, 1961); Translated from Russian: *Ustoichivost' Dvizheniya* 4th ed., rev. (Moscow: Nauka 1990)
120. Charney J, in *Proc. of the 9th General Assembly, UGGI, Assoc. Meteorol., Brussel* (1951) p. 47
121. Kurgansky M V *Izv. Atmos. Ocean. Phys.* **29** 444 (1994); *Izv. Ross. Akad. Nauk Fiz. Atm. Okeana* **29** 464 (1993)
122. Tassoul J-L *Theory of Rotating Stars* (Princeton, NJ: Princeton Univ. Press, 1978); Translated into Russian: *Teoriya Vrashchayushchikhsya Zvezd* (Moscow: Mir, 1982)
123. Maeder A et al. *Astron. Astrophys.* **553** A1 (2013)
124. Kalashnik M V, Svirkunov P N *Dokl. Earth Sci.* **349** 829 (1996); *Dokl. Ross. Akad. Nauk* **348** 811 (1996)
125. Kalashnik M V, Svirkunov P N *Russ. Meteor.* (4) 42 (1998); *Meteorolog. Gidrolog.* (4) 58 (1998)
126. Mu M, Shepherd T G, Swanson K *J. Atmos. Sci.* **53** 2918 (1996)
127. Mu M, Vladimirov V, Wu Y H *J. Atmos. Sci.* **56** 400 (1999)
128. Kurgansky M V *Quart. J. R. Meteor. Soc.* **135** 2168 (2009)
129. Eliassen A *Astrophis. Norvegica* **5** 19 (1951)
130. Rüdiger G, Arlt R, Shalybkov D *Astron. Astrophys.* **391** 781 (2002)
131. Shakura N I, Sunyaev R A *Astron. Astrophys.* **24** 337 (1973)
132. Velikhov E P *Sov. Phys. JETP* **36** 995 (1959); *Zh. Eksp. Teor. Fiz.* **36** 1398 (1959)
133. Chandrasekhar S *Hydrodynamic and Hydromagnetic Stability* (Oxford: Clarendon Press, 1961)
134. Balbus S A, Hawley J F *Astrophys. J.* **376** 214 (1991)
135. Balbus S A *Annu. Rev. Astron. Astrophys.* **41** 555 (2003)
136. Le Bars M, Le Gal P *Phys. Rev. Lett.* **99** 064502 (2007)
137. Le Dizès S, Riedinger X *J. Fluid Mech.* **660** 147 (2010)
138. Park J, Billant P *J. Fluid Mech.* **725** 262 (2013)
139. Rüdiger G et al. *Geophys. Astrophys. Fluid Dyn.* **111** 429 (2017)
140. Le Gal P et al. *J. Fluid Mech.* **907** R1 (2021)
141. Tassoul J-L *Stellar Rotation* (Cambridge: Cambridge Univ. Press, 2000)
142. Barnes J R *J. Atmos. Sci.* **41** 1536 (1984)
143. Polichtchouk I, Cho J Y-K *Mon. Not. R. Astron. Soc.* **424** 1307 (2012)
144. Sugimoto N, Takagi M, Matsuda Y *J. Geophys. Res. Planets* **119** 1950 (2014)
145. Goldreich P, Schubert G *Astrophys. J.* **150** 571 (1967)
146. Shibahashi H *Publ. Astron. Soc. Jpn.* **32** 341 (1980)
147. Knobloch E *Astrophys. Space Sci.* **116** 149 (1985)
148. Marcus P S, Press W H *J. Fluid Mech.* **79** 525 (1977)
149. Spruit H C, Knobloch E *Astron. Astrophys.* **132** 89 (1984)
150. Cabot W *Astrophys. J.* **277** 806 (1984)
151. Kitchatinov L L *Astron. Lett.* **39** 561 (2013); *Pis'ma Astron. Zh.* **39** 631 (2013)
152. Kitchatinov L L *Astrophys. J.* **784** 81 (2014)
153. Gilman P A *J. Atmos. Sci.* **24** 119 (1967)
154. Gilman P, Dikpati M *Astrophys. J.* **787** 60 (2014)
155. Gilman P A *Astrophys. J.* **853** 65 (2018)
156. Chiang E *Astrophys. J.* **675** 1549 (2008)
157. Klahr H H, Bodenheimer P *Astrophys. J.* **582** 869 (2003)
158. Klahr H H *Astrophys. J.* **606** 1070 (2004)
159. Lesur G, Papaloizou J C B *Astron. Astrophys.* **513** A60 (2010)
160. Adams F C, Watkins R *Astrophys. J.* **451** 314 (1995)
161. Barge P, Sommeria J *Astron. Astrophys.* **295** L1 (1995)
162. Ou S et al. *Astrophys. J.* **667** 1220 (2007)
163. Petersen M R, Julien K, Stewart G R *Astrophys. J.* **658** 1236 (2007)
164. Lorén-Aguilar P, Bate M R *Mon. Not. R. Astron. Soc. Lett.* **453** L78 (2015)
165. Barge P, Richard S, Le Dizès S *Astron. Astrophys.* **592** A136 (2016)
166. Richard S, Nelson R P, Umurhan O M *Mon. Not. R. Astron. Soc.* **456** 3571 (2016)